1994

A rheological investigation of electrorheological materials subjected to small strains

Andy H. Shiang
Lehigh University

AUTHOR:

Shiang, Andy H.

TITLE:

A Rheological Investigation of Electrorheological Materials Subjected to Small Strains

DATE: January 15, 1995

A Rheological Investigation of Electrorheological Materials Subjected to Small Strains

by

Andy H. Shiang

A Thesis

Presented to the Graduate and Research Committee

of Lehigh University

in Candidacy for the Degree of

Master of Science

in

The Department of Mechanical Engineering and Mechanics

Lehigh University

1994

CERTIFICATE OF APPROVAL

This thesis is accepted and approved in partial fulfillment of the requirements for the Master of Science.

Dec. 5, 1994
Date

Thesis Advisor
Dr. John P. Coulter

Chairperson
Dr. Robert P. Wei

"The chief aim of all investigations of the external world should be to discover the rational order and harmony which has been imposed on it by God and which He revealed to us in the language of mathematics."

Johannes Kepler

1571-1630

Acknowledgments

I would like to first acknowledge my parents—Mr. and Mrs. Cheng-Teh Shiang (Chao-Nan), for their constant love and encouragement throughout my life. I thank you for your emotional and financial support and for the sacrifices you have made for me.

Much appreciation is directed towards my advisor—Professor John P. Coulter. As Hipolito said in Hemingway's "The Chauffeurs of Madrid"—"Listen, we had a good time, didn't we?"

The support and encouragement of Mr. and Mrs. Henry Yao (Shirley) are appreciated. Thanks also goes to Mr. and Mrs. Christophe Dorier (Emily) for pleasant European summers. As for Mr. and Mrs. Clifford VerMulm (Hope), and Mr. and Mrs. Mark Gehman (Grace), thank you for being there, for the laughter, and for the sweetness of friendship.

To my "academic" comrades in arms, Ms. Melek Yalcintas, Ms. Evelitsa Higuerey, Dr. Hamdi Demirci, I bid you to march on!

Lunch time just would not have been the same without Mr. Doo Hwan Kim—a Ph.D. candidate in Applied Mathematics. It was truly a pleasure to have known you. A heart-felt thanks goes to Mr. Chao-Kun Chyu—a Ph.D. candidate in Mechanical Engineering and Mechanics. I have benefited from your guidance and friendship; I have enjoyed tremendously our stimulating discourses.

I would also like to acknowledge Drs. Keith Weiss and Ted Duclos of LORD Corporation for generously supplying the ER materials needed throughout this study. Lastly, this thesis research could not have been realized without the funding of Dr. Gary Anderson of the U.S. Army Research Office (Grant No. DAAL03-92-G-0388).

TABLE OF CONTENTS

LIST OF TABLES

LIST OF FIGURES

LIST OF FIGURES (CONTINUED)

LIST OF FIGURES (CONTINUED)

NOMENCLATURE

RHEOLOGICAL INVESTIGATION

A	Area
G^*	Complex Shear Modulus
G'	Complex Storage Modulus
G''	Complex Loss Modulus
G_n^*	Nonlinear Complex Shear Modulus
G_n'	Nonlinear Storage Modulus
G_n''	Nonlinear Loss Modulus
ϕ	Shear Stress/Strain Phase Angle
$\tan \delta$	Loss Tangent
τ	Shear Stress
τ_y	Dynamic Yield Stress
τ^*	Complex Shear Stress
γ	Applied Shear Strain
η	Apparent Viscosity
η_p	Bingham Plastic Viscosity
ω	Radial Sinusoidal Excitation Frequency
μ	Newtonian Viscosity

CONTROLLABILITY AND RELIABILITY INVESTIGATION

ΔE	Change in Electric Field Strength
t_e	Electric Field Application Time
f_n	Vibration Modal Frequency
δ	Modal Loss Factor
E	Electric Field
f_e	AC Electric Field Frequency

ABSTRACT

The present investigation focused on the study of the small strain, dynamic behavior of electrorheological (ER) materials at room temperature. Emphasis was placed on the influence of ER rheology on the long-term frequency response of ER material based adaptive structures. Both Alternate Current (AC) and Direct Current (DC) ER materials were tested for linearity (strain dependence) at small strain amplitudes. The results of the rheological experiments indicated that both AC and DC ER materials behaved in a nonlinear viscoelastic fashion; this rendered the linear viscoelastic theory invalid for the description and characterization of ER materials under dynamic shear. Factors which influenced the nonlinear viscoelastic properties were electric field strength, strain amplitude, and strain frequency. Investigations were conducted on adaptive structures which utilized ER materials as the damping layer. The reliability of these structures in terms of variations in vibration modal frequency and loss factor over time were found. The rheology of the two ER materials was found to have caused fundamental differences in the frequency response of the respective ER adaptive structures. Factors which affected the time response of these structures to on-off states in electric field were: electric field strength, electric field application time, and amplitude of excitation. The response of this class of adaptive structures to the application of electric field may be approximated as instantaneous, while the response to the removal of electric field could be extraordinarily long—especially at high excitation frequencies.

CHAPTER 1: INTRODUCTION OF ELECTRORHEOLOGICAL MATERIALS AND THEIR APPLICATIONS

1.1 ER Materials—What are They and What are They Used For?

Since Winslow's discovery of electrorheological (ER) fluids in 1949, much research has been conducted in this relatively new field. Although first called "electroviscous" fluids by Winslow, "electrorheological" fluids soon replaced the previous name. This is because while the apparent viscosity of these fluids does increase dramatically with the application of an electric field, "electrorheological" better describes the changes in viscoelastic properties of these fluids under deformation. The studies first conducted by Winslow (1949) were performed on silica powder in kerosene under the influence of an electric field. Winslow reported that the formation of the fibrils in the direction of electric field was responsible for the increase in shear resistance of the bulk fluid. The shear resistance of the fibrils, or chains, was an active agent in affecting the fluid's apparent viscosity under varying degree of electric field intensity. The reversibility of this phenomenon upon electric field removal was also reported in this pioneering work.

By definition, ER fluids are primarily a colloidal suspension of polarizable particles in a dielectric medium. In the absence of an electric field, the fluid flows freely, and the particulate distribution is random. But upon application of an external electric field, the particles align themselves in the direction of the field and form fibrils or chain-like structures between the electrodes. The formation of these fibrils or chains increases the viscosity of the fluid and changes the rheological behavior of the ER material, i.e. the ER material's ability to resist shear and deformation increases. When the electric field is removed, the bulk fluid returns to zero-field behavior. The response time of this reversible phenomenon is generally claimed throughout available literature to be on the order of a few milliseconds. The phenomenon described above is illustrated in Figure 1.1.

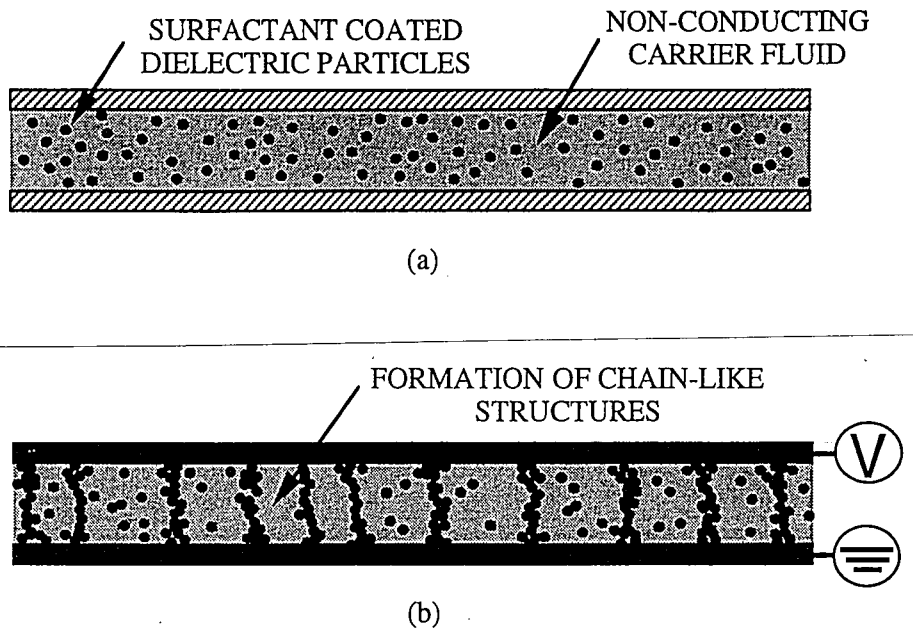

Figure 1.1 The ER effect. (a) Zero electric field and (b) the application of a non-zero electric field.

Perhaps a simpler description of the ER phenomenon is that the behavior of ER fluids changes from that of a liquid to that of a jell-form upon the application of electric field. Upon removal of the electric field, the ER material returns to the liquid state.

Several recent papers have reviewed the causes of the ER phenomenon (Weiss et al., 1993; Jordan and Shaw, 1989; Conrad and Sprecher, 1991; Block et al., 1990; Gast and Zukoski, 1989). The primary mechanism for the ER effect is thought to be the polarization of the particles and the resulting attraction forces between them in an electric field. Another theory is known as the Water-Glue Theory where the content of water—a highly polar molecule—in an ER material is thought to be responsible for the ER effect. However, highly sophisticated experiments have been performed which controlled water content (anhydrous ER fluids), yet the ER effect persisted. Other theories such as the Particle Fibrillation Theory and the Distorted Double Layer Theory also help to explain the causes for the ER phenomenon. Each of the above theories has it's own weakness, and a theory that is applicable to the multitude of ER materials and is universally accepted remains

to be found. In order to further develop ER material based applications, superior fluids are needed; the fundamentals of how ER mechanisms work need to be fully understood.

1.2 ER Materials in Academia and Industry

The composition of any ER material found in academia or industry is comprised of primarily four components: a particle constituent, a dielectric fluid medium, surfactants, and various additives. Weiss et al. (1993) gave a thorough summary of various ER materials available in the patent literature. Although a bewildering number of possible material combinations exist, the following statement can be made for any ER material: particle constituents—natural or synthetic—are minute (many ER materials have particle diameter of approximately 10 to 50 μm); carrier fluids have the common characteristic of being dielectric, i.e. non conducting, such as various mineral, silicone, castor oils, and a variety of other chemicals; surfactants are utilized to prevent particle flocculation; various additives such as water, glycerin, acids and alcohol may be added to enhance the ER effect.

Typically, researchers in the ER investigative community may either synthesize their own ER materials or procure samples from chemical companies specializing in ER material research and development. Researchers in materials science are interested in material composition, novel processes and synthesis, testing methodology, and of course, material properties. Those in the mechanical engineering discipline may also be interested in the above topics, but more commonly have particular interests in the application of these materials in devices such as valves, dampers and shock absorbers, clutches, and engine mounts, as well as noise and vibration control. Ultimately, the decision on whether to purchase or to synthesize depends on ones research interests and resources.

Presently in the US, the ER materials originating from academic research institutions are consumed specifically at the respective schools. Researchers such as Gamota and Filisko (1991a, 1991b, 1991c), Conrad et al. (1991), Conrad and Sprecher (1991), Choi et al. (1992) have utilized ER materials prepared in their own laboratories.

The experiments conducted included linear/nonlinear material behavior, temperature dependence, mechanical properties, and fluid composition. Commercialized ER materials are now available in the US and abroad with LORD Corporation being one of the first to offer their fluids to the public. Several researchers (Jordan et al., 1992; Don, 1993; Coulter et al., 1993b; Gong et al., 1993; Yalcintas and Coulter, 1993; Yalcintas et al., 1993; Yen and Achorn, 1991) have utilized commercial ER materials in their research. The details on the state of the art in ER material-related research is the subject of Section 2.4 of the present thesis. As evident from the previously mentioned paper by Weiss et al. (1993), the combinations of particles, base fluids, surfactants, and additives which form an ER material are numerous. This fact coupled with numerous testing methodologies is one of the reasons for the ER research field's lack of a standard method and fluid. Researchers in the commercial ER industry (Weiss et al., 1993) believe that one of the primary barriers for establishing commercial ER-related business has been a lack of satisfactory materials as well as an inadequate understanding of the ER phenomenon.

1.3 ER Materials Provided by LORD Corporation

The ER materials used throughout the present thesis research were supplied by LORD Corporation. Two types of ER fluids were used. Fluids which respond to Direct Current (DC) electric field, and fluids which respond to Alternate Current (AC) electric field of various field frequencies. These fluids are referenced throughout the thesis simply as DC and AC fluids.

1.3.1 VersaFlo ER-200

This ER material responds to an AC electric field frequency of 500 Hertz or greater. The material has an opaque, white appearance after mixing. According to material specifications supplied by LORD Corporation, a summary of the post-yield properties of ER-200 is provided in Table 1.1.

Table 1.1 Post-yield properties of LORD VersaFlo ER-200 (AC) at 25°C

AC Electric Field (kV/mm)	0	1.0	2.0	3.0
Dynamic Yield Stress (Pa)	50-200	200-300	900-1000	1600-2200
Bingham Viscosity (mPa-s)	200-400	200-250	250-350	200-800
Current Density ($\mu A/cm^2$)	—	400-470	760-830	1200-1500

1.3.2 VersaFlo ER-III

According to information supplied by LORD Corporation, ER-III is an ER material which responds to DC electric field. The material has a dark blue appearance after mixing. Some typical post-yield properties of this ER material are summarized in Table 1.2.

Table 1.2 Post-yield properties of LORD VersaFlo ER-III (DC) at 25°C

DC Electric Field (kV/mm)	0	1.0	2.0	3.0	4.0
Dynamic Yield Stress (Pa)	31	148	383	729	1326
Bingham Viscosity (mPa-s)	206	136	110	267	116
Current Density ($\mu A/cm^2$)	—	0.8	1.1	5.8	8.5

1.4 Potential Applications Related to the Present Research Investigation

The controllable rheological behavior of ER materials becomes useful to engineering systems when variable system performance is desired. When such a system is implemented with sensing and control capabilities, the result is an intelligent or adaptive system capable of sensing external stimuli and react according to pre-specified criteria. In this way, the optimal performance is always obtained.

Two regimes of ER material rheological behavior are generally referenced in ER research literature: the pre-yield regime and the post-yield regime. It is believed that in the pre-yield regime, ER materials behave in a linear viscoelastic fashion, and the equations of linear viscoelasticity are valid to describe the properties of these materials under dynamic strain. In the post-yield, or the continuous-flow regime the Bingham Plastic approximation:

$$\tau = \tau_y + \eta_p \dot{\gamma} \tag{1.1}$$

is often used. In Equation 1.1, $\dot{\gamma}$ is the shear rate, and τ_y is the dynamic yield stress of the ER material. The η_p, or the plastic viscosity, is a weak function of external electric field and is quite often assumed constant in the design of ER material based devices.

Essentially, there are two fundamental ER material/electrode interaction configurations found in commonly studied ER devices such as valves, dampers and shock absorbers, and clutches. These are generally referenced as the fixed electrode configuration and the sliding electrode configuration—as shown in Figure 1.2(a) and (b), respectively. In fixed electrode configuration devices, the electrodes containing the region of ER fluid flow are stationary. Flow of ER fluids in these devices is driven by the pressure gradient which exists between the entrance and exit region of the flow area. By controlling the voltage level on the electrodes and therefore the electric field, variable performance of the device is achieved. The electric field, ER material rheology, as well as device geometry are the governing factors between the pressure gradient and flow. For sliding electrode devices, one of the electrodes is subjected to a tangential force which results in the plate moving with a certain velocity. In these devices, the governing factors for the performance parameters, i.e. force and speed of the electrode, are electric field, device geometry, and ER material rheological properties.

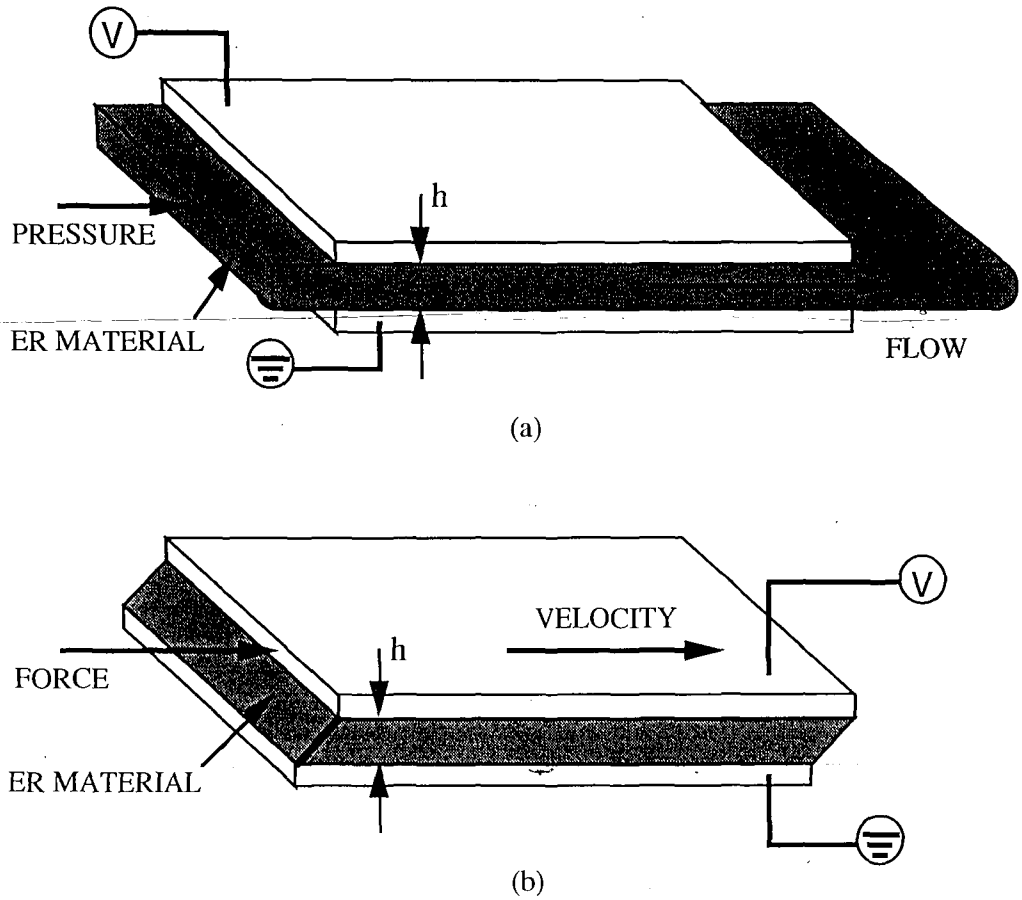

Figure 1.2 ER device component configurations: (a) fixed electrode and (b) sliding electrode.

1.4.1 Controllable Devices

The understanding of the two fundamental configurations mentioned above may lead to relationships which approximate actual ER device behavior. Utilizing the Bingham approximation characterized by Equation 1.1, the steady-state behavior of the ER device—fixed electrode or sliding electrode—may be explicitly determined. Of the numerous ER devices which exist in literature, the practical and potentially marketable, and therefore well-studied examples are: dampers and shock absorbers, valves, clutches and brakes, controllable machinery and engine mounts, and adaptive structures. A discussion on each of these applications is given in the subsequent sections.

1.4.1.1 Dampers and shock absorbers

Many real world devices requiring the use of dampers and shock absorbers are prime candidates for design improvements due to the controllable ER material rheology. A diverse range of potential applications exists from off-road vehicles and helicopter struts to aircraft landing gear. In these applications, both the fixed and sliding electrode configurations may be used. The primary difference exist in whether the moving piston drives the ER fluid across valve-like channels, or if the piston—which is itself an electrode, shears the ER material contained by an adjacent stationary electrode. Illustrations for both configurations are shown in Figure 1.3.

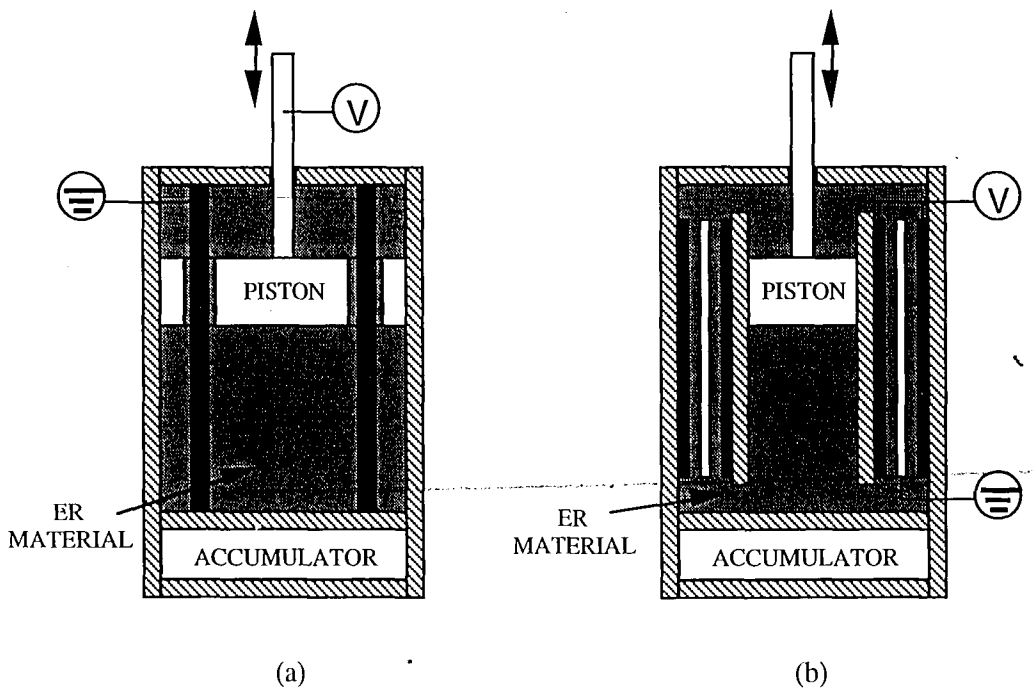

Figure 1.3 ER damper configurations: (a) sliding plate and (b) fixed plate.

Experimental and analytical evaluations of dampers and shock absorbers were conducted by several researchers where the successful use of these dampers were demonstrated. Significant and controllable variations in vibration amplitude, as well as overall system damping were observed especially at resonant frequencies. Although certain

devices such as aircraft landing gear require stronger ER materials, reasonable qualitative agreement between theory and experimentation were observed for this application.

1.4.1.2 Valves

The notion of a valve with no moving parts is an attractive one. Ask any engineer who is familiar with the maintenance and replacement of valves and he or she will most likely welcome the concept of an ER valve. Since there are no moving mechanical components, there are no seals to deteriorate, no springs to replace, and no hinges to be worn out. The implementation of ER valves into any fluid system, whether for pure fluid handling or for control purposes should significantly reduce maintenance requirements.

The concept of an ER valve was proposed and investigated by Winslow in the 1940's. The basic ER valve may be as simple as the plate-shaped device shown in Figure 1.2(a), or it may be more sophisticated such as the commonly studied concentric-cylinder valve shown in Figure 1.4. In either case, if the material flowing through the valve is electrorheological, the flow and pressure drop through the valve may be controlled by varying the electric field. In addition to low maintenance due to a lack of moving parts, the benefits of these valves include fast response time, and minimization of fluid/valve-part interaction effects such as water hammer and noise.

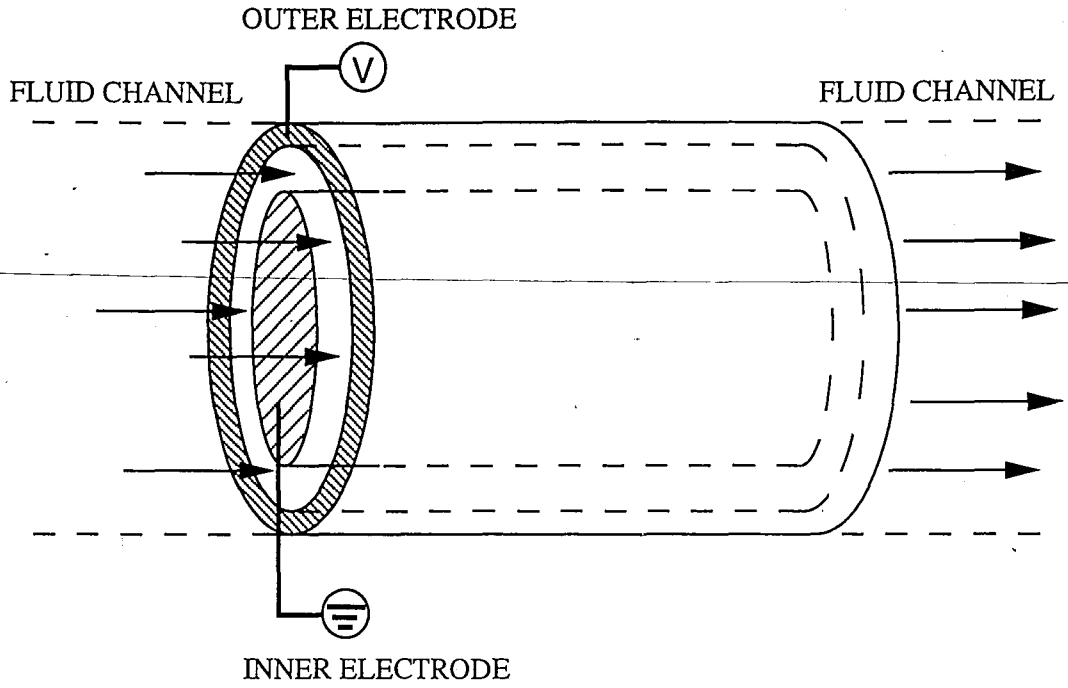

Figure 1.4 Concentric-cylinder ER valve.

Although ER valves are not practical for large fluid-power systems where the working fluid experiences thermodynamic phase changes, these valves have been proven useful. Several types of controllable devices have been developed as a result of incorporating ER valves into larger systems. Examples of such systems are controllable shakers or vibrators. Manufacturing applications also include machine part holders and valveless hydraulic robots—which use ER materials as the working fluid (Hartsock et al., 1991).

1.4.1.3 Clutches and brakes

Winslow's published work (1949) also included controllable clutches and brakes. Though the development of these devices were limited over the next three decades, they received much attention in the 1980's. Due to the nature of the device, the sliding electrode configuration is used. Typically either a concentric-cylinder geometry or a multiple parallel

disk configuration is used, as shown in Figure 1.5. The decision on which configuration to use depends on design input parameters such as load, operating temperatures, and rotation speed.

The unique method of using an ER clutch with variable power transmission has certain advantages. In addition to having low friction, the torque transmission of this power coupling mechanism is adjustable. Namely, in order to obtain a high power transmission ratio, one increases the electric field strength; if a low power transmission ratio is needed, one decreases the field strength. The usage of ER clutches with linear torque/applied-voltage relationship could facilitate computerization of high speed manufacturing processes requiring variable force or torque, thereby streamlining the process and reducing cost.

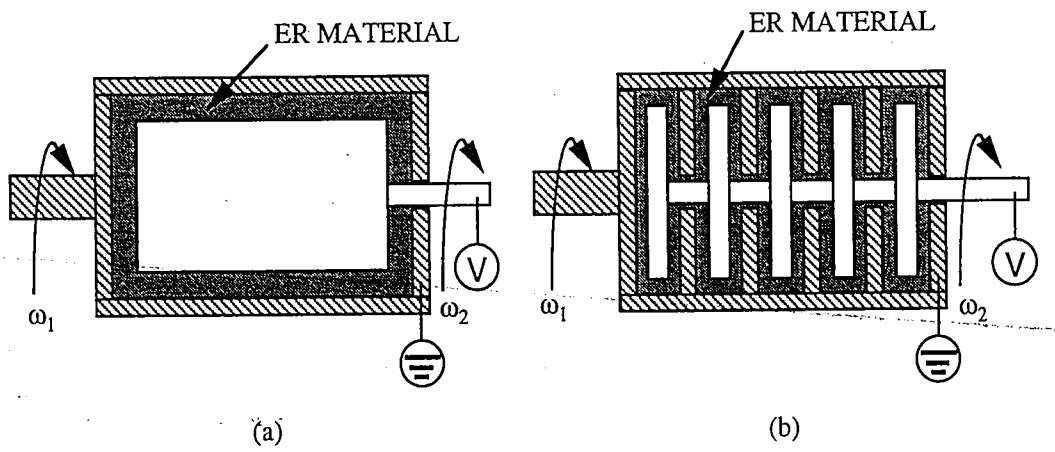

Figure 1.5 ER clutch configurations: (a) concentric cylinder and (b) parallel disk.

The nature of ER clutch and brake design is not without disadvantages. Attention is needed in the design and implementation of these devices in high-temperature applications. Since temperature increases of greater than 100°C may cause decreases in the apparent viscosity of certain ER materials (consequently ER effect diminishes), viscous heating of the fluid, and ohmic heating due to the electric field should not be ignored. Lastly in high speed ER clutches, the centrifugal acceleration experienced by the ER particulate matter will

also contribute to the deterioration of the ER effect by causing fluid/particulate separation. However, with attention in design and implementation of these unique devices, ER clutches may serve the engineer well in industrial processes requiring variable torque transmission and rapid response time.

1.4.1.4 Controllable machinery and engine mounts

Devices which also benefited from the incorporation of ER valve technology were machinery and engine mounts. Traditional liquid-filled mounts were designed to have fluid inertia track characteristics, as well as both bottom and top compliance values for the damping of specific forces at specific frequencies. In these application-specific mounts, the number, size and shape of the inertia tubes are fixed once the design parameters are set. But in using an ER valve as the inertia tube, the fluid flow between the top and bottom part of the mount is easily regulated, thereby achieving overall mount performance control. This concept is shown in Figure 1.6.

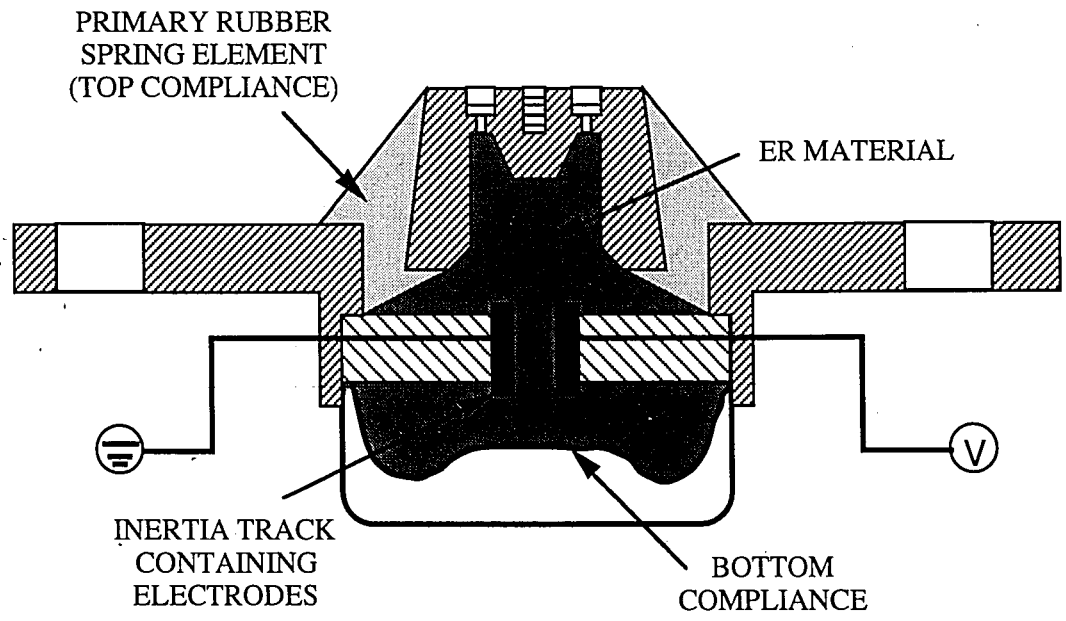

Figure 1.6 A proposed ER controllable machinery or engine mount.

Though the technology of ER engine and machinery mounts is still at an infancy, analytical and experimental work conducted thus far show promise for this class of devices. In relatively low excitation frequencies (< 50 Hertz), a significant range of controllability in terms of high damping and high dynamic spring rate has been noticed by several researchers. The overall positive control capabilities of these mounts at moderate temperatures (0°-100° C), as well as endurance to high service-life cycles were both proven.

1.4.2 Adaptive Structures

Since the mid 1980's, the utilization of ER materials for structural damping has been proposed and studied. Unlike the controllable devices discussed in Section 1.4.1, the use of ER materials for adaptive structures was thought to be based on the controllability of the ER materials in the pre-yield region. In environments where variable structural performance is desired, ER materials are potentially applicable due to the fast, reversible, and controllable changes in rheological behavior which they exhibit. When a structure with controllable stiffness and damping is combined with real-time sensing and control capabilities, the result is an intelligent system capable of adapting to a changing environment in the interest of performance optimization.

There are no set rules in the design and fabrication of ER adaptive structures, but two classes of ER material based adaptive structures have been studied thus far. They are referred to as shear configuration and extensional configuration, as shown in Figure 1.7. In adaptive structures where the ER particulate chains undergo shear deformation, the structures are classified as shear-configuration based. Likewise, for structures where the chains are in compressive and tensile loading, the structures are referenced as extensional-configuration based. ER adaptive structures found in the industrial or academic research communities may be placed into one of the two classifications.

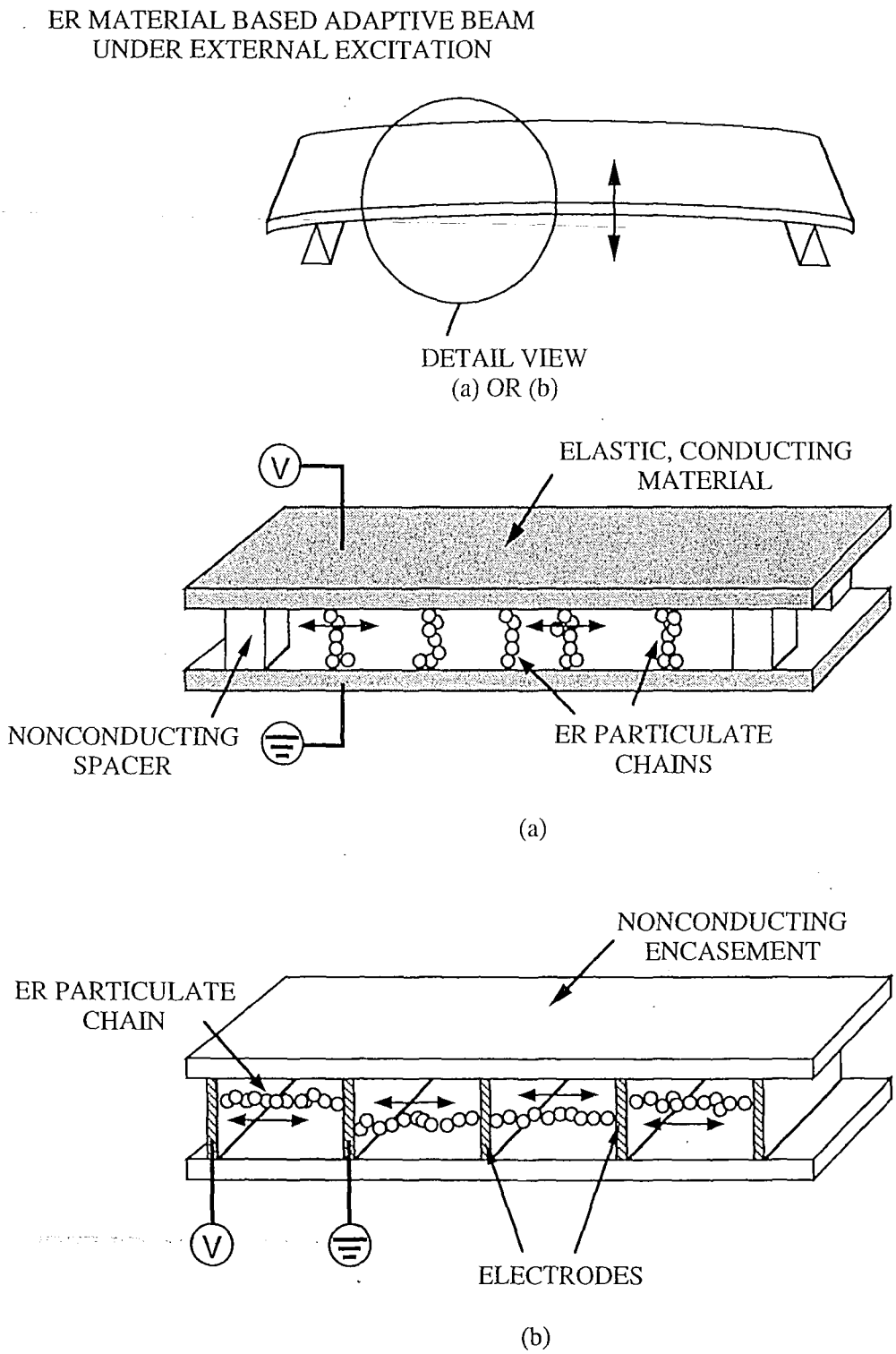

Figure 1.7 Basic configurations of ER material based adaptive structure: (a) shear configuration and (b) extensional configuration.

Recently, the advent of artificial-intelligence controlled smart structures combined with advanced stress sensing fiber optics had enabled researchers to design truly "intelligent" structural systems. Han et al. (1994) studied the vibration response of an ER material filled beam using fiber-optic sensors and a simple, manual control scheme. A neural-network control scheme was used on an ER dynamic damper by Morishita and Ura (1993) for successful vibration suppression of a monolithic cantilever beam. Flanders et al. (1994) also developed an ontogenic neural-network control system for vibration control of an ER material based beam incorporating multiple ER based control elements under multiple excitation sources. The key concept of a tunable ER material based composite structure is that if the designer wishes to avoid resonance over a given frequency range, the structures could be tuned by applying or removing the electric field so that the response to a given frequency of excitation is minimized. The integration of all three research areas—ER adaptive structural modeling, artificial-intelligence based controls, and fiber-optic sensing—is required for the successful operation of such advanced structural systems. Though alternate and more conventional control and sensing methods could be used, the nature and conditions of this type of application require the utilization of advanced techniques.

There are several reasons for employing artificial neural networks as the control algorithm for the ER beam subjected to external disturbances. Primarily, it is because neural networks represent non-parametric techniques for achieving arbitrarily complex functional mappings, which could provide the core of the solution to the vibration-control problem. Also, the variety of neural-network configurations and learning algorithms could lead to a practical, adaptive method for vibration control in increasingly complex structural systems.

The use of ER materials for semi-active damping of the structure is heavily dependent on the acquisition of precise and timely response from the structure in a form convenient for processing by the control system. Several techniques were used for in-situ measurement of the data which may be used to provide the information necessary to evaluate the effect of ER materials on the damping of the structure. In a laboratory environment, proximity probes may be used to monitor the structure's response. While this is quite adequate in the lab, real-world conditions may prove this to be highly impractical. Examples of this may include helicopter blade damping, aircraft body or skin vibration damping, and damping of automobile body panels. An alternative type of sensor that could be used are electrical strain gages attached directly to the structure. Though strain gages can provide adequate response in both sensitivity and frequency, they are sensitive to electromagnetic radiation. In addition to being susceptible to corrosion in a harsh environment, there is a need for electrical connections to carry the signal out of the structure, which also could be subject to electromagnetic influence. Due to the inherent fiber-optics insensitivity to electromagnetic radiation and their ability to withstand harsh environments, they are ideal for ER adaptive structure applications.

One such ER adaptive structure incorporating fiber-optic sensing and neural-network controls has been assembled and tested with limited success. The schematics of the smart structure is shown in Figure 1.8. Due to technical difficulties in the ER rheology part of the project—to be discussed in detail in Section 4.1—the implementation of this

intelligent structure has been successful only in the low frequency range (<50 Hertz). In comparison, the fiber-optic sensing and the neural-network controls have been less troublesome. However, in spite of the difficulties, the operation of such systems have gone beyond the proof-of-concept stage. More importantly, these early experiments have aided the researchers in identifying areas which need further attention and efforts. Thus far, the ER-rheology part of the project has been identified as such an area; the details for the arrival of this are the subjects of Chapters 3 and 4 of the present thesis.

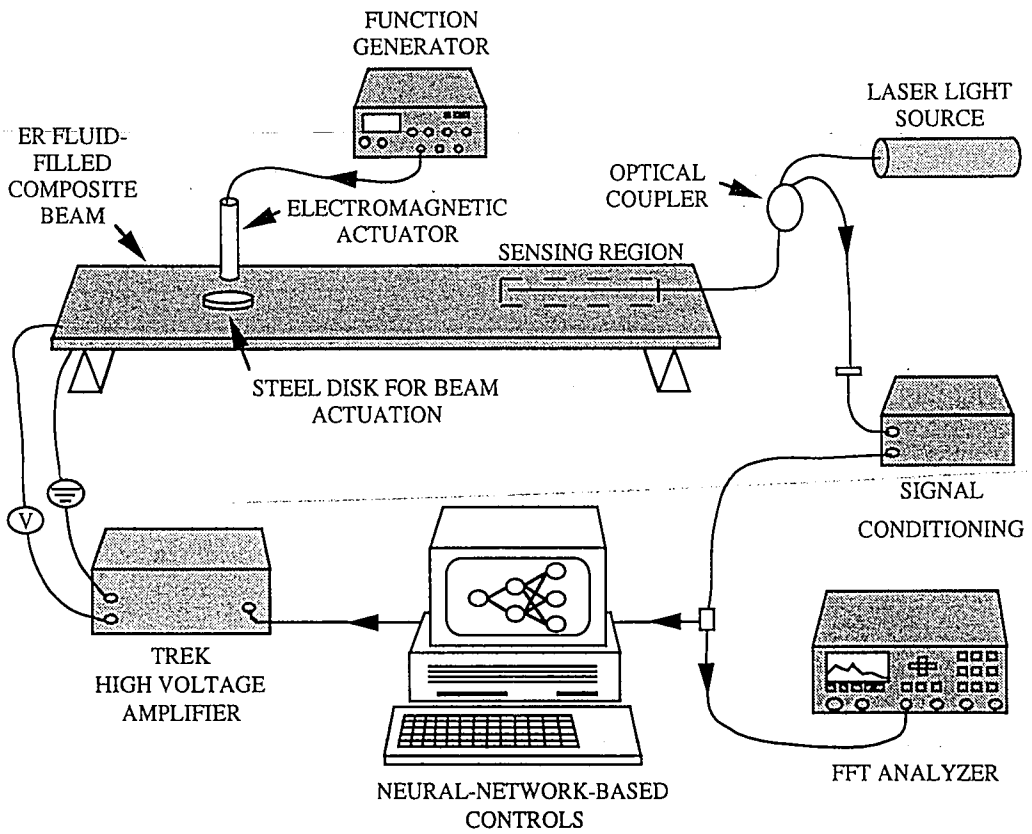

Figure 1.8 ER material based adaptive structure with fiber-optic sensing and neural-network controls.

1.5 Chapter Summary—Overall Focus and Structure of the Thesis

The concepts of Electrorheological (ER) materials and engineering with ER materials were introduced. Studies of these materials have been documented since the 1940's. ER materials are a special class of colloidal suspensions of polarizable particles in a dielectric fluid medium. The rheological properties of these unique materials change rapidly in response to changing external electric fields. The fast response time and controllable rheology of these materials have led to the design and study of numerous novel applications. These applications are classified into controllable devices and adaptive structures, the latter of which is the subject of this thesis research. Throughout this research project, only commercial ER materials—as supplied by the manufacture—were used in the fabrication of ER material based adaptive structures and for rheological testing.

Although considerable progress has been made recently in ER adaptive structures with the incorporation of control and sensing capabilities, the full implementation of such systems has had limited success. This is due to a lack of essential and fundamental information regarding electrorheology—as applied to vibration damping. Previous electrorheology research, much of which has focused on the post-yield, dynamic properties of ER materials and devices have not answered all of the questions. The present thesis focuses on the influence of ER rheology on the behavior of ER adaptive structures in small amplitude vibration.

Chapter 2: ELECTRORHEOLOGICAL TESTING—STATE OF THE ART REVIEW

2.1 Rheology—Some Introductory Concepts

Rheology is the science of the deformation and flow of matter. As stress is applied to a body, it alters its shape or size. The body is said to flow if its degree of deformation changes continuously with time. Ultimately, the objective of rheology is to predict the forces necessary to produce a certain deformation or flow within a material.

For a viscous fluid, the application of a force, however small, will result in flow. Moreover, the release of the force on the system will not result in the recovery of the body to its original state. If the body under question is an elastic solid, the application of a force will result in deformation, not flow. Upon release of the force, the body will return to the original state. For a plastic body under force, the body will flow once a critical value is exceeded; otherwise, the body will deform like an elastic solid. Real world materials exhibit neither idealized viscous, nor elastic behavior. In general, a real material such as steel or honey, will exhibit both elastic and viscous behaviors. Hence the definition of the term "viscoelasticity."

The science of rheology has many practical uses. In many branches of industry, the engineer or scientist is faced with the problem of designing apparatus or instruments to handle materials which are neither elastic nor viscous. Non-Newtonian fluids and plastics are frequently encountered in the food processing industry in the forms of pastes, suspensions, and soft-solids. Paper pulp suspensions exhibit unusual time-dependent effects; molten plastics also show pronounced viscoelastic behavior. Hence, rheology is not merely a branch of applied mechanics for the mathematician or the theoretician, but rather, abundant examples of applied rheology exist in everyday living. The understanding of rheology as it applies to material properties and behavior shed light on practical problems of the present day, including engineering applications of ER materials.

2.2 Theory of Linear Viscoelasticity

The ideal behavior of an elastic solid under tensile stress may be expressed by the constitutive equation of the form,

$$\sigma = E\varepsilon \tag{2.1}$$

where σ is the applied force per unit area, ε is the strain or relative change in length, and E is the Young's Modulus. If the same solid is subjected to shear loading, the constitutive equation is:

$$\tau = G\gamma \tag{2.2}$$

where τ represents shear stress, G is the shear modulus, and γ is the shear strain. An illustration of an elastic body under loading is shown in Figures 2.1.

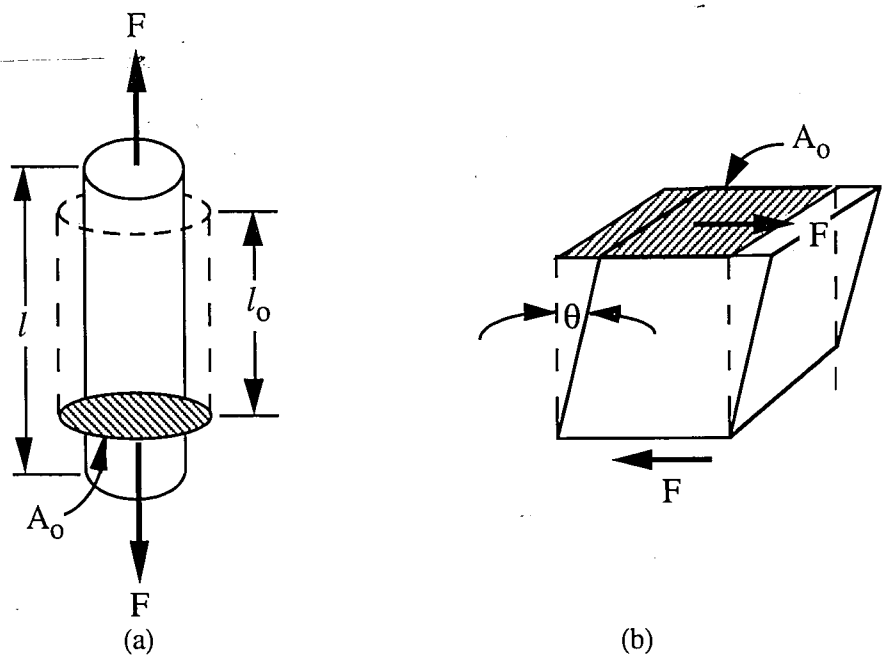

Figure 2.1 Elastic body under stress, (a) tensile loading and (b) shear loading.

The constants of proportionality E and G are a measure of the material's stiffness, or ability to resist deformation. The linear region, i.e. the region where the ratio of the overall stress to the overall strain on a material is independent of the magnitude of the stress and strain, is known as the Hookean region of the material.

When an ideal viscous fluid is sheared as depicted by Figure 2.2, the constitutive equation is:

$$\tau = \mu \frac{du}{dy} \tag{2.3}$$

where τ is the shear stress applied to the fluid and $\frac{du}{dy}$ is the rate of strain (or shear rate). The constant of proportionality, μ, is the absolute (dynamic) viscosity. An important point that should be noted is that a fluid is said to be Newtonian if the viscosity does not depend on the shear rate.

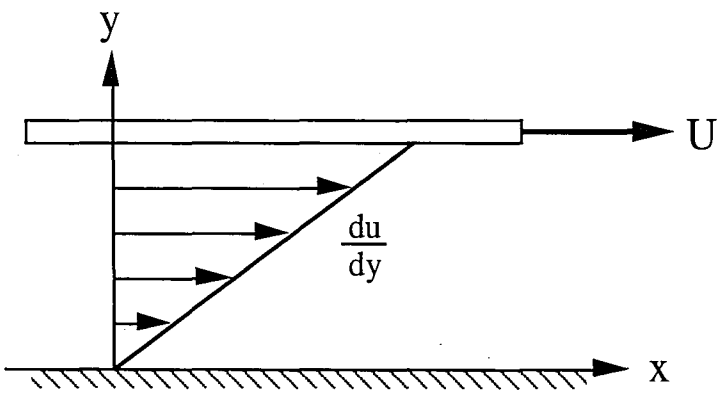

Figure 2.2 Newtonian fluid under shear.

In non-Newtonian fluids the viscosity is not constant, but rather is a function of shear rate. A familiar example is toothpaste. Toothpaste behaves as a "fluid" when squeezed from the tube, but it does not run out by itself when the cap is removed. There is a yield stress above which the toothpaste "flows." Such non-Newtonian behavior may be classified as time-dependent, or viscoelastic. Typical shear rate dependence of several

fluids are shown in Figure 2.3. When defined in this manner, the apparent viscosity, or $\eta(\dot{\gamma})$ characterizes the ratio between shear stress and shear rate.

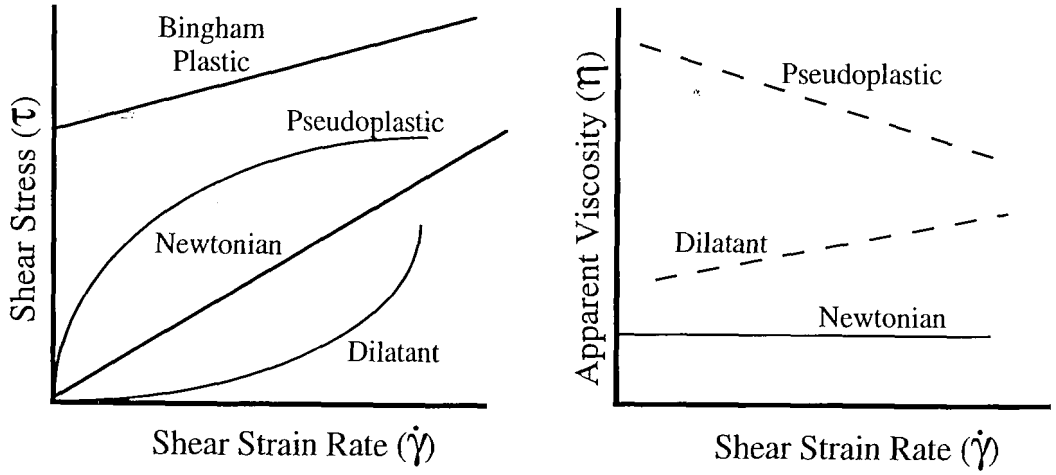

Figure 2.3 Shear rate dependence of several materials.

Fluids in which the apparent viscosity increases with increasing shear rate are termed dilatant (or shear thickening). Some examples include aqueous dispersions of clay and sand. When the apparent viscosity of a fluid decreases with increasing shear rate, the fluid is termed pseudoplastic (or shear thinning). The majority of non-Newtonian fluids fall into this category. Familiar examples are polymer solutions, colloidal suspensions, and emulsions. A material such as toothpaste that behaves as a solid until the "threshold," or yield stress τ_y, is reached, and subsequently exhibits a linear relationship between stress and shear rate is called a Bingham Plastic. Other examples of Bingham Plastics are drilling mud, and concentrated coal slurries.

In real materials, rearrangements take place inside the material when a strain or stress is imposed on it. The time required for the rearrangements may be very short or very long. When changes occur so rapidly that the time is negligible compared with the time of the experiment, the material is regarded as purely viscous. All energy required to produce the deformation in a purely viscous material is dissipated as heat. When the material

rearrangements take virtually infinite time, the material is said to be purely elastic. In a purely elastic material all of the energy required to produce deformation is stored and is completely recovered upon removal of the force. In principle, all real world materials are viscoelastic, i.e. energy of deformation is partially dissipated and partially stored.

Since the material rearrangements within a viscoelastic material depend on the time of the arrangement (i.e. neither zero nor infinite as in cases of viscous and elastic behavior), the relation between stress and strain, or rate of strain may not be expressed by material constants. Rather, these relationships are time and temperature dependent.

The familiar quantities of Young's Modulus (E), and Shear Modulus (G) in Equations 2.1-2.2 are from quasi-static measurements. When cyclical motions are imposed upon viscoelastic materials, it is more convenient to discuss the dynamic mechanical moduli of the materials. If the applied strain varies with time in a sinusoidal fashion, the strain may be expressed by:

$$\gamma = \gamma_o \sin \omega t \tag{2.4}$$

where γ_o is the strain amplitude and ω is the angular frequency in radians/sec. The shear rate is of course the time derivative of γ, or

$$\dot{\gamma} = \gamma_o \omega \cos \omega t \tag{2.5}$$

Since in an ideal elastic material there is no energy dissipated, the stress response is

$$\tau = G\gamma = G\gamma_o \sin \omega t \tag{2.6}$$

In an ideal viscous fluid with no energy stored, the stress response is:

$$\tau = \eta \dot{\gamma} \tag{2.7}$$

or

$$\tau = \eta \gamma_o \omega \cos \omega t \tag{2.8}$$

Through trigonometric identities, it may be shown that Equation 2.8 is also equal to

$$\tau = \eta\omega\gamma_o \sin\left(\omega t + \frac{\pi}{2}\right) \tag{2.9}$$

This essentially means that for an ideal elastic material, stress and strain are in phase. For an ideal fluid, stress and strain are out of phase by 90°, or $\frac{\pi}{2}$ radians. The angle which stress and strain are out of phase is known as the phase angle ϕ. For viscoelastic materials, the phase angle is in between zero and ninety degrees. This is shown in Figure 2.4.

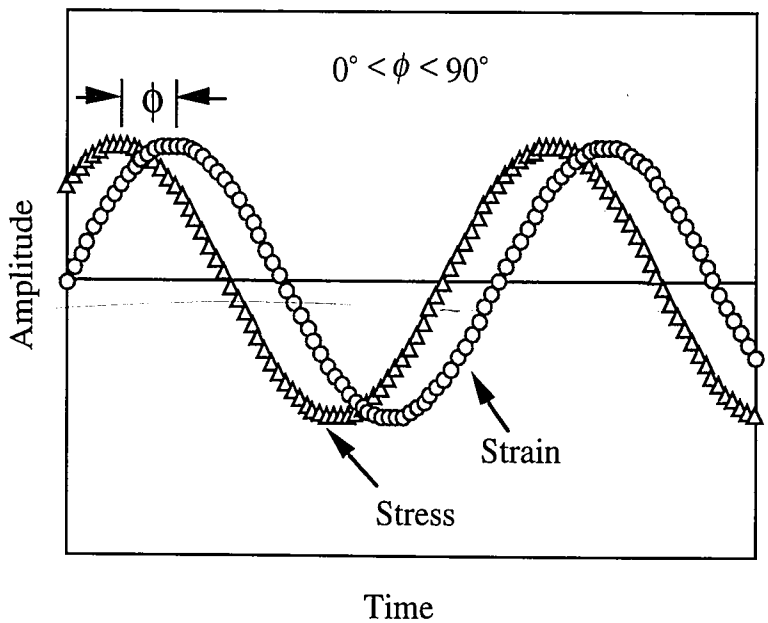

Figure 2.4 Stress/strain response of a viscoelastic material.

In a viscoelastic material with applied strain as expressed by Equation 2.4, the stress may be written as

$$\tau = \tau_o \sin(\omega t + \phi) \tag{2.10}$$

After the substitution of trigonometric identities, the following equation is yielded:

$$\tau = \tau_o \left[\sin(\omega t)\cos(\phi) + \cos(\omega t)\sin(\phi)\right] \tag{2.11}$$

This may be further separated into an elastic stress in phase with the strain expressed by

$$\tau' = \tau_o \cos\phi \tag{2.12}$$

and a viscous stress in phase with the strain rate written as

$$\tau'' = \tau_o \sin\phi \tag{2.13}$$

The two stresses, τ' and τ'', quantify the degree of viscoelasticity of the material. The two stresses are frequently expressed in terms of complex notation as:

$$\tau^* = \tau' + i\tau'' \tag{2.14}$$

where i is the complex number $\sqrt{-1}$.

The dynamic shear moduli of the viscoelastic material is obtained from dividing the complex shear stress by the applied strain:

$$G^* = \frac{\tau^*}{\gamma} \tag{2.15}$$

or in complex notation:

$$G^* = G' + i\,G'' \tag{2.16}$$

where

$$G' = \frac{\tau'}{\gamma} = G^* \cos\phi \tag{2.17}$$

and

$$G'' = \frac{\tau''}{\gamma} = G^* \sin\phi \tag{2.18}$$

G' is the storage modulus, which is a measure of energy stored elastically during deformation; G'' is the loss modulus, which is a measure of the energy dissipated as heat.

Another equation widely used is:

$$\tan\delta = \frac{G''}{G'} \tag{2.19}$$

where $\tan\delta$ is called the loss tangent and is a ratio of the two components of the complex modulus. The two quantities—G" and $\tan\delta$ expressed by Equations 2.18 and 2.19, respectively—are of interest for vibration damping. If these quantities are small for a given vibration frequency and electric field intensity, then the damping will be small; for large values of $\tan\delta$ and G", the damping will be large. Therefore, depending on the application, an ER material with damping capabilities will be useful in vibration control with additional benefits of controllability and instantaneous response time.

In controlled stress or controlled strain rotational rheometers, the magnitude of the complex shear modulus G^* may be obtained from Equation 2.15. In this equation, the complex shear stress amplitude τ^* is obtained from torque (moment of shear stress) and area relationships. When τ^* is divided by the applied shear strain amplitude γ_o, which is a measured quantity, G^* is obtained. In knowing the measured phase angle ϕ between stress and strain, the complex loss and storage moduli are obtained from Equations 2.17-2.18.

It is critical to emphasize that the above equations represent the properties of a viscoelastic material (polymer, emulsion, or electrorheological) in the linear region. In this region, the complex shear modulus is a constant of proportionality of shear stress over shear strain. Above a critical yield strain γ_y, the shear moduli vary with strain. When this occurs, the material behavior is said to be nonlinear and the equations of linear viscoelasticity are no longer valid for the description of dynamic properties. Many viscoelastic materials, including polymers and emulsions, behave linearly up to some γ_y, and become nonlinear at larger strains. ER materials, primarily suspensions, are believed to behave in this linear viscoelastic fashion at small strains, becoming nonlinear at strains greater than γ_y.

2.3 Significance of Pre-Yield and Post-Yield Behavior in the Application of ER Materials

In the application of ER materials, two classifications are made. The first is controllable devices, and the second is adaptive structures. The significance of each class may be representative of the corresponding regimes they occupy in electrorheology. Controllable devices such as valves, dampers, shock absorbers, and clutches are based on the post-yield, large deformation shear behavior of ER materials. Small amplitude, dynamic shearing of ER materials, such as would occur in adaptive structures applications, has been assumed by many researchers to fall in the pre-yield range (Coulter, 1993a; Don, 1993; Gamota and Filisko, 1991a, 1991b, 1991c; Jordan et al., 1992). The ideal dynamic behavior of ER materials under increasing strain amplitude is shown in Figure 2.5(a). Transition from linear to nonlinear viscoelastic regions is represented by the deviation of storage modulus and loss modulus from linear functions. Once the shear strain exceeds the yield strain γ_y, the equations of linear viscoelasticity no longer hold. The behavior of the ER material is far more complex; more sophisticated theories and methods are required to analyze material properties and behavior.

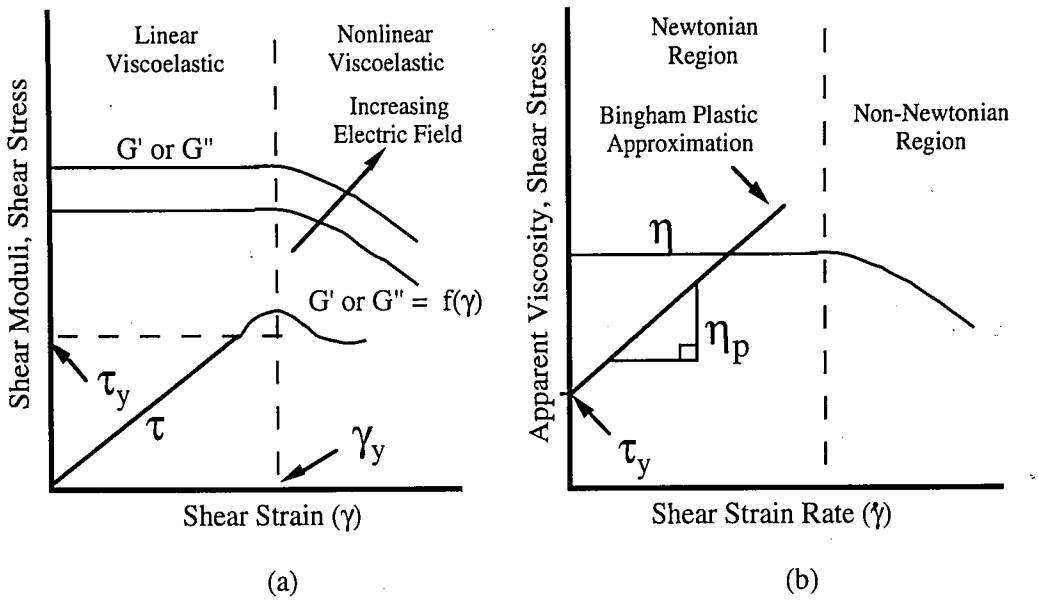

Figure 2.5 Dynamic behavior of viscoelastic materials. (a) Shear moduli and stress versus strain, and (b) apparent viscosity and Bingham Plastic approximation in the post-yield region.

The Bingham Plastic approximation previously described in Section 1.4 is often used to model ER materials under continuous shear for post-yield applications. The equation is listed again for convenience:

$$\tau = \tau_y + \eta_p \dot{\gamma} \tag{2.20}$$

As it is shown in Figure 2.5(b), the shear stress of ER materials after yielding consists of the dynamic yield stress (τ_y), and a component governed by the shear rate and the Bingham plastic viscosity (η_p), which is the slope of the line. $\dot{\gamma}$ is the applied shear rate. It should be noted that τ_y is a strong function of electric field and η_p is a weak function of electric field often assumed constant in the design of controllable devices.

Within the regime of linear viscoelasticity, the storage and loss moduli are of interest for the design and modeling of ER material based adaptive structures. These properties are well known in the literature to be a function of electric field strength,

temperature and excitation frequency. Though some research has been conducted on the influence of temperature on ER material behavior (Conrad et al., 1991), the primary concern of the present thesis research has been focused on the room-temperature behavior and properties of these materials.

2.4 State of the Art Review

The two primary areas of interest related to this thesis are electrorheology and ER adaptive structures. In the area of electrorheology, research efforts have been completed on many of the various aspects of ER materials such as material composition, mechanical properties, testing methodology, temperature effects, ER mechanism modeling, and shear strain dependence effects. A state of the art review of recent research work conducted in electrorheology is presented in Section 2.4.1. For the ER adaptive structures area, research interests may include vibration suppression, control and sensing, time response, and fluid reliability and durability. A state of the art review of ER rheology as related to ER adaptive structures is presented in Section 2.4.2.

2.4.1 Electrorheology

In Klass and Martinek's pioneering work (1967) on ER fluids, the rheological and electrical properties of ER fluids were investigated and presented. Their ER fluids were made of silica or calcium titanate suspended in a naphthenic carrier fluid. The authors investigated the rheological properties of the ER fluid using a couette, continuous shear (post-yield) apparatus that is capable of shear rates upwards of 5000 sec^{-1}. From their experiments, several important results were concluded: 1) Under zero field conditions, the suspension behaved as Newtonian fluid, but when subjected to an electric field, the ER material exhibited non-Newtonian, pseudoplastic behavior; 2) As electric field was increased, the electroviscous effect also increased; and 3) Electroviscosity was proportional to the square of the field strength. A brief explanation of the ER effect was also given by

the authors. The primary mechanism responsible for the effect was thought to be the induced polarization of the double layer surrounding the particles.

The temperature dependence of the electrical properties and strength of an zeolite particle/silicone oil ER fluid was investigated by Conrad et al. (1991). The authors used a mechanical testing machine to provide strains of up to 500 percent at a constant strain rate of 0.085 sec^{-1}. The temperature during testing ranged from 25-160°C. The authors defined yield stress as the stress at a predetermined strain and strain rate; more clearly, it is the region where stress does not change significantly with strain. An E^2 relationship was noticed for yield stress. The authors also provided data for the dielectric constant of the ER fluid as temperature was increased.

In Conrad and Sprecher's review paper (1991), rheology and electrical characteristics of typical ER fluids were reviewed. The authors emphasized that yield stress or flow stress is the shear stress at a given shear strain, strain rate, and temperature. The relationships between yield stress and electric field, material composition, and temperature were given. With regard to electrical properties, current density versus electric field relationship were given. Static and dynamic structures that occur within ER fluids were discussed. As electric field increased, the particles formed clusters and complete chains. Further increases in electric field strength increased the number of chains. Two theories for the ER effect were also discussed by the authors, namely, the Water Bridge Theory and the Point Dipole Theory (polarization of particles).

Among the particle size effects studies completed on ER materials is the recent paper by Coughlin and Capps (1994) on the steady shear properties. ER fluids consisted of synthetic silica particles in silicone oil were tested on a modified Brookfield viscometer with a couette attachment. The authors measured the ER effects using steady shear testing. ER material apparent viscosity and shear stress were recorded at varying shear rates and electric field strengths. For ER materials of varying primary particle size and composition, the results showed that the ER effect was dependent on particle sizes.

Attempts were made by Brooks (1993) to simplify equations used in the design of ER material based devices. The key areas of concern involving the ER devices were introduced as the off-state, the on-state, and the power requirement. The author summarized, for each of the areas, benefits, problems, and conditions for ER device design. Among the issues discussed were volume fraction, temperature, shear rate, and electric field. The summary of the paper introduced five equations reduced from volumes of ER material data. When these equations are used within the established limitations and within reason, the design process for common ER devices should be simplified.

Filisko and Radzilowski (1990) proposed a mechanism for an alumino-silicate/paraffin based ER fluid which does not require water. The preparation of this ER fluid utilized high temperature drying and thermal-vacuum mixing. The water content of the ER fluids was determined using infrared spectroscopy. Rheological measurements were performed using a modified Weissenberg rheogoniometer with a couette attachment. A series of post-yield tests were performed at a steady shear rate of 45 sec^{-1} and at room temperature. Apparent viscosity of the ER fluid was found to be strongly influenced by water content. From the results, the authors concluded that the morphology and the chemistry of the particles were responsible for the ER effect, since tests were performed in which the water content was undetectable.

Bullough et al. (1993) examined a couette type clutch for its performance with ER fluids of varying volume fraction. The ER fluid used was a mixture of silicone oil and fluorolube with lithium polymethacrylate particles. The particle volume fraction range in their tests varied from 20 to 40 percent. The authors found that in their tests, the volume fraction of the solid had little effect on the time-dependent properties of the ER fluid, although the shear stress did increase dramatically. Shear rates in their tests ranged from 0 to 19,000 sec^{-1}, and torque response was investigated for a temperature range of 15 to 50 °C.

Brooks et al. (1986) utilized shear wave propagation to investigate the viscoelastic properties of an ER fluid consisted of lithium polymethacrylate in chlorinated hydrocarbon oil. In this paper, results for G' and G" as a function of applied electric field (0-600 V/mm) at various volume fractions were given. All tests were conducted using a shear wave propagation frequency of 1200 rad/sec, or 190 Hertz. The results of their investigation showed that the viscoelastic properties G' and G" increased to a maximum at approximately 300 V/mm, then decreased as electric field was further increased. This finding is contradictory to the generally observed E^2 relationship. It should also be noted that the fluid used in this investigation was a commercial ER fluid supplied by Laser Engineering of London. Unlike ER researchers with materials engineering emphasis, the authors used the fluid as obtained, instead of making the fluids themselves from components.

The rheological behavior of ER materials was classified into three regimes by Gamota and Filisko (1991a): pre-yield, yield, and post-yield. They claimed that in the pre-yield region, the deformation of ER materials may be interpreted using linear viscoelastic theory, and that the loss and storage moduli can be calculated. In this regime, energy storage and dissipation properties are increased by the application of an electric field. They reported that in the yield region, the yield stress for ER materials is a function of field strength. Lastly, they concluded that for these ER materials, the yield regime is marked by continuous shearing at constant rates so that flow is initiated and maintained.

Gamota and Filisko (1991b) also studied the linear/nonlinear dynamic behavior of an alumino-silicate/paraffin oil ER material. The results were presented for tests in the 10-50 Hertz range. The authors identified that strain amplitude and electric field strength were key factors affecting ER fluid response. Furthermore, yield strain was found to be a function of frequency and field strength, and yield stress was determined to be an increasing function of electric field.

Gamota and Filisko (1991c) studied the high frequency (300-400 Hertz) dynamic response of an alumino-silicate/paraffin oil ER fluid. They identified the pre-yield region in their tests by using elliptical hysteresis loops, and then proceeded to give dynamic moduli and loss tangent as a function of electric field and frequency. In this room-temperature study, a couette setup was used on a modified Rheometrics Mechanical Spectrometer with a constant strain amplitude of 2.4%. The result of their tests indicated that the ER material behaved as a linear viscoelastic body when subjected to a zero electric field and sinusoidal shear strain. When electric field was increased, the shear modulus and the loss modulus both increased steadily. The authors also presented a rheological model for the ER material in the pre-yield region. Namely, a Zener model consisting of a spring in series with a Kelvin model. Using this model, they were able to predict the frequency dependence of the loss modulus at four different electric fields. In all cases, a maximum of the loss modulus was predicted within the frequency range of interest.

Jordan et al. (1992) investigated the small strain, dynamic behavior of commercial ER materials for field strength and strain dependence. The rheometer used in their tests was a Rheometrics Mechanical Spectrometer with both parallel-plate and couette geometries. The influence of electric field on volume fraction were presented in this study. The most important results presented, however, dealt with the dependence of dynamic moduli on strain. Specifically, they showed that the dynamic moduli was strain independent for up to 4%. The strain frequency for the presented linear behavior was low (ω = 1 rad/sec), however. It is interesting to note that the authors remarked on the system (rheometer) dependency of the magnitudes of G' and G". Nonlinear behavior was shown for the material for parallel-plate geometry at low frequency (ω = 0.159 rad/sec) and relatively high electric field strength (E = 2.5 kV/mm).

Yen and Achorn (1991) studied the dynamic behavior of an ER fluid consisted of a hydrated lithium salt of poly(methyl methacrylate) in chlorinated paraffin oil. Dynamic stresses as functions of strain were studied for various volume fractions and electric field

strengths. No strain dependence analysis for G' and G" was performed, but instead, the authors relied on the deviation of stress response from sinusoidal behavior for the determination of yielding.

Thurston and Gaertner (1991) presented additional testing on the viscoelastic nature of ER materials. A rectangular, oscillating channel flow device was utilized, and therefore the strain level experienced by the ER materials was high. In certain cases, the authors claimed that the ER materials stayed linear viscoelastic at strain levels in excess of 20%. The fluids used consisted of corn starch in mineral oil.

The electrorheology of silica suspensions in silicone oil was studied by Otsubo et al. (1992). In addition to examining the steady shear behavior of this ER fluid for varying volume fractions, the dynamic viscoelastic response was presented. Dynamic moduli were plotted against strain frequency for several strain amplitudes. However, the paper did not recognize the significance of establishing the dynamic yield strain and stress. The smallest strain amplitude (1%) utilized in the tests was an approximation obtained from material stress response similar to results described for Yen and Achorn (1991). If the actual behavior of the ER materials was indeed in the nonlinear region, the reported results are virtually meaningless. The realization of the limits of linear viscoelastic theory must precede any frequency-dependence investigation.

Mechanisms of electrorheology were reviewed briefly by Block et al. (1990), with a specific emphasis placed on mechanisms involving dispersion polarization. The authors tested acenequinone radical polymers (PAQRs) dispersed in silicone or partially chlorinated petroleum fractions for various concentrations. In addition to measuring dielectric properties and static yield stress of their ER fluid, they also measured the dynamic rheological properties using a commercial Carri-Med controlled-stress rheometer. The test geometry used was a couette-type cell. Post-yield testing in this paper ranged from a shear rate of 0-3000 sec^{-1}. Volume fraction ranged from 15 to 20 percent. Results were

presented for only two discrete electric fields of 1.5 and 2.0 kV/mm. Also reviewed were theories and hypothesis for the mechanisms of electrorheology.

In Coulter et al.'s review paper (1993a), a summary of the state of art ER materials applications was given. The paper reviewed the post-yield rheological behavior of ER materials, as well as the equations of pressure drop and force in fixed electrode and moving electrode configurations. Equations for ER material volume and electrical power requirements were also given. The paper then gave a review of present accomplishments in ER material based devices such as valves and shakers, engine mounts, clutches and brakes, dampers, and adaptive structures. The authors clearly identified that in order to tap into the potential ER devices market, further investigations are required to answer some fundamental questions regarding ER materials behavior.

2.4.2 ER material based adaptive structures

An advantage of using ER materials in structural vibration damping is fast response time. Tanaka et al. (1992) studied the stress response of a DC ER material due to step electric field and sinusoidal strain. The stress response to step electric field in their tests were found to be on the order of milliseconds. Hill and Van Steenkiste (1991), and Hill et al. (1992) examined the time response of an ER fluid composed of micron-sized glass spheres in silicone oil. They found that the response time varies exponentially with particle/fluid area ratio. The response time of these series of experiments spanned a range of three orders of magnitude (1-1000 milliseconds). From these results, it is clear that ER materials respond to external electric fields within seconds. These investigators also reported the tendency of particle/fluid separation for AC electric field excitation, particularly at low volume fractions.

Hosseini-Sianaki et al. (1992) investigated the response time of an ER fluid in a couette type rheometer. Their results indicated the response time was on the order of tens of milliseconds. Temperature and shear rate increases both contributed to the decrease of

time response. More importantly, increasing the voltage level shortened the response time. Though direct conclusions should not be drawn, higher voltage level (electric field) is expected to shorten time response of ER material based structures.

Several research groups (Gandhi and Thompson, 1990, 1989, 1988; Don 1993; Coulter et al. 1993b; Choi et al., 1992; Yalcintas et al., 1993; Yalcintas and Coulter, 1993; Ehrgott and Masri, 1992; Wereley, 1994) have recently investigated the response of ER material filled composite structures. Though Wereley (1994) concluded that stronger ER materials are needed for damping of high flexural rigidity helicopter rotor blades, significant structural damping was noticed by other researchers using less stiff elastic layers. The damping of vibration and increases in natural frequencies of the structures were found as a function of applied electric field. Control schemes were introduced (Han et al., 1994; Gong et al., 1993; Morishita and Ura, 1993; Flanders et al., 1994) which could minimize the vibration response of these structures over a broad frequency range. However, these control schemes assume instantaneous response, i.e. zero response time of the ER structures to on-off states in the electric field. The previously mentioned papers (Hill and Van Steenkiste, 1991; Hill et al., 1992) studied response time of ER fluids, not ER material based adaptive structures. In addition, there has been a lack of literature on the response time of ER fluids to the removal of electric field. For successful implementation of adaptive structures with sensing and control capabilities undergoing external excitation, it is necessary to study the response time due to both application and removal of electric fields. Particular attention must be focused on high frequency-low amplitude vibration where there is less motion.

It is well known that ER fluids, primarily suspensions, have a tendency to phase separate over extended time. In certain applications such as high speed centrifuges and clutches, phase separation, or the settling of the particulate in the oil, will cause a gradual deterioration in device performance. Other researchers (Johnson et al., 1993) in performing high speed clutch tests also concluded that with post-yield devices, separation

tests must be conducted under realistic conditions, not just with gravitational loading alone. Boyle (1992) tested a prototype ER shock absorber for fluid durability. Successful performance of an ER material under actual service conditions was proven. The particle/fluid separation issue was not explicitly mentioned, but viscosity, shear stress, and response time were found to be properties which could depend on device service life cycle. In any adaptive structures vibrating at low frequency, high amplitude or high kinetic energy motion could provide the agitation necessary to prevent particle/fluid separation. High frequency vibrations, however, will have low amplitude which may not prevent fluid/particle separation.

Energy dissipation is a significant factor in analyzing the small amplitude vibration response of ER material based adaptive structures. Gamota and Filisco (1991a, 1991b, 1991c) and Ehrgott and Masri (1992) utilized stress-strain hysterisis curves to investigate the rheology of ER materials. They found that energy dissipation in the fluids is an increasing function of strain amplitude, strain frequency, and electric field. In a composite beam containing a viscoelastic ER fluid layer, this means that the vibration response of the beam will depend on excitation frequency and amplitude, electric field, and location along the beam. It should be emphasized that the viscoelastic properties of the ER layer may be difficult to quantify since as the beam undergoes modal transitions, the displacement and shear varies along the structure and is mode dependent. In particular, since the viscoelastic properties of ER materials are strain amplitude dependent, the design and modeling of these structures must not assume a beam with constant properties, unless the shear strain is known to be in the linear viscoelastic range.

2.5 Chapter Summary—Specific Objectives of the Present Investigation

An objective of the adaptive structures research group at Lehigh University is to further the understanding of the rheology of ER materials subjected to small dynamic strains. Specifically, the investigations performed were targeted in the commonly referenced pre-yield region. The design and modeling of ER adaptive structures need the rheological properties of the ER materials. Furthermore, essential information is needed in how the rheology of these materials affect the controllability and reliability of ER adaptive structures.

The specific objectives of this thesis research are thus summarized:

- Determine the linearity of the available commercial ER materials at small strains (0.1%-10%) using a commercial rheometer. Specifically, determine the yield strain below which the material behaves in a linear viscoelastic fashion.
- Determine the effect of strain frequency and electric field on the viscoelasticity of the ER materials.
- Ascertain the effect of time on the reliability of ER material based adaptive structures. Reliability in this case is defined in terms of modal frequency and damping loss factor repeatability over time.
- Investigate the controllability (in terms of time response) of ER adaptive structures due to the application and removal of electric field.
- Determine the overall influence of electrorheology on the vibration frequency response of ER material based adaptive structures.

CHAPTER 3: DYNAMIC MECHANICAL ANALYSIS

3.1 Introduction

The dynamic testing of various engineering materials will enable the engineer or the scientist to know about the materials' behavior under oscillating loading conditions. A common test of this nature when performed on elastic materials is the fatigue test, where the material is loaded under dynamic, compression-tension cycles. The primary purpose of this test is, of course, to determine how the mechanical properties and therefore service life of the material is affected as a function of dynamic load cycles. While tests of this nature are not usually performed on Newtonian materials, the results, when analyzed as special cases in viscoelastic theory, will yield material viscosity.

When dynamic testing is performed on a viscoelastic material, much more information will be obtained than in the elastic and viscous cases due to the nature of the material. Within the linear region, an ideal elastic material deforms immediately under stress, and recovers instantly upon the removal of stress. An ideal viscous material deforms continuously under stress but does not recover upon the removal of stress. Viscoelastic materials combine both of these behaviors—showing time-dependent, but incomplete recovery. Thus, the interpretation of the dynamic testing results of viscoelastic materials requires the equations of viscoelasticity.

Among the equations of linear viscoelasticity introduced in Section 2.2, that which is of primary interest to the present research is the complex shear modulus, G^*. Written in complex notation:

$$G^* = G' + i\,G'' \tag{3.1}$$

and consists of the storage modulus, G', and loss modulus, G". As stated in Chapter 2,

$$G' = G^* \cos \phi \tag{3.2}$$

and

$$G'' = G^* \sin \phi \tag{3.3}$$

where ϕ is the phase angle.

The above equations were discussed in length in Section 2.2. The emphasis here is upon the notion that G' represents the ability of the viscoelastic material to store the energy of deformation, and G" represents the ability of the material to dissipate the energy of deformation as heat. The phase angle is an indication of whether the material is more solid-like, or liquid-like.

Many commercial rheometers are available to find the viscoelastic properties of a variety of materials such as polymers, melts, liquids, solids, and emulsions. While most rheometers are designed for testing the viscoelastic properties of materials at frequency ranges below 20 Hertz, the use of the time-temperature superposition principle (Sperling, 1992) allows the experimenter to find the properties at much higher or lower frequencies.

Depending on the physical form of the sample material, e.g. solid, liquid, or pastes, several testing geometries may be utilized in stress/strain rheometers. Regardless of the geometry utilized and the form of the sample, however, oscillatory loading is imposed on the sample and the corresponding force response is recorded as a function of time. These dynamic stress-strain responses are monitored as a function of frequency (temperature), and in the case of ER materials: electric field intensity. Much useful information is provided when these dynamic stress-strain responses are presented in terms of G^*, G', G", and $\tan \delta$.

Abundant applications of dynamic mechanical analysis exist. In the field of polymer science and engineering, dynamic testing allows the researcher to evaluate miscibility in polymer blends. Through this method, the service temperature of the polymers could be determined, as well as the detection of the onset of molecular motion. Lastly, the utilization of dynamic mechanical analysis allows the characterization of

viscoelastic behavior, thereby permitting the researcher to determine the applicability of a material for vibration damping.

3.2 Significance of Yield Strain Related to ER Material Based Adaptive Structures

The equations of linear viscoelasticity introduced in Section 2.2 are relevant in analyzing the small amplitude vibration of ER material based structures. When applied to viscoelastic materials, these equations become a powerful tool for the characterization of material behavior and properties. However, as discussed previously, these equations are valid within the bound established by the yield strain, γ_y. For a viscoelastic material, the dynamic moduli as a function of strain frequency and temperature are described by these equations. Outside of γ_y, the dynamic properties are no longer simple functions of stress, and the material is said to exhibit nonlinear behavior. More sophisticated techniques are needed for the analysis of nonlinear behavior.

When an elastic or an ER composite beam undergoes transverse vibration, strain amplitude is a function of location along the structure, as shown in Figure 3.1. As this structure undergoes modal transition, the strain amplitude continues to change according to the mode shapes and location along the longitudinal axis. It was anticipated that the ER material contained in the composite beam under sinusoidal, small strains will be in the linear range. In the modeling of these structures, therefore, the controllable dynamic moduli of the ER fluid layer will be influenced by excitation frequency, temperature, and of course, electric field strength.

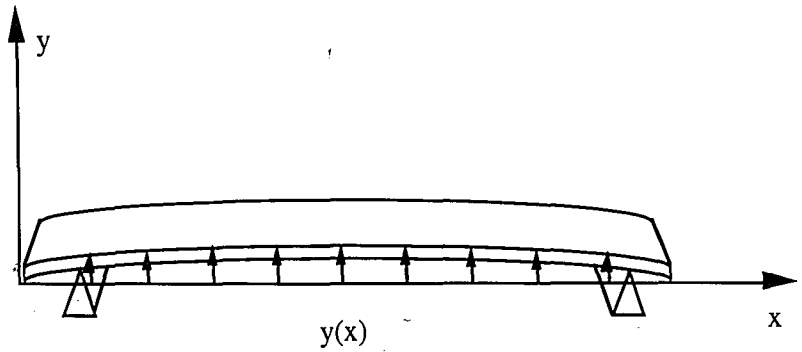

Figure 3.1 Strain variation of a simply-supported beam under transverse vibration.

When the ER adaptive structures are under high frequency-low amplitude vibration, the ER material may be in the linear range since strain will be small everywhere along the beam. But discretion is needed in the modeling of ER adaptive structures under low frequency-high amplitude vibration since strain is large under these conditions. If the strain is large enough to exceed γ_y, the behavior of the ER material layer will be nonlinear; its dynamic properties could not be described by linear equations. In this case, the assumption of a damping layer with uniform rheological properties would be erroneous.

The design and modeling of an ER adaptive beam with a nonuniform damping layer would be a challenging task. But should linear viscoelastic behavior be observed for the ER materials, especially if γ_y is found to be relatively high (1-10%), then the modeling task at hand would be significantly simplified.

The fundamental understanding of the vibrational behavior of ER material based structures starts from the knowledge of whether or not the ER materials behave linearly. Ultimately, ER rheology governs the dynamic behavior of these structures.

3.3 Experimental Apparatus and Procedures

Rheological experiments were conducted on a Rheometrics RDA II rheometer equipped with an ER testing option. Several geometries are available for the testing of various materials, e.g. couette cup and bob, cone and plate, parallel plate, and rectangular

torsion. The utilization of various geometries allows the experimenter to test solids, liquids, melts, and pastes.

Since the present objectives included the determination of yield strain for ER materials, strain-sweep tests were needed. Prior to the actual testing of ER materials, testing of other materials was performed. Poly(dimethyl siloxane), or PDMS, is a linear viscoelastic material used by Rheometrics Inc. for the calibration of its rheometers. S-8000 oil is a viscous material standard manufactured by The Cannon Instrument Company for the calibration of viscometers and rheometers. Strain sweeps were performed on both of these materials to verify that PDMS and S-8000 oil were indeed linear viscoelastic and viscous, respectively, and that the rheometer was functioning properly.

The testing of PDMS utilized the parallel-plate geometry with a diameter of 25 mm. After pre-heating the parallel plates to 30°C, the sample was placed between the plates. The sample was trimmed and the plates were brought together so that a 2.0 mm-thick sample was formed. At the completion of sample loading and trimming, the PDMS had a bowed appearance at the plate edges. Upon completion of preparatory procedures, the control computer provided motor input which produced strain, and the resultant output torque was fed back to the computer—where the raw data was processed and analyzed. The strain range investigated was from 0.1 to 100 percent. The parallel-plate geometry and the instrumentation utilized are shown in Figure 3.2.

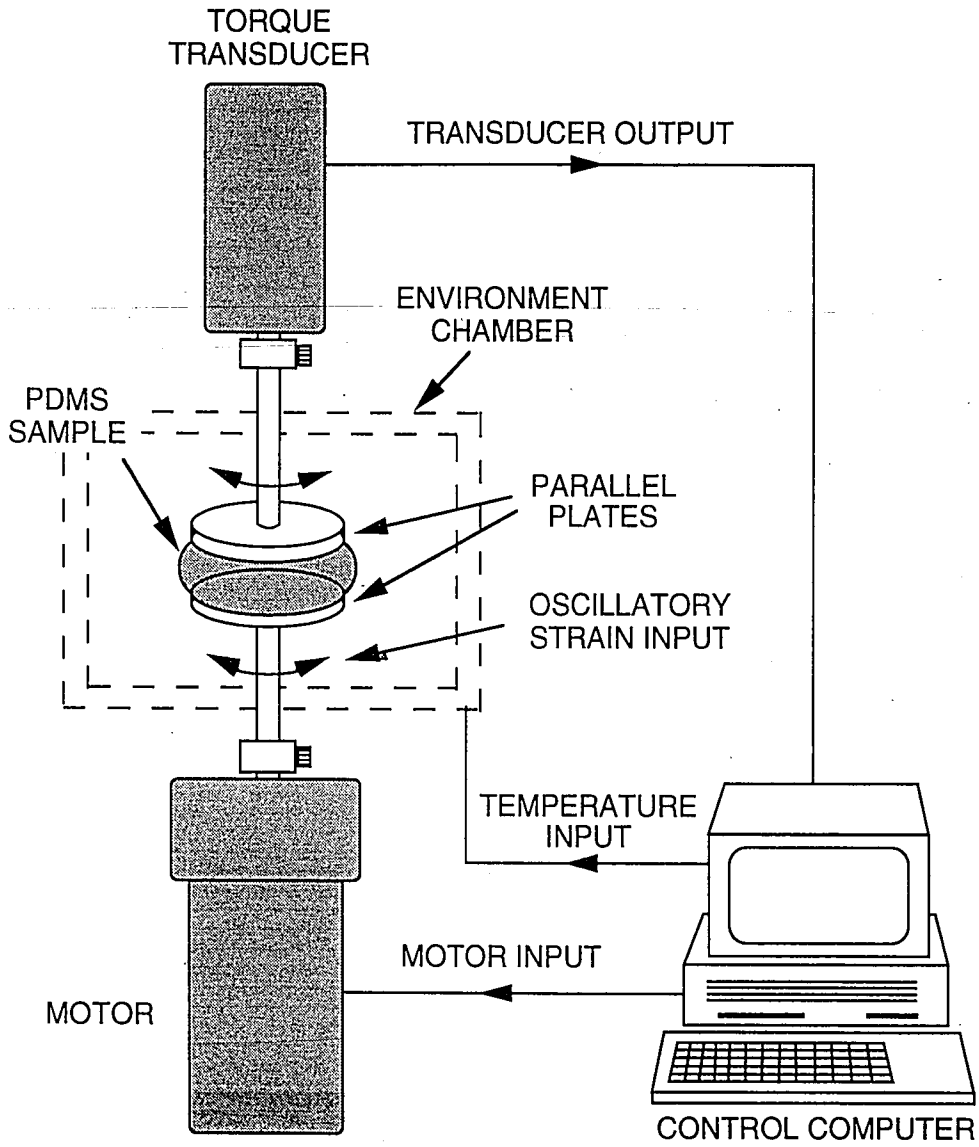

Figure 3.2 Schematic diagram of the Rheometrics RDA II Dynamic Analyzer with parallel-plate geometry.

The instrumentation schematic used for ER materials testing is shown in Figure 3.3. The objective was to first perform strain sweeps to find γ_y of the ER materials at discrete values of electric field. Following this, a secondary objective was to perform testing at strain levels below γ_y and obtain the storage and loss moduli for strain frequencies of interest, e.g. 10, 15 Hertz. When shearing the ER materials, care was taken

to choose the rheometer testing geometry which will provide both uniform electric field and uniform shear rate throughout the sample. Unlike parallel plate and cone and plate geometries, the shear rate and electric field in the couette geometry is everywhere uniform, therefore it was used in the present experiment. The ER materials, after mixing and desiccation, were placed in the couette cup. The diameter and length of the couette bob were 25 mm and 32 mm, respectively, and the inner diameter of the couette cup was 27 mm. A sample thickness of 1 mm was formed. Since the yield strain of the ER materials is expected to be low (Don, 1993; Jordan et al., 1992), strain sweeps were performed from approximately 0.1 to 10 percent.

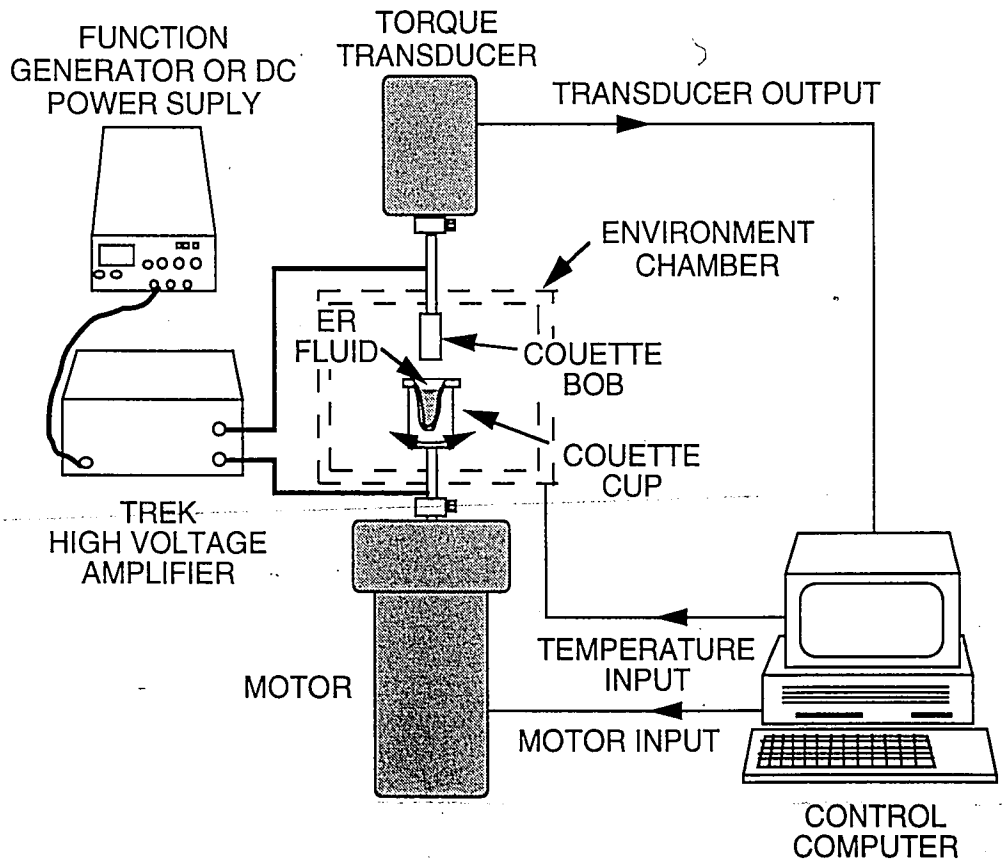

Figure 3.3 Schematic diagram of the Rheometrics RDA II Dynamic Analyzer with ER testing option.

Strain sweeps of S-8000 oil were performed using the couette cup and bob geometry previously described. The strain range investigated for this highly viscous material was from approximately 1 to 100 percent. The instrumentation used was identical to that shown in Figure 3.3, except the high voltage amplifier remained disconnected.

3.4 Results and Discussion

The results of the rheological experiments performed are presented in the subsequent sections. First, the results of strain sweeps performed for the S-8000 oil is presented in Section 3.4.1. In Section 3.4.2, the strain sweeps for the PDMS is presented and analyzed. In Sections 3.4.3 and 3.4.4, the results of strain sweeps (linearity analysis) for the AC, and for the DC ER materials are presented, respectively.

3.4.1 Newtonian material

From Figure 3.4(a), it may be observed that the S-8000 oil is indeed a highly viscous material. The G' values were less than one Pa (actual average value was 0.53 Pa) and exhibited a decreasing trend as strain was increased. G" values on the other hand, were high and remained constant as strain was increased. The average loss modulus for the strain range investigated was 160 Pa. In Figure 3.4(b), it may be observed that the phase angle was approximately 90 degrees (actual average value was 89.8 degrees), and is strain invariant. As previously discussed, all real-world materials will exhibit elastic and viscous responses. The phase angle of 0 degrees for the elastic material, and 90 degrees for the viscous material are only ideal cases, as demonstrated presently.

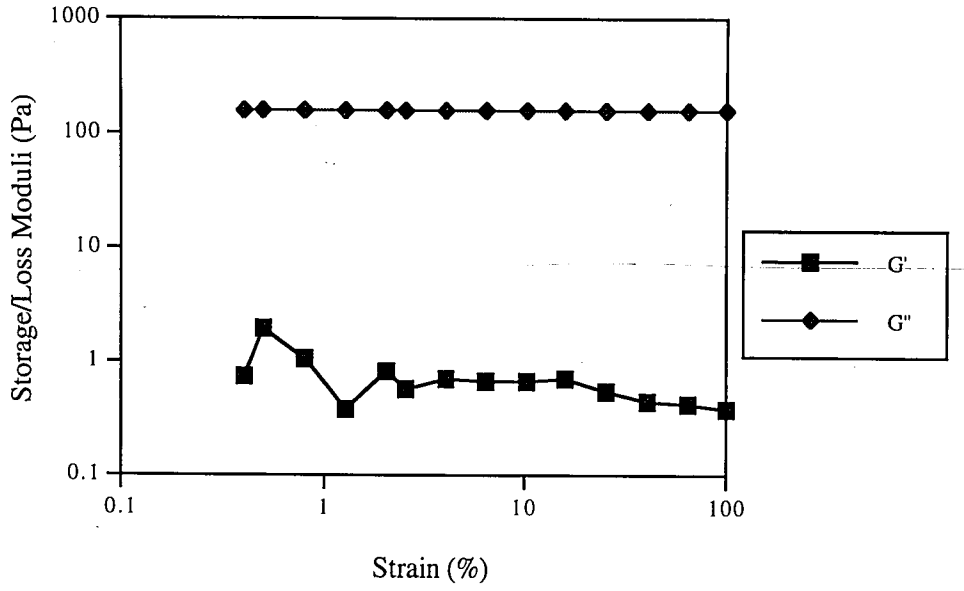

(a)

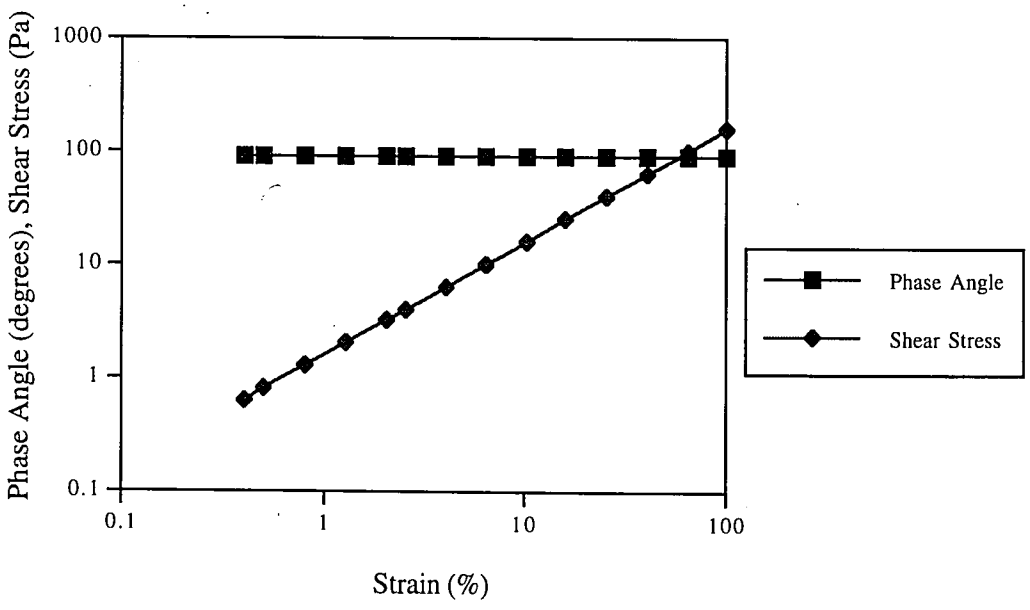

(b)

Figure 3.4 Strain sweep of S-8000 Newtonian oil for strain frequency of 1 Hertz and temperature of 24°C. (a) Storage and loss moduli versus strain, and (b) phase angle and shear stress versus strain.

The dynamic shear stress versus shear strain for the S-8000 oil is also shown in Figure 3.4(b). As may be observed from the figure, the shear stress exhibited a continued linear increase up to 100 percent strain, with no indication of yielding. Since this is a highly viscous material, yielding does not apply in the same sense as a viscoelastic material. Rather, through complex viscosity relationships (Sperling, 1992), it may be shown that for low, fixed frequency tests, e.g. one Hertz, the dynamic shear stress versus shear strain curve is comparable to a stress versus shear rate curve such as those described in Section 2.2. Comparing the Newtonian curve of Figure 2.3 with the shear stress curve of Figure 3.4(b), it may be concluded that the S-8000 oil closely approximates ideal Newtonian behavior, and under the strain range investigated, does not deviate from it. The utilization of the RDA II as a viscometer was thus established.

3.4.2 Linear viscoelastic material

The results of PDMS rheological studies are presented in Figures 3.5 and 3.6. In these Figures, the rheological properties (G', G", or ϕ) as a function of strain are plotted for five discrete excitation frequencies (0.1, 1, 5, 10, and 16 Hertz). The objective was to show the linear viscoelastic behavior of the PDMS by examining the effects of strain and frequency on rheological properties of interest.

Observe that in Figures 3.5(a) and (b), both the storage and loss moduli exhibited linear viscoelastic behavior. That is, both G' and G" remained strain invariant up to some critical yield strain. The G' data started to deviate from a linear relationship at approximately 24% strain. Likewise, the yield strain determined from G" was consistently observed at approximately 27%. Also, from these two Figures, the rheological properties of the PDMS can be clearly observed to be a function of frequency. As excitation frequency was increased, both storage and loss moduli exhibited an increasing trend. However, the relationship between the dynamic properties and frequency should be investigated separately using a frequency sweep.

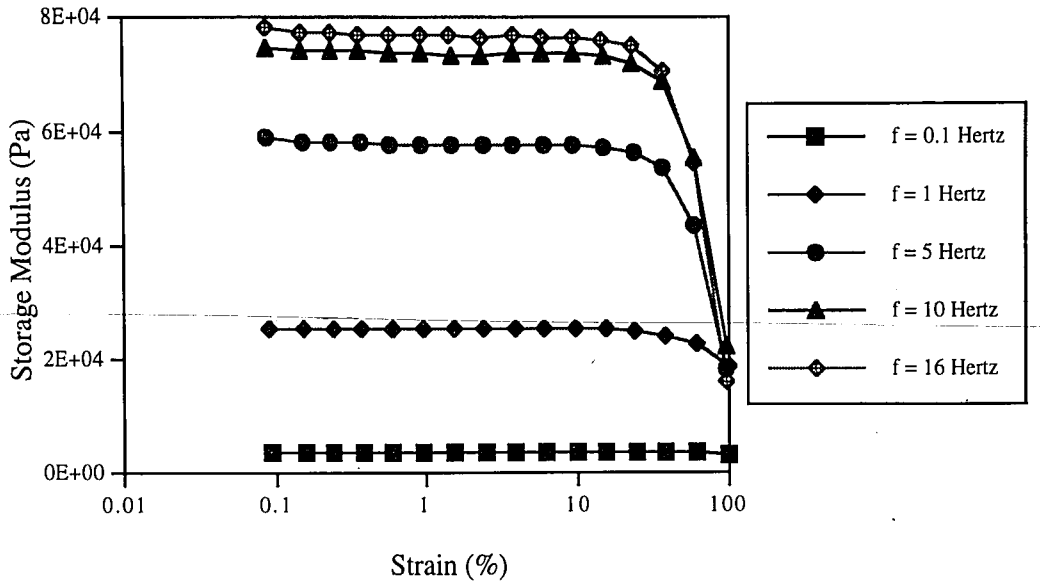

(a)

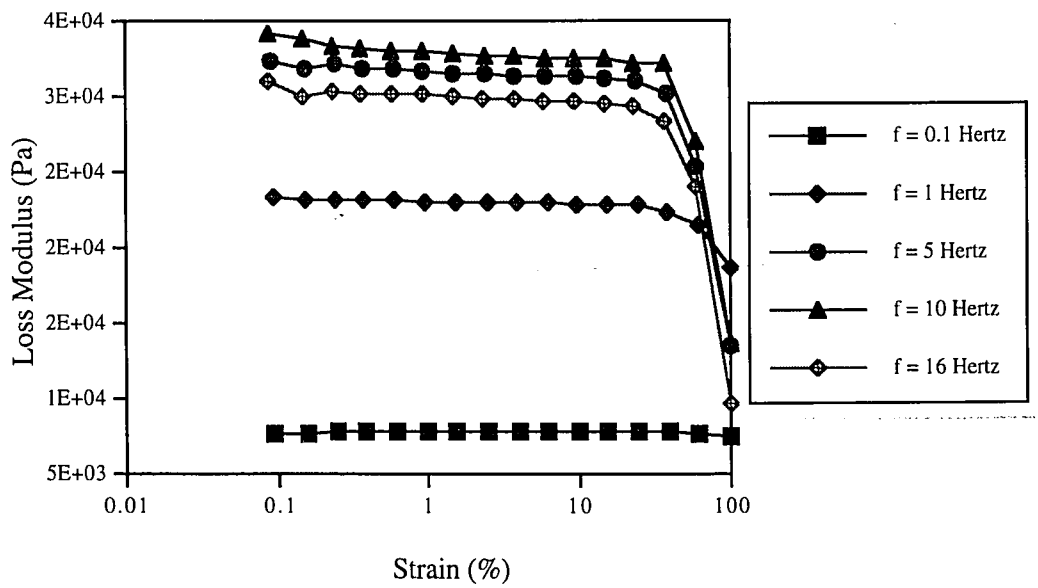

(b)

Figure 3.5 Strain sweep of PDMS at 30°C. (a) Storage modulus and (b) loss modulus.

In Figure 3.6(a), the phase angle as a function of strain and frequency is shown. The material is viscoelastic ($0° < \phi < 90°$). For low frequencies (0.1 and 1 Hertz), ϕ remained relatively strain invariant, the material did not become more viscous nor more elastic at higher strains. However, at frequencies of 5 Hertz and above, the phase angle started to increase towards 90 degrees at a strain of 38%—which was an indication of the onset of molecular motion, i.e. the material had become more viscous. The general downward shift of the phase angle indicated that at high frequencies, the material had become more elastic. In other words, as the material was being sheared at faster rates, the polymer chains did not have time to start the yielding, or flow process. Therefore, overall the material was shown to have become more solid-like at higher excitation frequencies.

In addition to being an increasing function of frequency, it can be observed from Figure 3.6(b) that the shear stress of PDMS started to show yielding at approximately 60% strain. This did not correspond well with the storage and loss moduli's deviation from linear relationships at 24% and 27% strain, respectively. The interpretation of this is that shear stress is not as reliable as the dynamic moduli in determining the linearity of the viscoelastic materials; a more detailed explanation follows in Section 3.4.4. The combination of yielding shown by the shear stress and the strain dependence of dynamic moduli are indicative of the material's transition from linear viscoelastic to nonlinear viscoelastic behavior.

It should be emphasized that the linear behavior exhibited by the PDMS is an exception rather than the rule. Also, the simple linear relationships shown in Figures 3.5 and 3.6 should not be expected without research for other materials such as polymers, emulsions, and colloids. However, through the course of this thesis research, rheological experiments were conducted on Prell Shampoo—an emulsion—which also exhibited linear viscoelastic behavior comparable to that of the PDMS. Though technically not a material standard, Prell Shampoo is used by PenKem, Inc. of Bedford Hills, New York, for calibration of its rheometers.

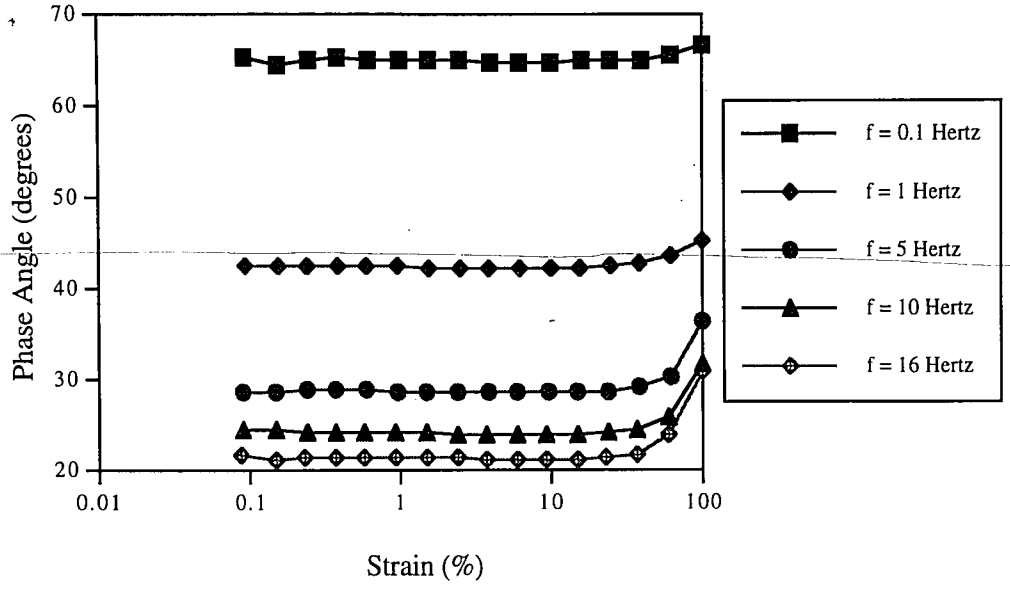

(a)

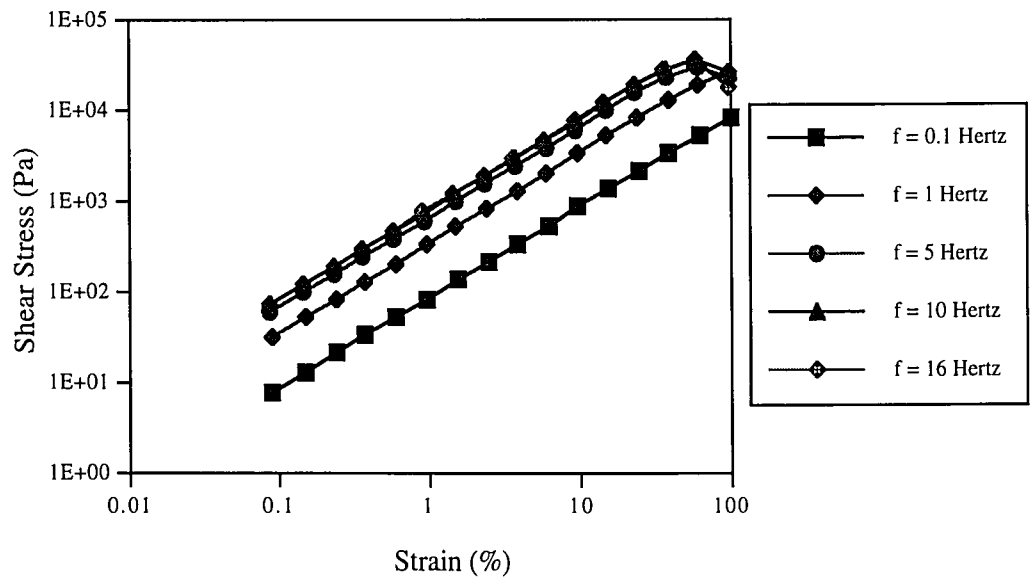

(b)

Figure 3.6 Strain sweep of PDMS at 30°C. (a) Phase angle and (b) shear stress.

3.4.3 AC ER material

Strain sweeps were performed on the AC ER material at small strain levels to find the yield strain, or the limit of validity of linear viscoelastic theory. Though experimental work was conducted for several electric field intensities, an emphasis was focused on a relatively high field level of 3 kV(rms)/mm. This was because the ER effect was strongest at this electric field level. For an applied electric field of 3 kV(rms)/mm, results are presented for 1, 5, 10, and 16 Hertz in Figures 3.7 and 3.8. If the material is linear viscoelastic, it is likely that it will be so at lower frequencies, similar to the results (Figure 3.5(a) and (b)) presented for PDMS. Since high excitation frequency did affect viscoelastic properties, it was anticipated that the testing of ER materials in the low frequency range (1-5 Hertz) would reveal linear behavior.

From Figure 3.7(a) and (b), it can be observed that, unlike PDMS, the behavior of ER-200 is clearly nonlinear, i.e. G' and G" are strain dependent. Therefore, the yield strain—if it exists for the material—is less than 0.1 %. Observe that even at 5 Hertz and 1 Hertz, the material is still nonlinear. Since the material is nonlinear, the linear viscoelastic equations may not be used. It becomes necessary to differentiate linear properties from their nonlinear counterpart. The nonlinear storage modulus will therefore be referred to as G_n'; the nonlinear loss modulus will be designated as G_n''; the total complex nonlinear shear modulus will be defined as G_n^*.

Also it can be observed from Figure 3.7(a) and (b) that at 0.1% strain, G_n' and G_n'' values were approximately equal. As the strain level was increased, however, the relative contributions of G_n' and G_n'' in the total G_n^* differed. Specifically, G_n'' was found to be larger than G_n' at a strain level of near 10%. This of course means that if this ER material is utilized for damping, its overall damping capability changes with the magnitude of applied shear strain.

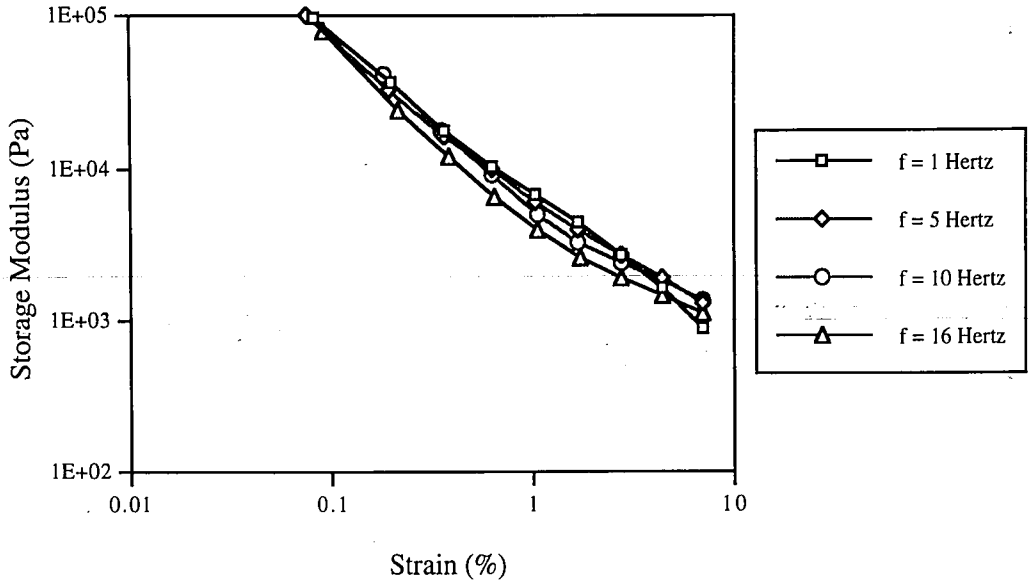

(a)

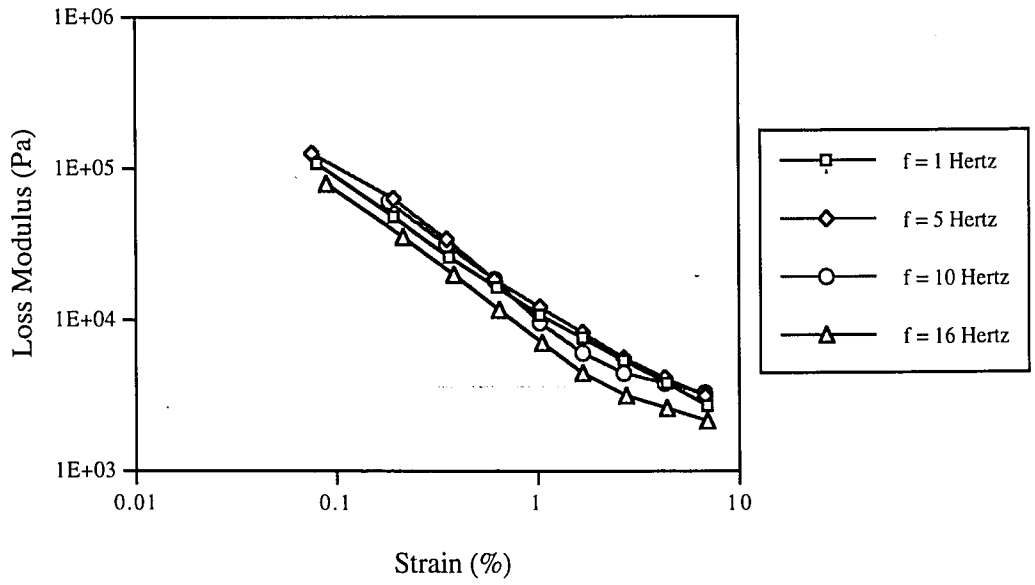

(b)

Figure 3.7 Strain sweep of ER-200 for electric field of 3 kV(rms)/mm. (a) Storage modulus and (b) loss modulus.

The viscoelastic nature of the ER-200 may be clearly observed from Figure 3.8(a), in which the phase angle is plotted as a function of strain amplitude. Unlike the viscous S-8000 oil, which has a phase angle of nearly 90 degrees and is strain invariant, the phase angle for the ER-200 varies with strain. The viscous nature of this material in the strain range investigated is evident from the predominantly high phase angle values, i.e. >45 degrees as strain amplitude is continually increased. While the effect of frequency on the degree of viscoelasticity (in terms of ϕ) could not be clearly established from Figure 3.8(a), it could be seen from this Figure that the phase angle reached a plateau of approximately 60 degrees at 1% strain. Further increases in strain induced flow-like behavior in the material as seen from the data trend towards 90 degrees. This plateau of the phase angle and the lack of a trend with frequency modification support the nonlinear results of Figures 3.7(a)-(b). Similar unclear frequency dependency of shear stress was also observed, as shown in Figure 3.8(b). In summary, none of the results for the AC ER material indicated yielding similar in nature to that of Figure 3.6(b) for the PDMS.

It was anticipated that at an electric field level of 3 kV(rms)/mm and at low frequencies of 1 and 5 Hertz the ER material would exhibit linear behavior. Since this was found to be untrue and the behavior at all frequencies investigated was nonlinear, the subsequent determination of the rheological properties as a function of electric field was only performed for a frequency of one Hertz.

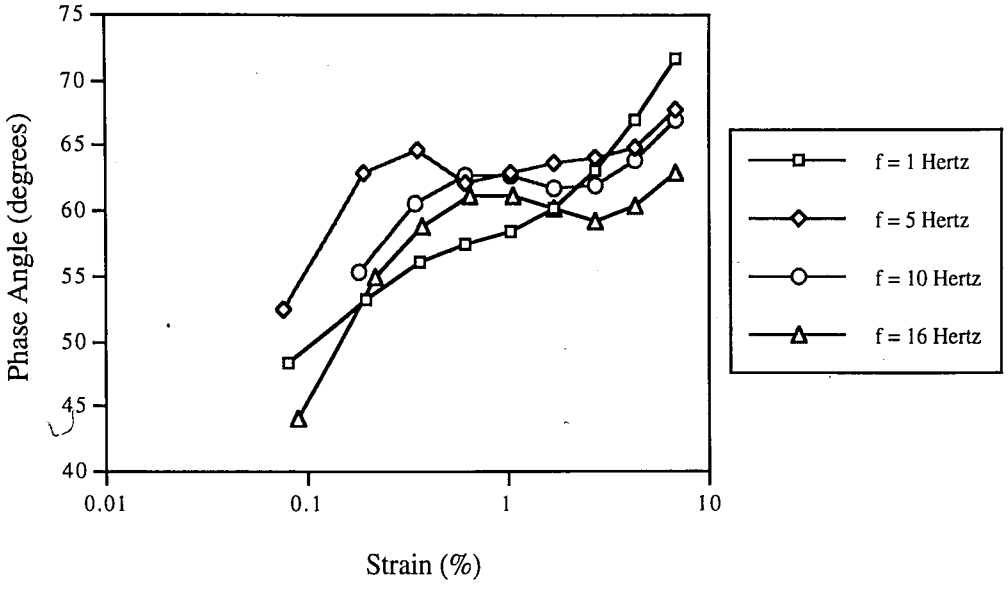

(a)

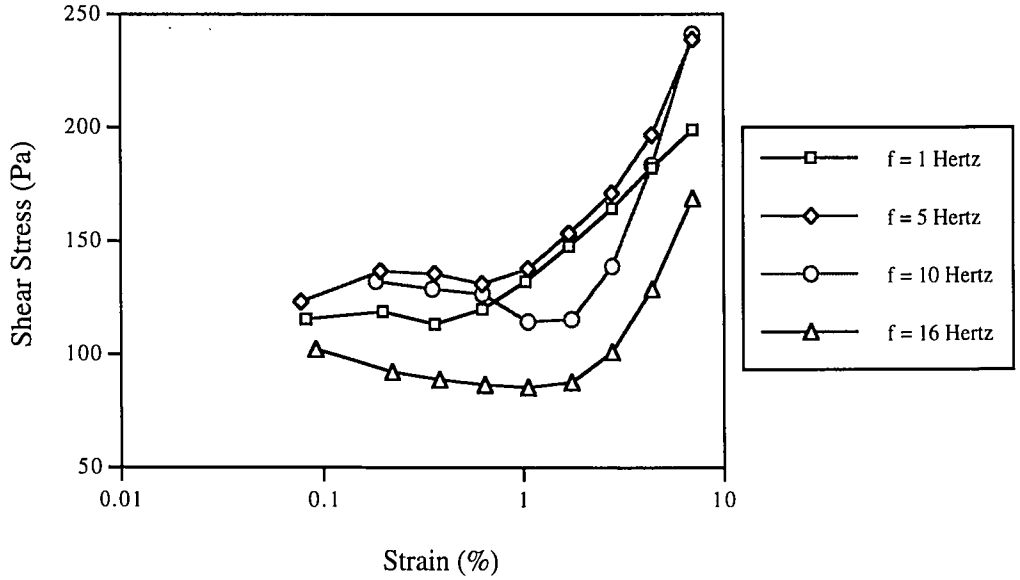

(b)

Figure 3.8 Strain sweep of ER-200 for electric field of 3 kV(rms)/mm. (a) Phase angle and (b) shear stress.

The resultant observed nonlinear storage and loss moduli are presented in Figure 3.9(a) and (b). It can be seen that both the nonlinear storage and loss moduli were found to be highly dependent on the strength of the electric field. For example, in Figure 3.9(a), in the absence of electric field and at 0.1% strain, G_n' was found to be 320 Pa; while for approximately the same strain amplitude and an electric field of 3 kV(rms)/mm, G_n' was found to be 95,000 Pa.

Likewise, for the nonlinear loss modulus at a strain level of about 0.1%, the G_n'' value was 610 Pa at zero electric field, and was 107,000 Pa for an electric field of 3 KV(rms)/mm. Such pronounced differences in rheological properties as electric field is intensified exemplify the uniqueness of this class of materials. Unfortunately, at the same time the nonlinear behavior of these materials poses new challenges in understanding the material mechanical properties as a function of frequency and electric field strength.

As discussed previously, the phase angle is useful since it relates to the degree of material viscoelasticity. The viscoelastic nature of ER-200 is shown in Figure 3.10(a). The general data trend exhibited is that the phase angle decreased at higher electric field levels, i.e. the material became slightly more elastic. As strain amplitude increased, however, the phase angle approached 90 degrees. In addition, it should be noted that at a strain level of about 0.1 %, the minimum phase angle was still above 40 degrees. This again suggests that this ER material is primarily viscous in nature, as supported by a comparison of the relative magnitudes of G_n' and G_n'' (Figure 3.9(a) and (b)).

An examination of the shear stress in Figure 3.10(b) does not reveal much new information. One sees that shear stress increased as electric field was strengthened due to the increased ER material complex moduli. The shear stress data showed no yielding, which supports the findings concluded from the phase angle results.

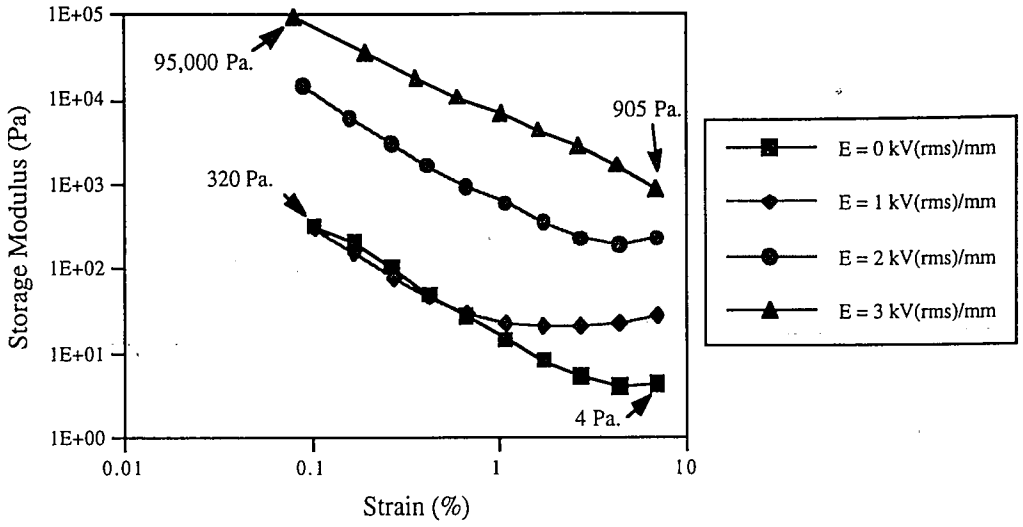

(a)

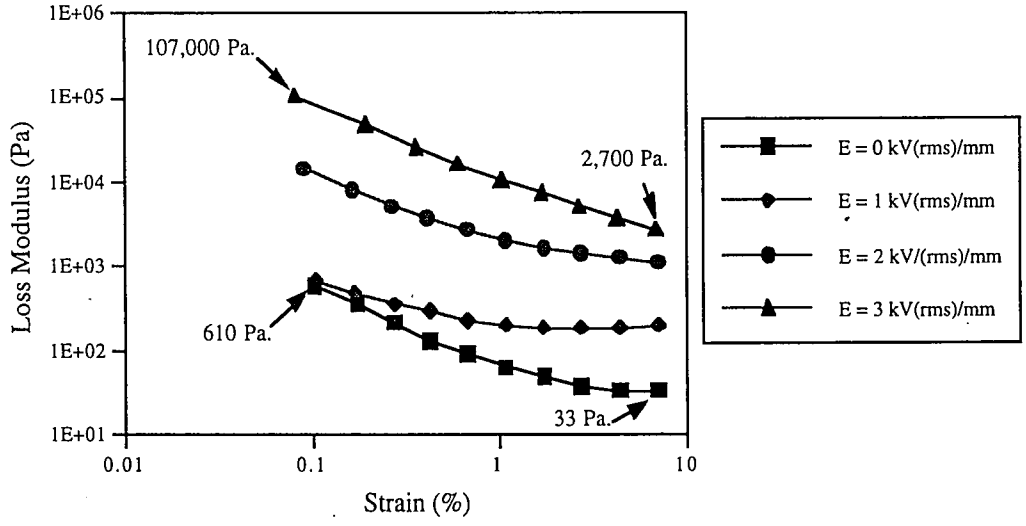

(b)

Figure 3.9 Strain sweep of ER-200 for strain frequency of 1 Hertz. (a) Storage modulus and (b) loss modulus.

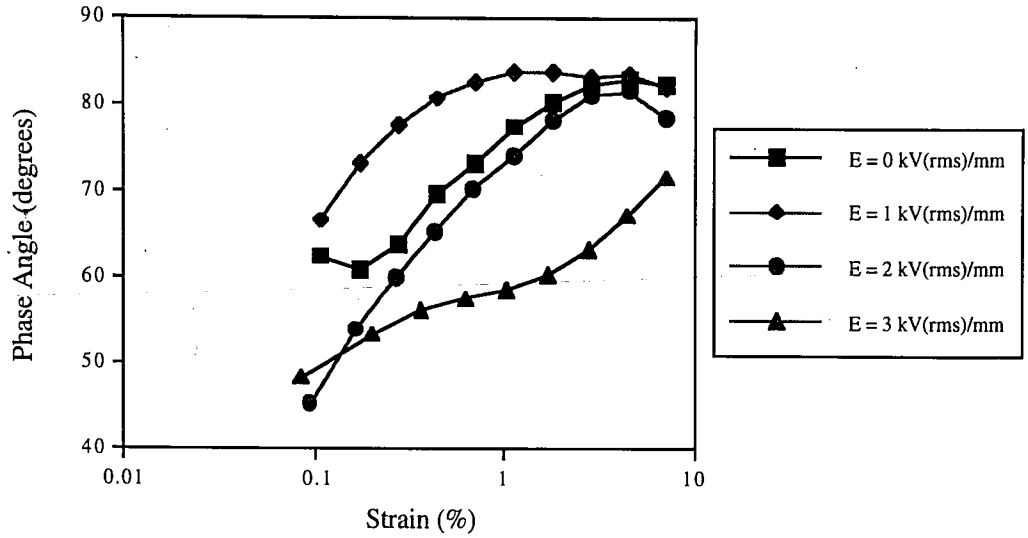

(a)

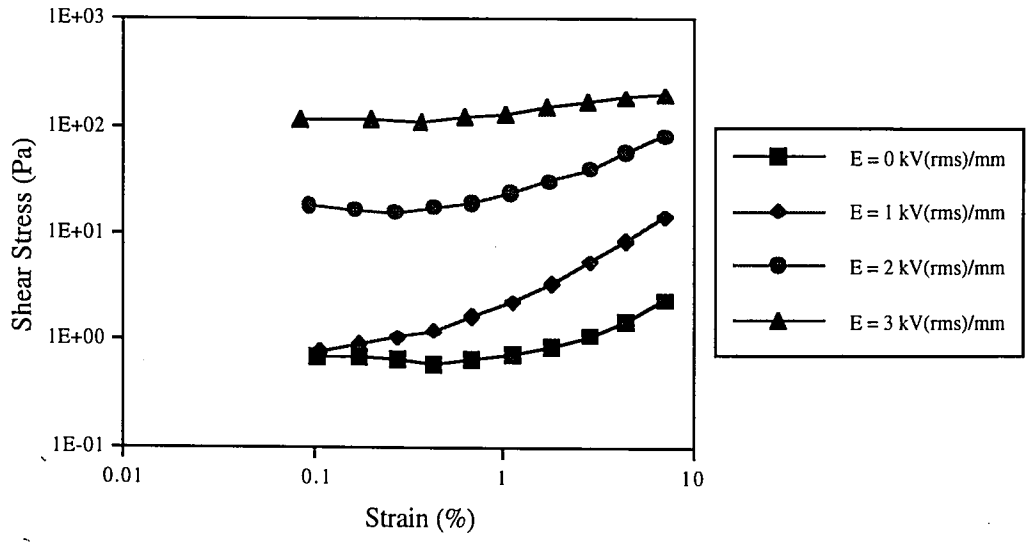

(b)

Figure 3.10 Strain sweep of ER-200 for strain frequency of 1 Hertz. (a) Phase angle and (b) shear stress.

In summary, the rheological behavior and properties of the AC ER material were found. The small strain behavior was found to be nonlinear viscoelastic, i.e. strain dependent, even at low excitation frequency and high electric field strength. For this material, the rheological properties (G_n', G_n'', and ϕ) are indeed functions of strain frequency. It was also shown that these rheological properties are strongly influenced by electric field intensity; as much as three decades of differences in magnitude were observed for this material between the zero and high-intensity electric fields.

3.4.4 DC ER material

For the DC ER material, essentially the same linearity analysis was performed. Namely, at a high electric field setting (3 kV/mm), strain sweeps were performed at four strain frequencies (1, 5, 10, 16 Hertz). Then the tests were repeated, but strain frequency was held constant at 1 Hertz, and electric field intensity was varied. It should be noted that although the previous AC electric field level mentioned in Section 3.4.3 may have the same numerical value as that of DC fields, e.g. 3 kV(rms)/mm versus 3 kV/mm, the two fields are not equivalent. In AC electric fields, the voltage varies with time in a sinusoidal fashion, whereas in the DC field case, an offset and time-invariant voltage is applied. Since the instrumentation was designed to give AC field readings in root-mean-square (rms) values, all AC fields utilized in this thesis research were referred to in terms of root-mean-square values. Of course, an AC field of 3 kV(rms)/mm does not equal a DC field of 3 kV/mm, but electric field levels of these intensities are considered quite high for the respective ER materials. Therefore, the comparisons of rheological properties between AC and DC electric fields are qualitative in nature.

In Figure 3.11(a) and (b), the nonlinear behavior for both the storage and loss moduli of the DC material is presented. All measured quantities, therefore, are more precisely known as G_n' and G_n''. As with the ER-200, even at a low strain frequency of 1 Hertz and high electric field of 3 kV/mm, the material still behaved non-linearly.

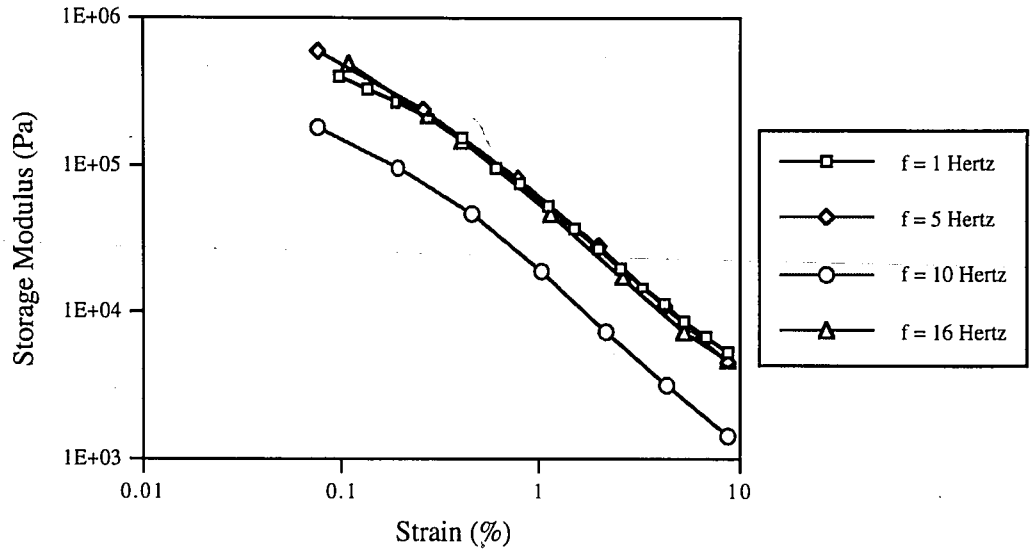

(a)

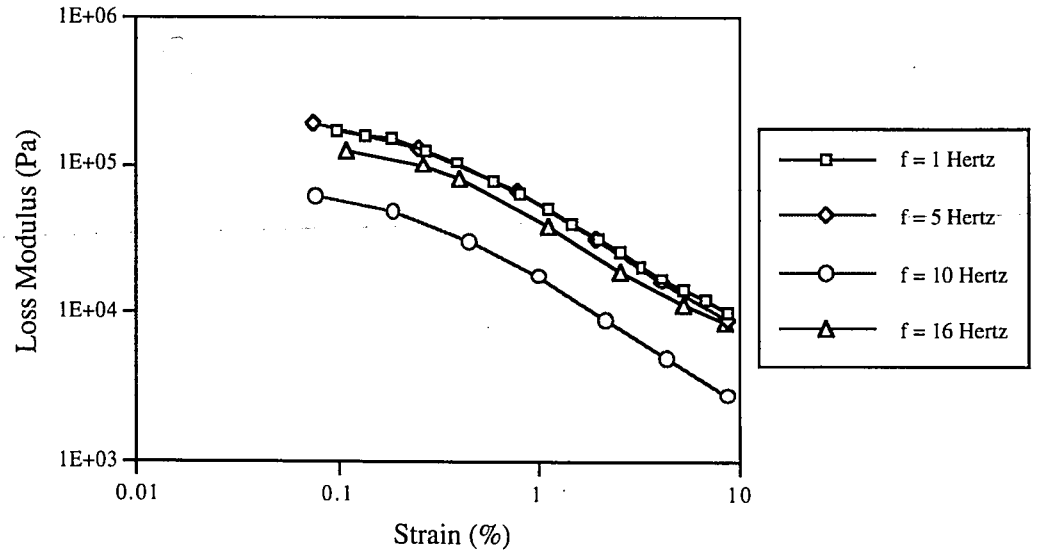

(b)

Figure 3.11 Strain sweep of ER-III for electric field of 3 kV/mm. (a) Storage modulus and (b) loss modulus.

Excluding the aberrant 10 Hertz results, a comparison of Figures 3.11(a) and (b) with Figures 3.7(a) and (b) yields the following observation: In the frequency range investigated, the DC rheological properties are less frequency dependent than those of the AC material. This may be seen from the smaller data spread over the frequency range investigated. It should be understood that the frequency range tested was considered low and narrow, and in order to further investigate $G_n^{'}$ and $G_n^{''}$ dependence on frequency, the upper limit of frequency (16 Hertz) should be increased. Should the DC material properties be found to be frequency independent, the design and implementation of DC ER adaptive structures would be made considerably easier. But most likely, the results are simply identifying the limitations of the present setup to test for frequency dependence of ER-III.

From Figures 3.12(a) and 3.8(a), profound differences between and DC and AC ER materials can be noticed. For comparatively high electric fields, much more elastic behavior was seen for the DC than the AC ER material. Specifically, observe in Figure 3.12(a) that at a strain of 0.1%, the phase angle for the four frequencies tested were approximately 20 degrees. For the AC material presented in Figure 3.8(a), the phase angles were 40 degrees and above. This means that at small strains, the DC ER material behaves much more elastically than the AC ER material. But this of course also means that the AC material has higher viscous damping capabilities than its DC counterpart. Note that the plateau region seen in Figure 3.8(a) does not exist in Figure 3.12(a), i.e. the viscoelastic transition of the DC material is less complicated than the AC material. Also from Figure 3.12(a), the ideal case of yielding was not observed, i.e. at no point was there a sudden transition in phase angle from near 0 to 90 degrees.

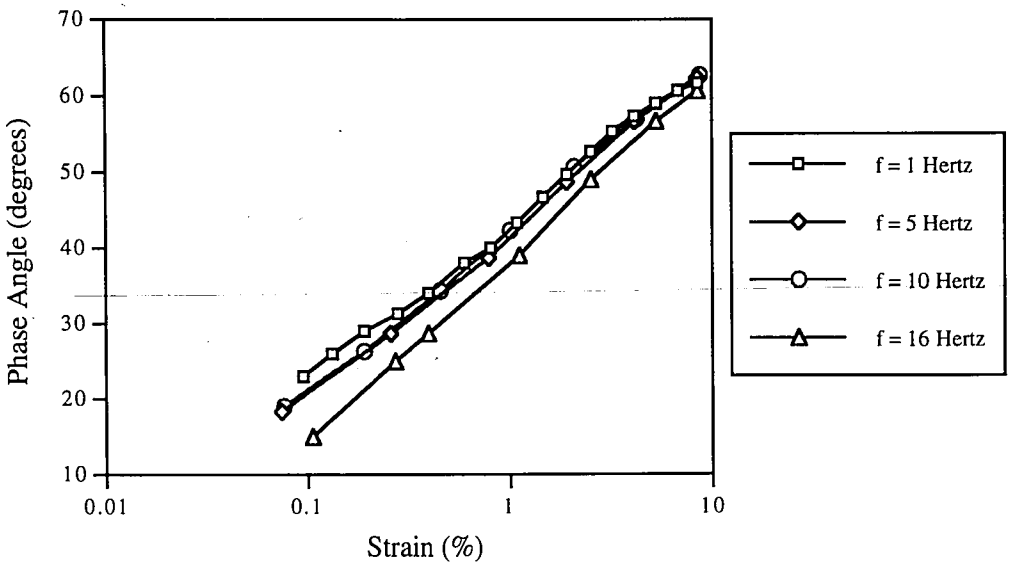

(a)

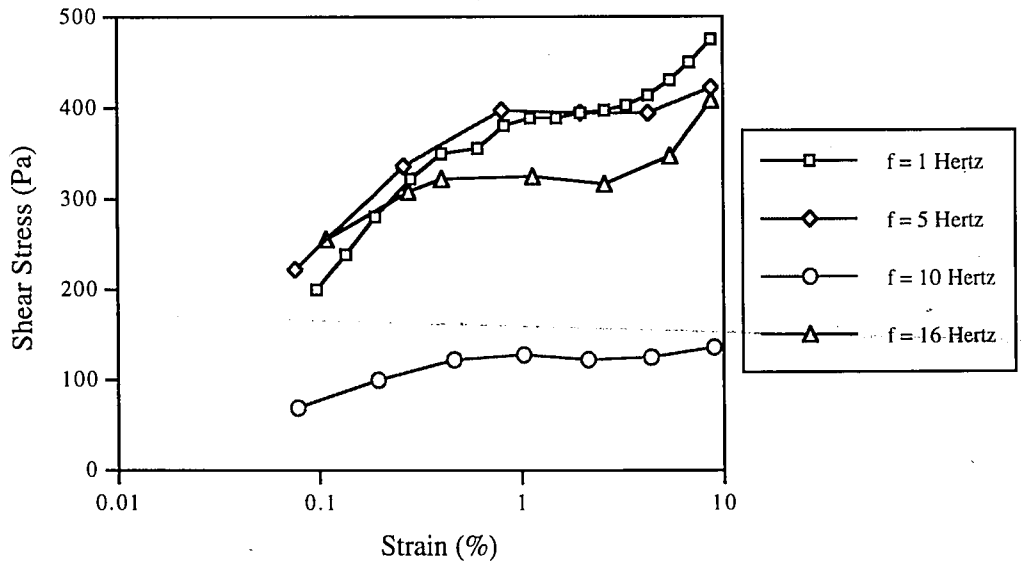

(b)

Figure 3.12 Strain sweep of ER-III for electric field of 3 kV/mm. (a) Phase angle and (b) shear stress.

The lack of yielding described for the phase angle is further supported by the shear stress/strain curves of Figure 3.12(b) where true yielding of the material was not observed. Yielding would have been exhibited by a maximization followed by a rapid decrease of stress as the strain amplitude level was increased. In Figure 3.12(b) however, the data does show a more pronounced frequency dependence as compared to Figures 3.11(a) and (b)—excluding the aberrant 10 Hertz results.

A fine point should be raised regarding the reliability of using shear stress as an indicator of linear/nonlinear viscoelastic behavior. In shear strain tests of this nature, the governing equation is

$$\tau^* = G^*\gamma \tag{3.4}$$

as first introduced in Section 2.2. According to the theory of linear viscoelasticity, in the linear region, G^* is constant up to some critical strain, γ_y. Essentially what this means is that if one increases γ, the measured shear stress must increase proportionally to keep G^* constant. Likewise, decreases in stress must proportionally match decreases in strain. Therefore, even though pre-yield and post-yield regions are indeed synonymous with linear and nonlinear viscoelastic behavior, examination of τ^* alone may not be reliable, since τ^* as written in Equation 3.4 includes G^*. Thus in terms of a reliable indicator of linear/nonlinear behavior of a viscoelastic material, Equation 3.4 should first be solved for G^* in terms of τ^* and γ. Then, from the measured shear strains and stresses, G^* should be obtained and plotted against corresponding γ's. If the G^* values are strain independent, the material is linear; otherwise, if G^* depends on strain, the material is nonlinear. Another important point to be made regarding the theory of linear viscoelasticity is that within the linear region, dynamic moduli are a function of only temperature and excitation frequency. Specifically for ER materials at room temperature, dynamic moduli should only be functions of external electric field and excitation frequency in order for linear viscoelastic theory to apply.

As was done with ER-200, strain sweeps for the DC material were performed at a high electric field strength throughout the frequency range of the RDA II. Since even at low frequencies, the behavior was seen to be nonlinear, the nonlinear rheological properties will be presented as a function of electric field strength for one Hertz. Rheological properties as functions of strain and electric field are presented in Figures 3.13 and 3.14.

In Figures 3.13(a) and (b), G_n' and G_n'' of ER-III are seen to be strongly influenced by electric field strength. As much as four decades of differences in the dynamic moduli were observed between field strengths of 0 and 3 kV/mm. Although for the ER-200, this electric field dependency was also noticed, significant differences were observed for the overall composition of G_n^* of the two materials. As discussed in Section 3.4.3, G_n'' of ER-200 dominated over G_n', and the material behavior was predominantly viscous. However, for ER-III, G_n' could be seen from Figures 3.13(a) and (b) to be significantly larger than G_n'' at a strain of approximately 0.1%. A higher contribution of G_n' to the overall G_n^* is equivalent to a predominantly elastic behavior of the material. Notice that at a strain of nearly 10%, a cross-over occurred and G_n'' became greater than G_n'; thus for this material, damping capabilities improved at larger strain amplitudes.

Supporting the above mentioned damping capabilities of ER-III is the phase angle versus strain curve of Figure 3.14(a), where ϕ values started in the elastic region (<45 degrees) and approached the viscous region (90 degrees) smoothly. In general, increases in electric field strength were marked by the material's exhibition of more solid-like behavior, i.e. the downward shift of phase angle curves. This smooth approach to the flow region was accompanied by a lack of yielding of Figure 3.14(b), though the dependence of shear stress on electric field could be easily identified. And once again, the emphasis of the ER material behavioral linearity should be placed upon the strain dependence of the dynamic moduli, not on the yielding of shear stresses.

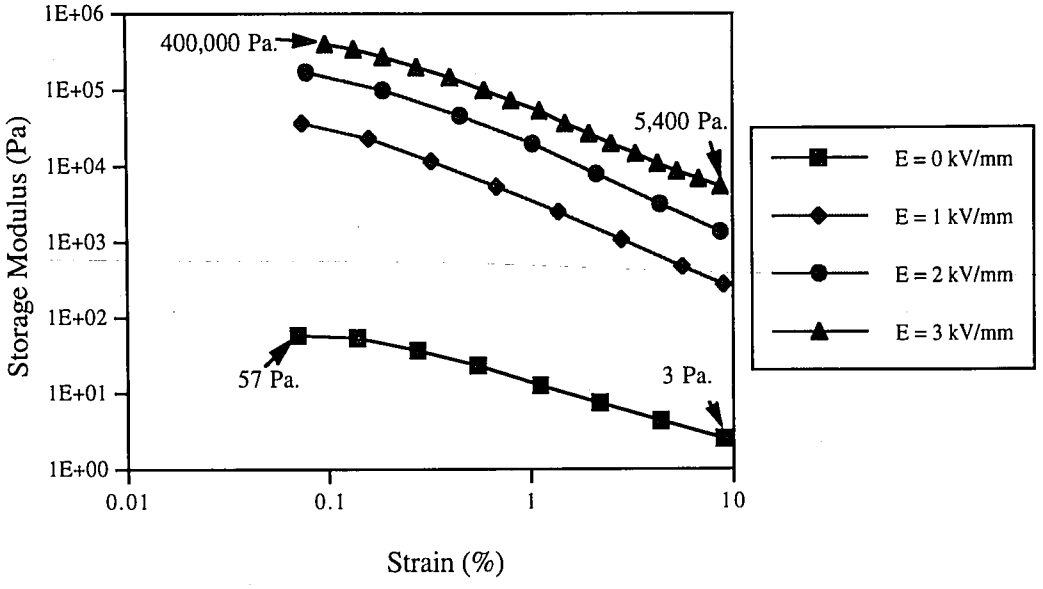

(a)

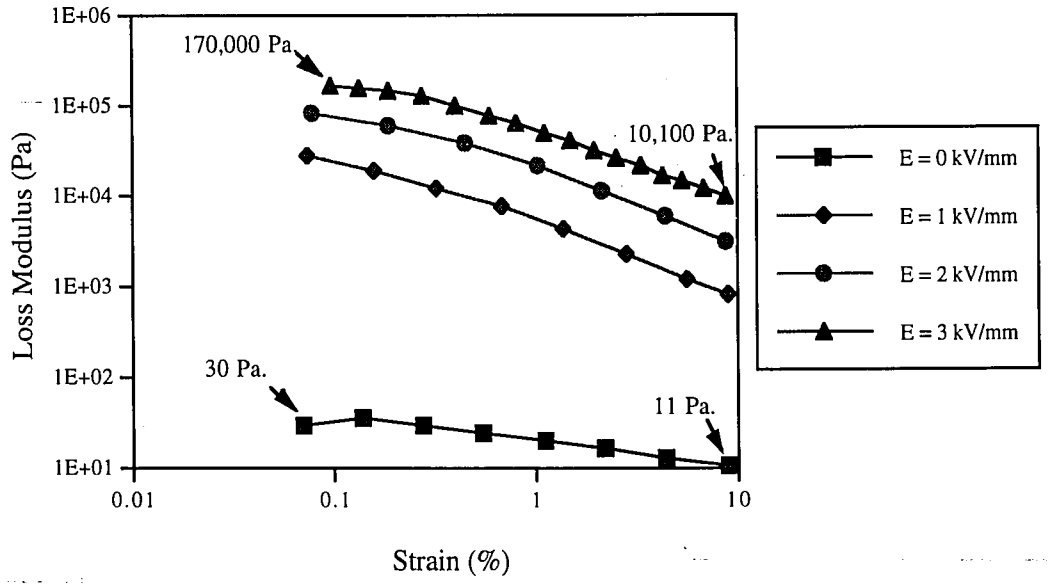

(b)

Figure 3.13 Strain sweep of ER-III for strain frequency of 1 Hertz. (a) Storage modulus and (b) loss modulus.

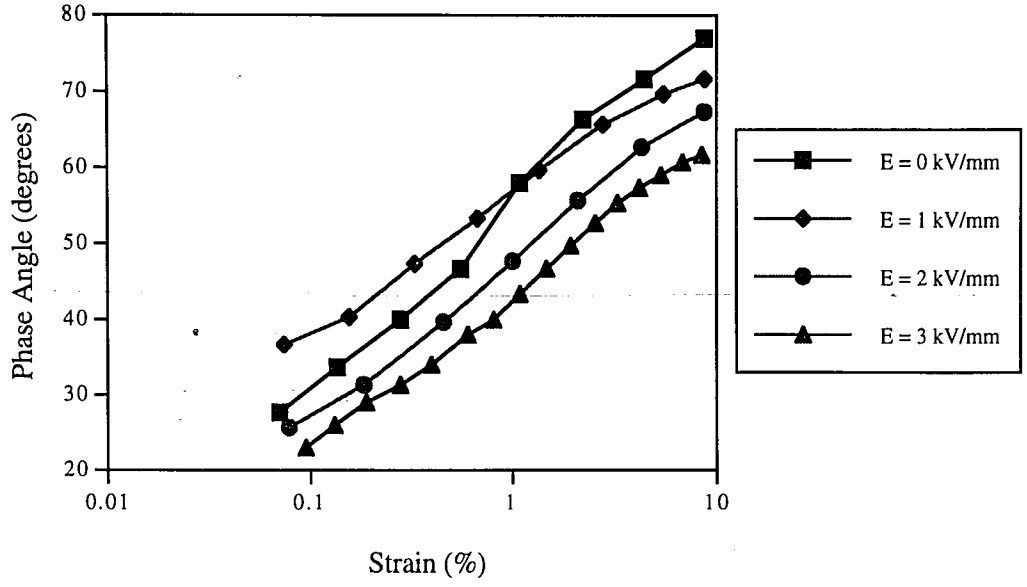

(a)

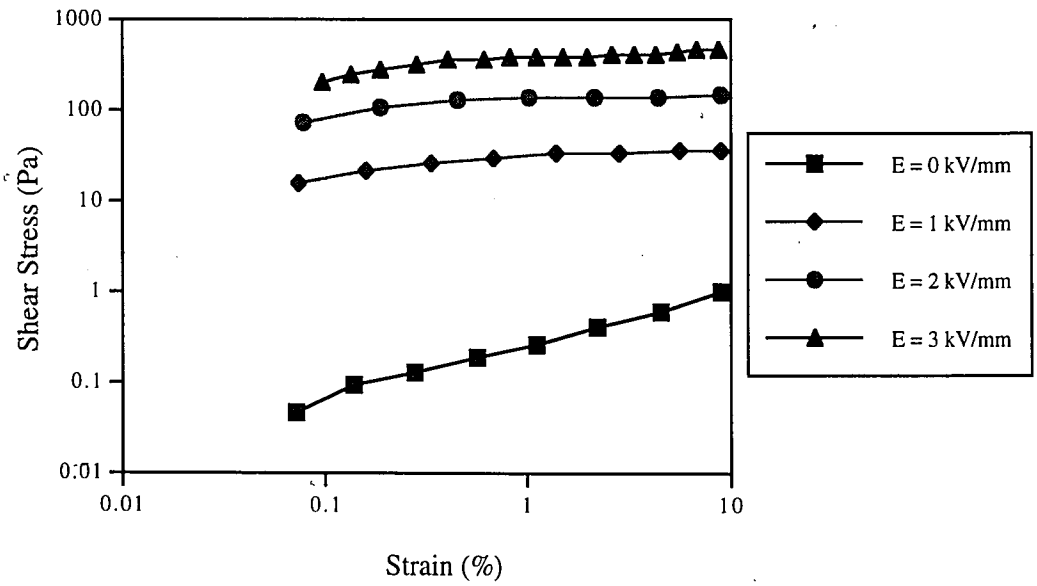

(b)

Figure 3.14 Strain sweep of ER-III for strain frequency of 1 Hertz. (a) Phase angle and (b) shear stress.

3.5 Chapter Summary

The viscoelasticity of several materials was investigated under increasing strains. For the highly viscous S-8000 oil, it was proven that the rheometer was functioning properly as a viscometer. Strain sweeps performed showed that the material was Newtonian; high G" and very low G' values were consistently observed. Also established was the validity of using the stress/strain phase angle as an indicator of material viscoelasticity. For a highly viscous fluid such as the S-8000 oil, the ϕ value should be slightly less than 90 degrees, as it was proven to be in Section 3.4.1.

PDMS—a linear viscoelastic material—was tested for its dynamic moduli at increasing strain amplitudes. It was found that for this material, a critical strain, or yield strain γ_y did indeed exist below which G' and G" both stayed strain invariant, i.e. linear viscoelastic. Also important is the realization that γ_y is influenced by the strain frequency. For this material, γ_y decreased as strain frequency increased. The usefulness of the phase angle in establishing the degree of viscoelasticity was also discussed. In addition to the benefits of using ϕ to indicate deviation from linear behavior, the material properties (whether solid-like or liquid-like) as a function of frequency is shown clearly by the phase angle. As discussed previously, the ideal elastic material has a stress/strain phase angle of 0 degrees; the ideal viscous material has a phase angle of 90 degrees. The procedures and utilization of the RDA II for the testing of linear viscoelastic materials have been established at the completion of the PDMS experiments.

Both AC and DC ER materials were shown to have behaved in a nonlinear viscoelastic manner. At the smallest obtainable strain output of the rheometer with a couette attachment (approximately 0.1% strain), the materials were found to be strain dependent. Yield strains, if they exist at all, were smaller than 0.1%. It is certainly possible that the ER materials are linear at strain frequencies of smaller than one Hertz. But unfortunately, limited numbers of real-world engineering applications of ER materials exist in these low frequency ranges. From other evidence shown by the gathered data, the rheological

properties of these materials were found to be highly dependent on electric field strength and moderately dependent on strain frequency.

Alternative experimental or analytical methods are needed to find the yield strains of these behaviorally complex materials. Rheometers capable of outputting minute, dynamic strains of less than 0.1% strain are needed; this type of rheometer will most likely need special design and will not be a commercialized product like the Rheometrics RDA II. However, the evidence presented in Sections 3.4.3 and 3.4.4 indicated that the behavior of these materials was quite complex and was highly nonlinear. It is doubtful that a rheometer capable of smaller than 0.1% will be sufficient in solving the present linearity problem. Instead, other methods should be employed to analyze and model the behavior and properties of this unique class of colloidal suspensions under sinusoidal strain.

CHAPTER 4: RELIABILITY AND CONTROLLABILITY OF ER MATERIAL BASED ADAPTIVE STRUCTURES

4.1 Introduction

In Section 2.5, the purpose of the present investigation was first introduced; namely, to ascertain the utility of ER materials for structural-vibration damping. While ER rheology is certainly a subject worthy of intensive research efforts, there are benefits when a rheologist performs research using actual adaptive structures. The most important reason is that with the background and understanding of the relationship between stress and deformation of matter, a rheologist is able to explain how material properties affect the vibration response of these adaptive structures. Indeed, the design and modeling, as well as the understanding of these advanced structures require an in-depth knowledge of ER material viscoelasticity.

Several technical challenges were encountered during the early phases of the Lehigh University-U.S. Army Adaptive Structures research project with which the current investigation was affiliated. During the start-up phase of the project, several ER adaptive beams with fiber-optic sensors were tested using neural-network controls. Frequency sweeps in the moderate range (1-200 Hertz) were performed on these structures at various electric field settings. The information obtained from these tests were utilized to successfully train neural-network controllers. However, after the neural network was trained and the frequency sweeps repeated on the structures, two problems were apparent with the neural-network controlled behavior. These problems are illustrated by the results shown in Figure 4.1.

In Figure 4.1, the displacement response of a location on a vibrating ER material based adaptive beam is plotted as a function of vibration frequency. Two of the curves included are for constant applied electric field levels of 0 and 2.5 kV/mm, respectively. The third curve represents the response observed when a neural-network controller—trained to determine and apply optimum electric field levels for minimized vibration

response at each frequency—was used in an effort to demonstrate a truly "smart" ER material based adaptive structure. Ideally the resultant displacement response curve obtained using the neural-network controller would be below the other two constant electric field curves for all frequencies. As can be observed in Figure 4.1, such was not the case.

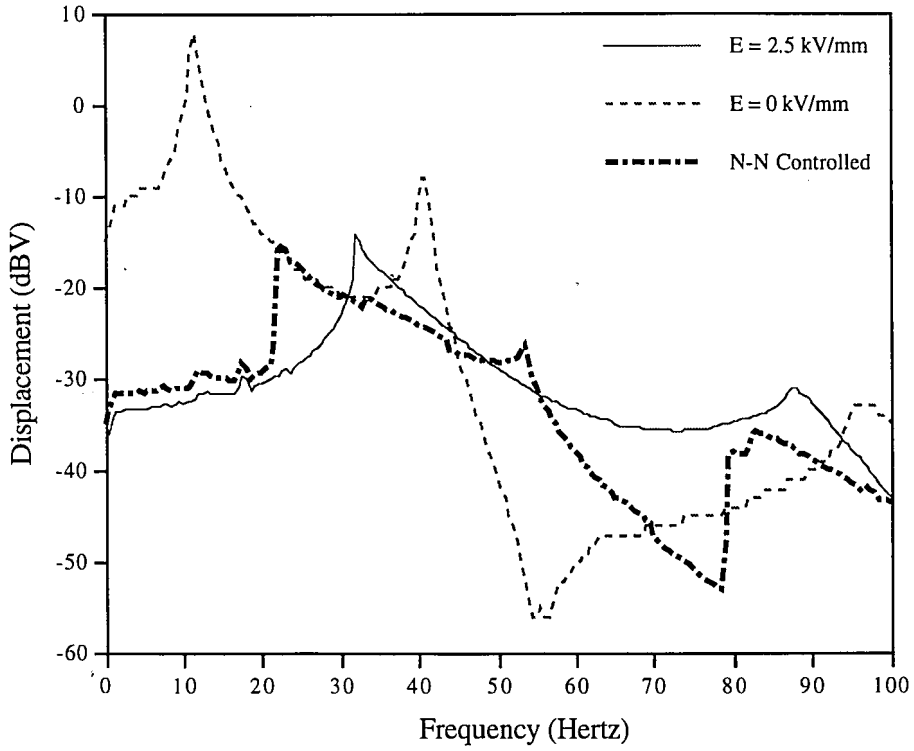

Figure 4.1 Comparison of neural-network-control response to control-free response of an ER adaptive beam.

The foremost problem encountered was as follows. For vibration frequencies less than 30 Hertz, the optimum electric field for vibration amplitude minimization was 2.5 kV/mm. The neural-network controller successfully applied this electric field level at all vibration frequencies less than 20 Hertz. As can be seen, the results were satisfactory. Between 20 and 30 Hertz, the neural network inappropriately applied a zero electric field, and as can be seen the structure responded at the corresponding zero-field level. The application of this "non-optimal" electric field level over the 20 to 30 Hertz range served to

test the ability of the adaptive structure to switch between on and off states in this frequency range. In the higher frequency range of from 45 to 90 Hertz, the optimum field needed for vibration minimization was 0 kV/mm. As the structural excitation frequency was increased steadily in a swept-sine fashion, the neural-network controller did indeed remove the applied electric field at 45 Hertz. It can be observed from Figure 4.1, however, that the neural-network response did not follow the electric field "off" curve immediately, but a delay in the adaptive structure adjustment to the new "off" field level could be seen.

As a result of experiments such as this, the following observation was made: the ER adaptive beam worked quite well for low frequency-large amplitude vibrations, but the beams failed to respond immediately to off states in electric field—especially during high frequency-small amplitude vibration. The controllability of these adaptive structures was, therefore, questioned for the first time. It was postulated that for this ER material (LORD ER-III) under small amplitude-high frequency shear deformation, perhaps the millisecond response time so often alluded to in literature simply did not apply.

A second potential problem can also be identified by looking at the results shown in Figure 4.1. Observe that, as mentioned previously, at approximately 20 Hertz the neural-network response returned to zero-field. For optimized vibration reduction, however, the switching off of electric field should have occurred at 30 Hertz. The neural network switched off early in this particular case. However, several days before the data presented in Figure 4.1 was collected, the neural network was trained using the same beam. The optimum electric field at 20 Hertz for vibration minimization during the training period was indeed 0 kV/mm. Changes in the ER material based adaptive structure must have occurred which led to the early switch off of electric field by the neural network. Consequently, the long-term reliability of these ER structures was questioned.

The controllability and reliability problems described above prevented the successful implementation of a truly intelligent structural system such as shown in Figure 1.8. Fundamental questions regarding ER beam time response and reliability needed to be

addressed. Therefore, ER material based beams were built, and experimental procedures were formulated to find answers to these questions.

4.2 Construction of ER Material Based Adaptive Beams

The ER sandwich beam utilized in this investigation was based on a shear configuration. Two aluminum plates of length 381 mm, width 25.4 mm, and thickness 0.76 mm were used as the two outer layers of the total composite structure. The two plates were separated by one millimeter thick polycarbonate spacers to ensure uniform ER material thickness. The beam was sealed on all sides with a thin latex material. The ER fluid, after mixing and desiccation, was injected into the beam. Wires were bonded to the surface of the aluminum plates for connection to the high voltage power amplifier. A diagram of the beam configuration utilized is shown in Figure 4.2. Through the course of this thesis study, two separate ER material based beams were constructed. The beams were identical except one was filled with the AC ER material (LORD ER-200), and the other was filled with the DC ER material (LORD ER-III).

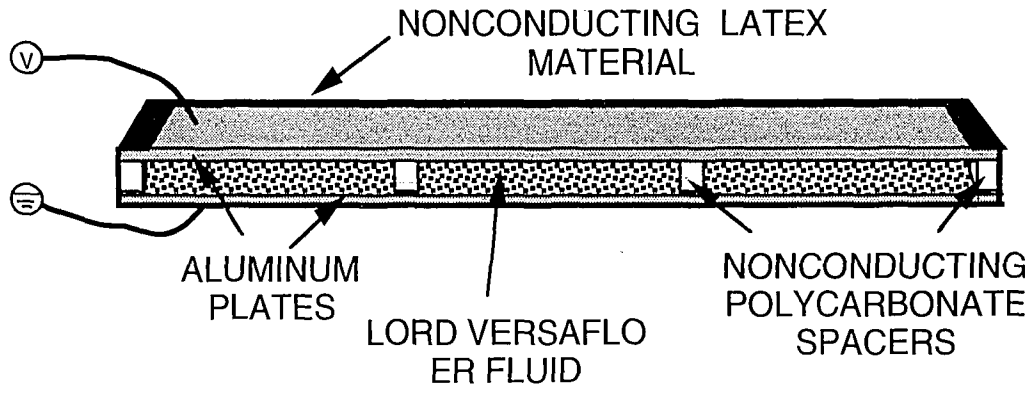

Figure 4.2 Basic components of an ER material based adaptive structure.

4.3 Experimental Setup

The instrumentation used in both the reliability and time response studies is shown in Figure 4.3. An Ono Sokki CF-920 FFT Analyzer with a built-in function generator was used to analyze captured data both in the time and frequency domain. The built-in function generator provided the input signal for the electromagnetic actuator used to excite the structure. A Bentley Nevada Series 7200 Proximity Sensor provided displacement data of the beam. For AC ER fluids, a B&K-Precision Model 3022 Sweep/Function Generator provided the input AC signal to the TREK Model 609C-6 high voltage amplifier. For DC ER fluids, an HP Model E3611A DC Power Supply provided the needed DC voltage to the TREK. Output of the amplifier was monitored using a Fluke Model 87 digital multimeter. For all cases considered, the beam under investigation was set up on a test bench which was designed to isolate external disturbances.

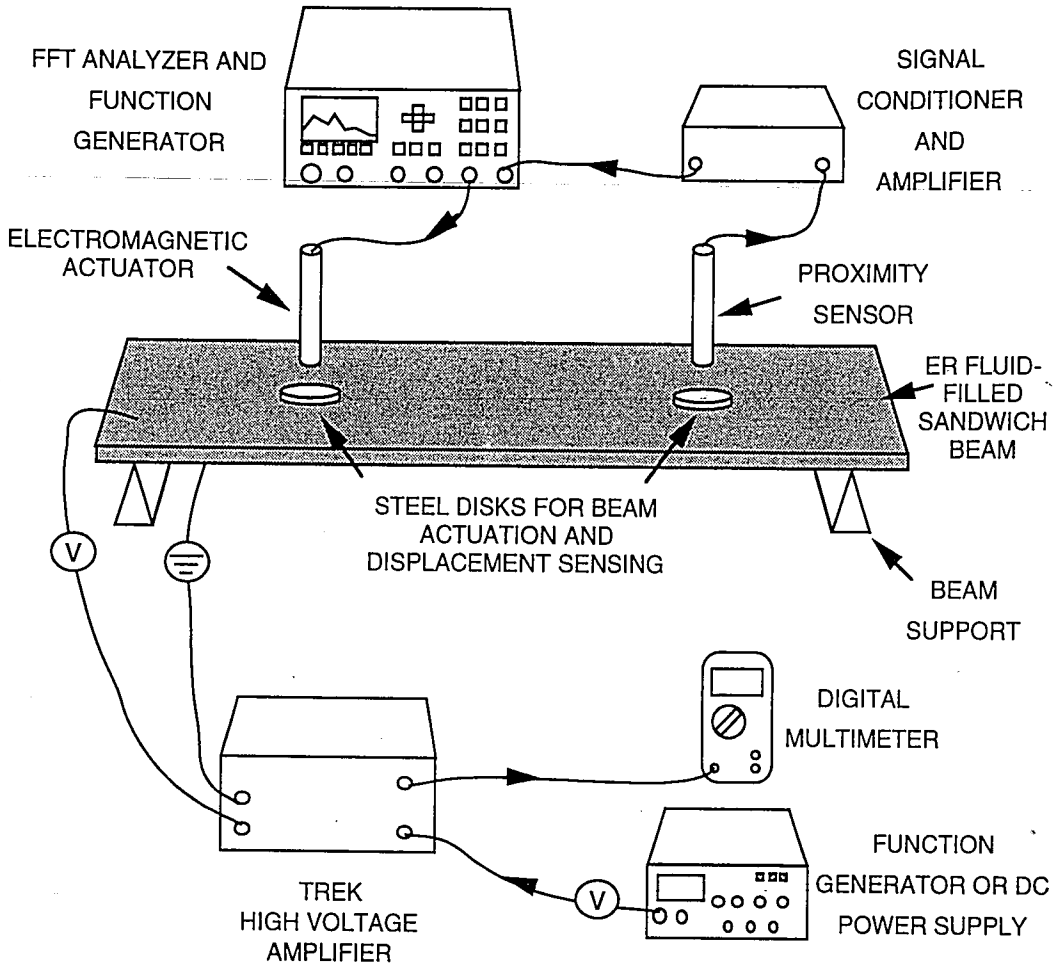

Figure 4.3 Experimental setup of ER adaptive structure reliability and controllability investigations.

4.4 Experimental Procedures

Since the reliability and controllability of the ER adaptive structures were two separate problems, experimental procedures were devised for each. The reliability testing procedures are described in Section 4.4.1 and the controllability testing procedures are described in Section 4.4.2.

4.4.1 Reliability

In the ER adaptive beam reliability analysis, the vibration response of the structures was studied over a period of three weeks. Data was taken on an average of once every 70 hours for the AC structure, and once every 100 hours for the DC structure. The test consisted of providing a sine wave of increasing frequency (0-250 Hertz) to the electromagnetic actuator and observing the frequency response of the structure at each discrete electric field setting. A typical frequency response of an ER material based structure is shown in Figure 4.4 for a discrete value of electric field E_i. As the electric field changes, the curve shifts due to changing ER material complex moduli. The objective of the test was to determine, as a function of time, the reliability of modal frequencies and loss factors at various applied electric field intensities. All tests performed on the AC structure utilized an applied AC frequency of 600 Hertz and an electric field of 0-1500 V(rms)/mm in increments of 500 V(rms)/mm. Electric fields of 0-3000 V/mm in increments of 1000 V/mm were used on the DC structure.

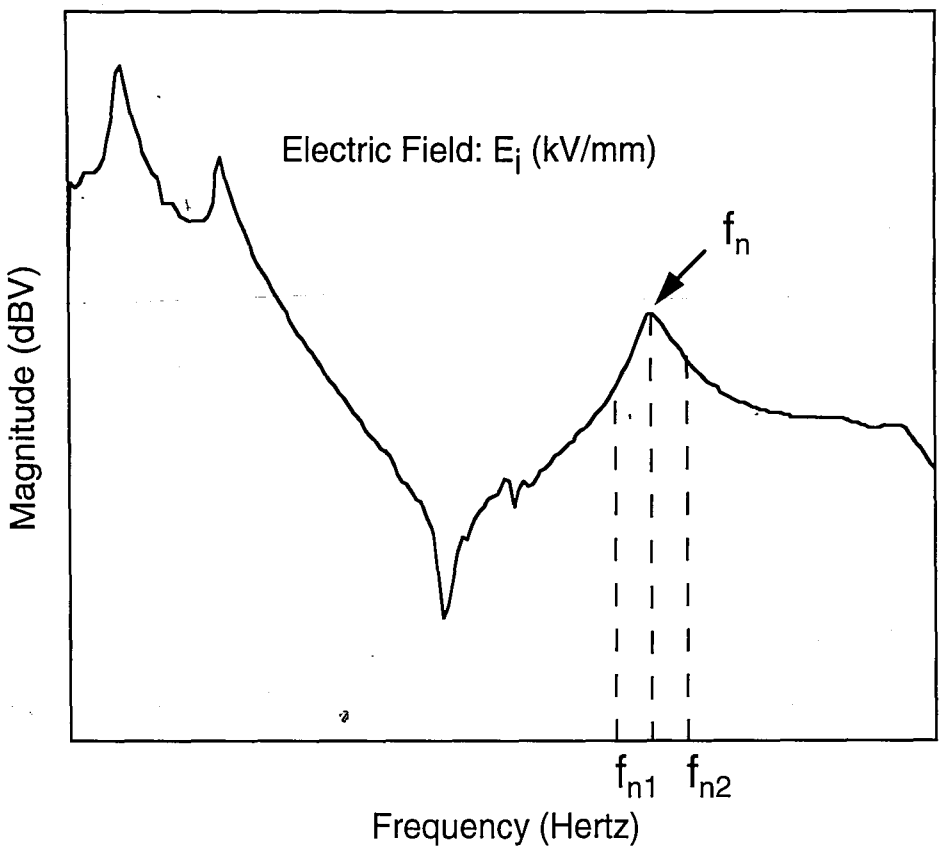

Figure 4.4 Typical frequency response of an ER adaptive beam in forced vibration.

4.4.2 Controllability

The ideal time response of an ER adaptive structure is instantaneous, i.e. there is no delay in the structure's response to turning on and off of the electric field. As the electric field is turned on, the structure's vibration amplitude is immediately adjusted with no delay. Likewise, the vibration amplitude returns to the zero-field state instantaneously when the electric field is turned off. This idealized behavior is represented in Figure 4.5. The beams used in the reliability studies were also used for the time response studies. The first and second fundamental frequencies of the beams at zero-field were obtained from reliability testing. Since the ER damping effect at these frequencies was easily observed, it was decided that all time-response testing would be performed at these frequencies, which were 15 and 34 Hertz for the AC beam, and 14 and 39 Hertz for the DC beam. As for the

reliability tests, all AC beam response time tests were conducted using an applied AC field frequency of 600 Hertz.

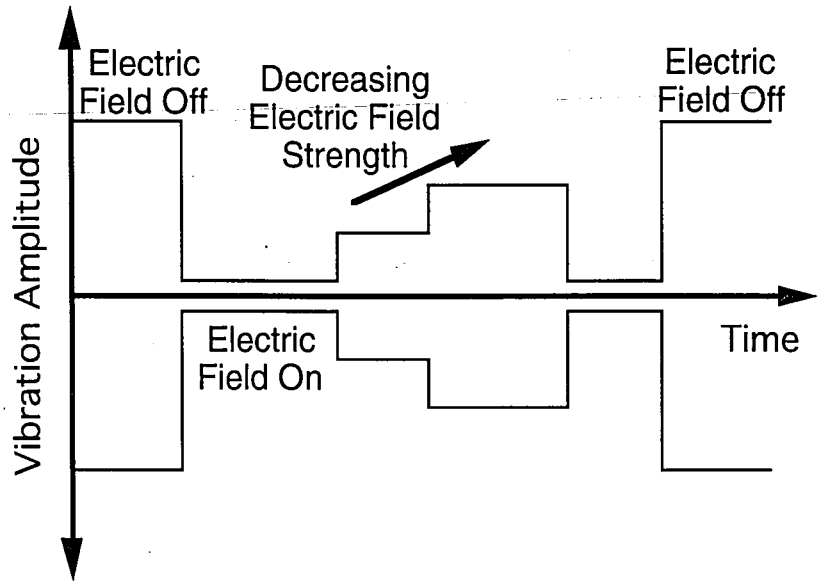

Figure 4.5 Ideal time response of ER adaptive structures.

In studying the AC adaptive structure's time response to increases in electric field strength, the function generator was used to provide a sine wave of known amplitude to the electromagnetic actuator. The actuator provided the excitation to the structure at one of the two fundamental modal frequencies. When the structure reached stable oscillation, the amplifier preset at a discrete electric field, e.g. 1000 V(rms)/mm, was switched on. The resulting time domain signal was recorded on the FFT analyzer. The same test was repeated for the DC structure using the DC Power Supply to provide the input offset voltage for the TREK. Switch-On Time was defined as the time period between the last wave form of the zero electric field and the onset of steady state oscillation with the electric field on.

In studying the beam response time for switching off of the electric field, the electric field application time became a factor in the investigation. Four values of electric field application time, t_e, were investigated: 5, 30, 60, and 120 seconds. For the AC and

the DC beam, at each fundamental frequency and each t_e, changes in vibration amplitude due to switching off of the electric field were recorded on the FFT Analyzer. The electric field strength change levels studied were 1500-0, 1000-0, and 500-0 V(rms)/mm for the AC beam; and 3000-0 in descending increments of 500 V/mm for the DC beam. Switch-Off Time was defined as the time period between the last steady wave form with electric field on, and the onset of steady state oscillation with zero electric field.

4.5 Results and Discussion

The results of the controllability and reliability experiments are presented in Sections 4.5.1 through 4.5.5. The results for the reliability analysis are presented in Section 4.5.1. The frequency responses of these adaptive beams—an issue indirectly related to reliability—are presented and discussed in Section 4.5.2. The influence of ER rheology on frequency response is presented in Section 4.5.3. And lastly, the controllability of these ER adaptive structures due to the application of electric field is presented in Section 4.5.4; the effect due to the removal of electric field is discussed in Section 4.5.5.

4.5.1 Modal frequency and loss factor stability

In Figures 4.6-4.8, the reliability of the AC ER material based beam in terms of modal frequency stability over time is presented. Ideally, the curves would be horizontal and linear over time, i.e. the viscoelastic layer of ER materials would have constant damping properties unaffected by time. Any changes in the properties of the ER material, particularly deterioration of ER effect, will cause corresponding changes in frequency response curves. In the case of deteriorating ER effect, or loss of damping capabilities, it is expected that the beam will exhibit shifting of the frequency curve, thereby changing the corresponding modal frequencies. Furthermore, in viscoelastic terms, the effect of time on the ER materials' storage modulus (G') and loss modulus (G") directly affects the

structures' performance over time. For this reason, research in ER material based adaptive structures must not only be concerned with changes in vibration response, but also with understanding fundamental ER rheology as applied to the present problem.

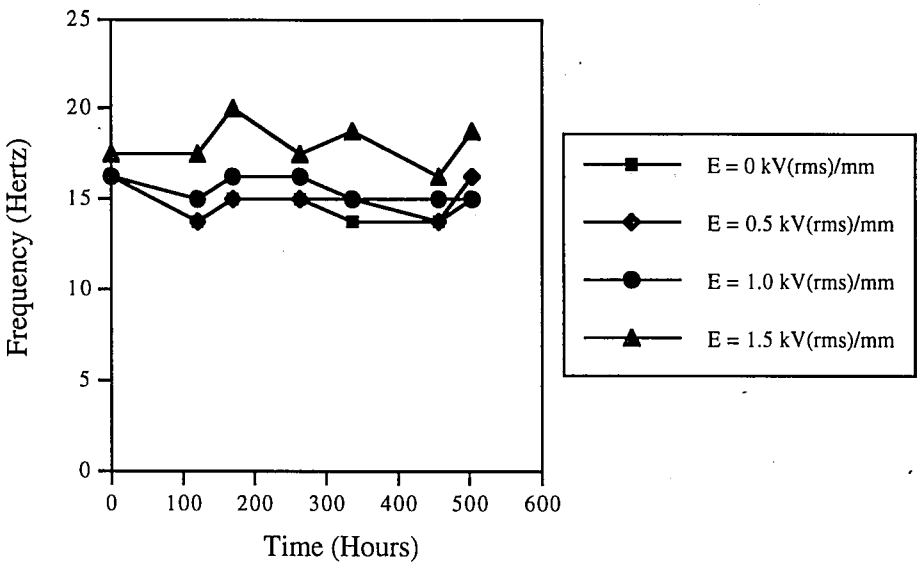

Figure 4.6 Variation of AC beam Mode One frequency over time.

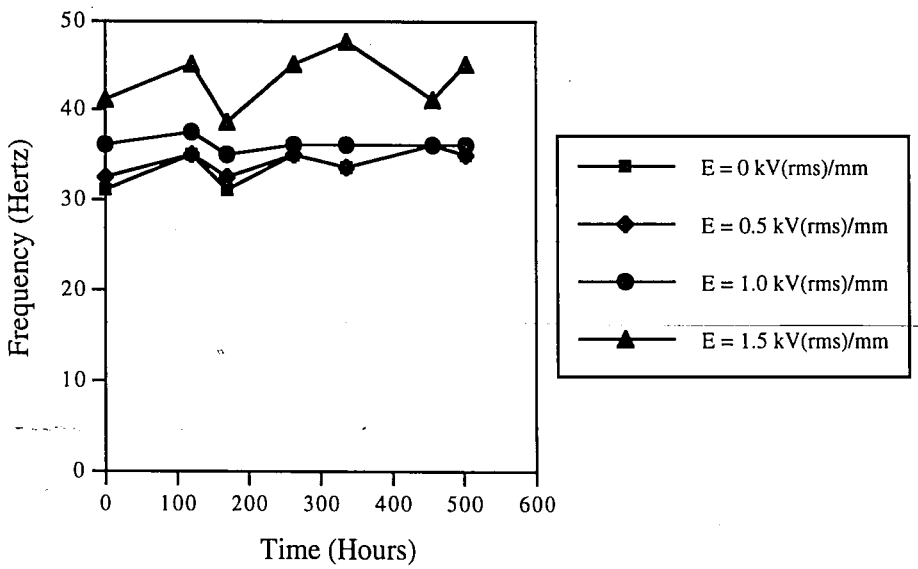

Figure 4.7 Variation of AC beam Mode Two frequency over time.

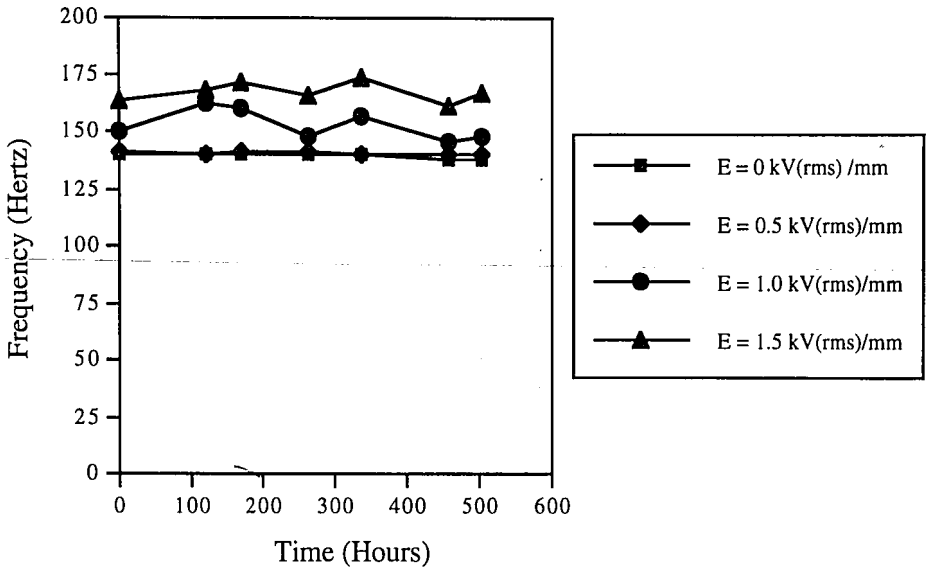

Figure 4.8 Variation of AC beam Mode Three frequency over time.

As apparent from Figures 4.6-4.8, the actual behavior of the modal frequency over time is not a linear function. Variations in fundamental frequencies occurred over the 500 hour study period. In Table 4.1, a summary of mean frequency values and standard deviations for each mode and each applied AC electric field is provided.

Table 4.1 Averages and standard deviations of observed natural frequencies for the AC ER material based adaptive structure

	Applied AC Electric Field (kV(rms)/mm)			
	0	0.5	1.0	1.5
Mode One				
Mean Frequency (Hz)	14.64	15.00	15.54	18.04
Standard Deviation (Hz)	0.95	1.02	0.67	1.22
Mode Two				
Mean Frequency (Hz)	33.93	34.29	36.25	43.39
Standard Deviation (Hz)	1.97	1.42	0.72	3.04
Mode Three				
Mean Frequency (Hz)	139.64	140.54	153.39	167.50
Standard Deviation (Hz)	0.61	0.67	6.44	4.27

From these Figures, it may also be observed that at 500 V(rms)/mm, the increases in vibration frequencies due to increasing ER fluid complex moduli were small. Mode 2 frequency increases of 28 percent above zero field values were observed at 1500 V(rms)/mm. It is apparent that overall, the beam exhibited no trend in modal frequency change over time.

In an oscillatory system, the amount of damping present may be determined from the system's frequency response. Specifically, for a forced vibration system such as an ER adaptive structure subjected to external excitation, frequency response graphs such as shown in Figure 4.4 could be generated. As the electric field intensity changes, the frequency response curve changes and shifts according to the amount of damping and compliance present in the ER material. The damping, or the energy absorption capability may be determined directly from frequency response graphs.

The loss factor for the beams under investigation was calculated for each electric field setting at each resonant frequency. The results for the AC beam loss factor over time are shown in Figures 4.9-4.11. Note that the data exhibits—in general—an upward shift in loss factor as the electric field is increased. In contrast to modal frequency variation over time, a wide scatter of loss factor over time was observed. But just as for the modal frequency results shown in Figures 4.6-4.8, neither increasing nor decreasing trends in loss factors were observed over the 500 hour study period. This means that although the actual damping may vary from day to day, the long term damping capability of the ER materials remains reliable.

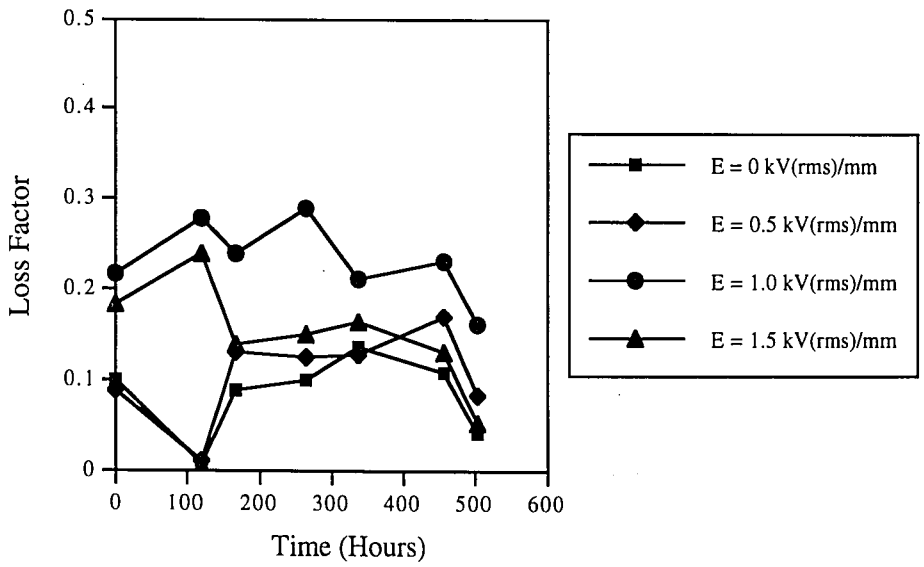

Figure 4.9 Variation of AC beam Mode One loss factor over time.

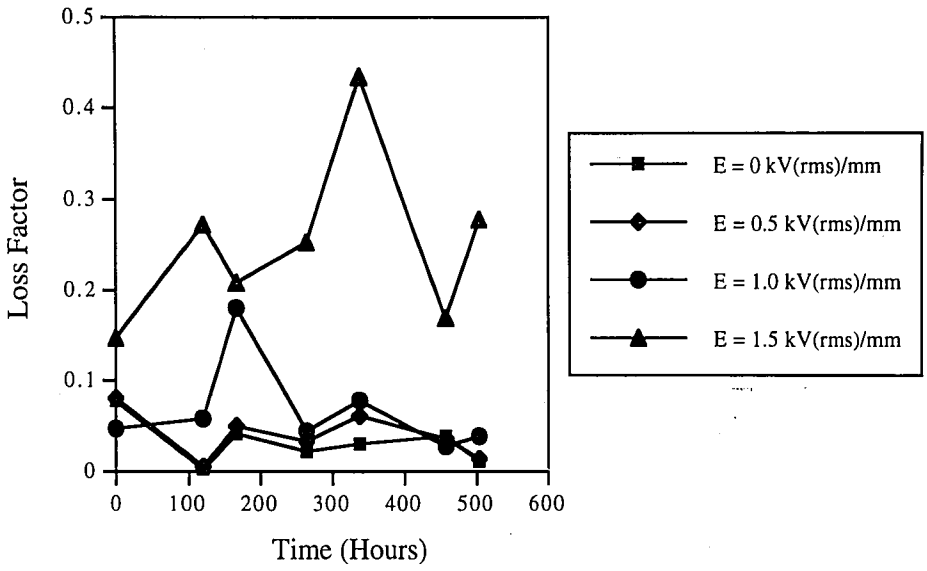

Figure 4.10 Variation of AC beam Mode Two loss factor over time.

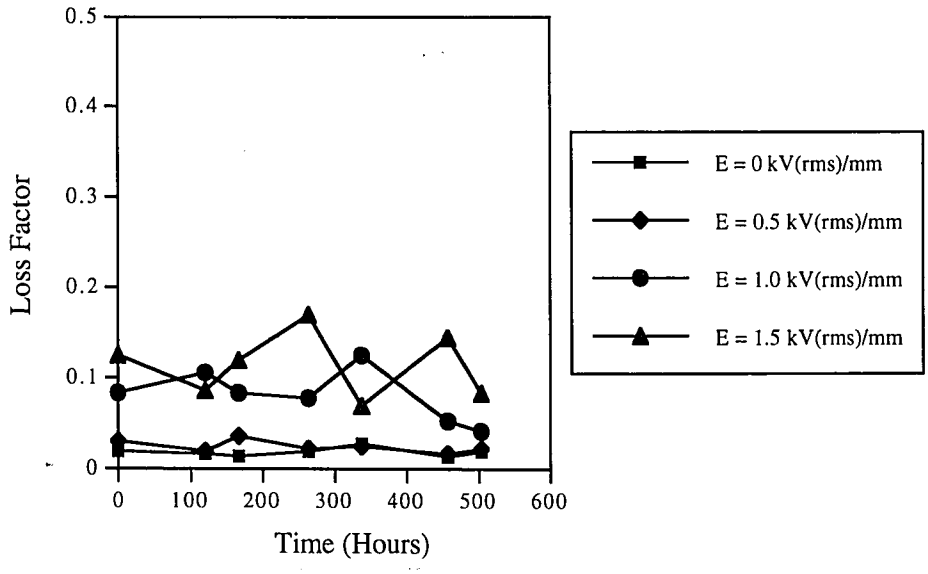

Figure 4.11 Variation of AC beam Mode Three loss factor over time.

The question remains as to the cause of such large deviations in loss factor over time. There are several possible causes for the phenomenon. Since the determination of damping is dependent upon the frequency response curves, any changes in these curves affect the loss factor. The foremost contribution to fluctuations in the frequency response curves is changes in ER material properties over time. In a composite structure such as an ER adaptive beam shown in Figure 4.2, the mechanical properties of the two elastic layers do not change with time. In addition, the latex sealant material had insignificant structural stiffness contributions, and its properties were also expected to be time invariant. Therefore the only other component capable of causing significant viscoelastic changes in the structure is the ER material. Other causes for loss factor variations may be attributed to the boundary conditions. Although attempts were made to duplicate the exact boundary conditions from day to day, it was possible that slight changes still existed which could contribute to the frequency response curves. Changes in loss factor over time may also have been caused by effects of ER particulate chain dynamics, since the ER material contained in a composite structure experiences many alignment-dispersion cycles. The continued variations in the chain structure, the reorientation of particles, as well as changes in the inter-particle forces could contribute significantly to changes in the viscoelastic behavior of the bulk fluid—thereby affecting the loss factor. The effect of time on the properties of these complex materials—which are subjected to many control variables—remains to be more fully understood.

The reliability of the DC beam was studied in terms of modal frequency and loss factor variation over time, similar to that of the AC beam. In Figures 4.12-4.14, it can be observed that for the DC beam, the modal frequency was relatively stable over the period of study. The mean frequency values and standard deviations for each mode and each applied DC electric field are summarized in Table 4.2.

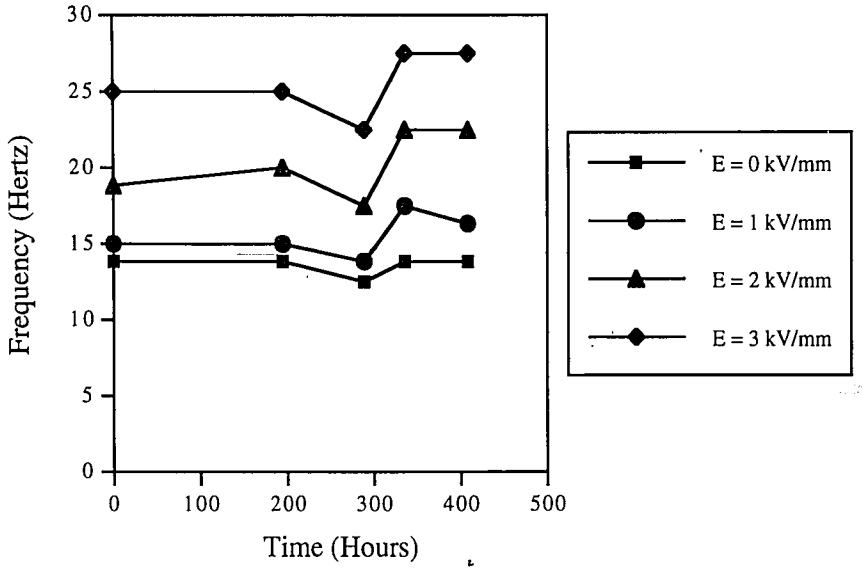

Figure 4.12 Variation of DC beam Mode One frequency over time.

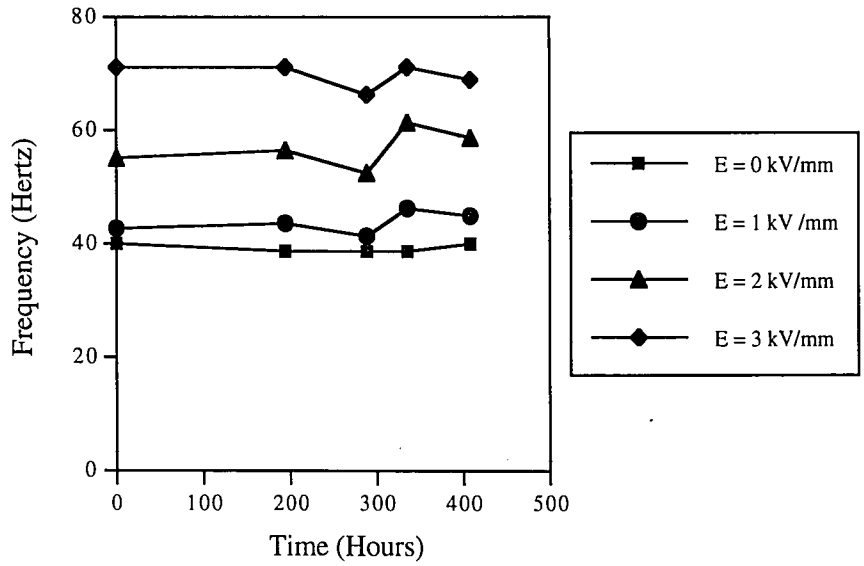

Figure 4.13 Variation of DC beam Mode Two frequency over time.

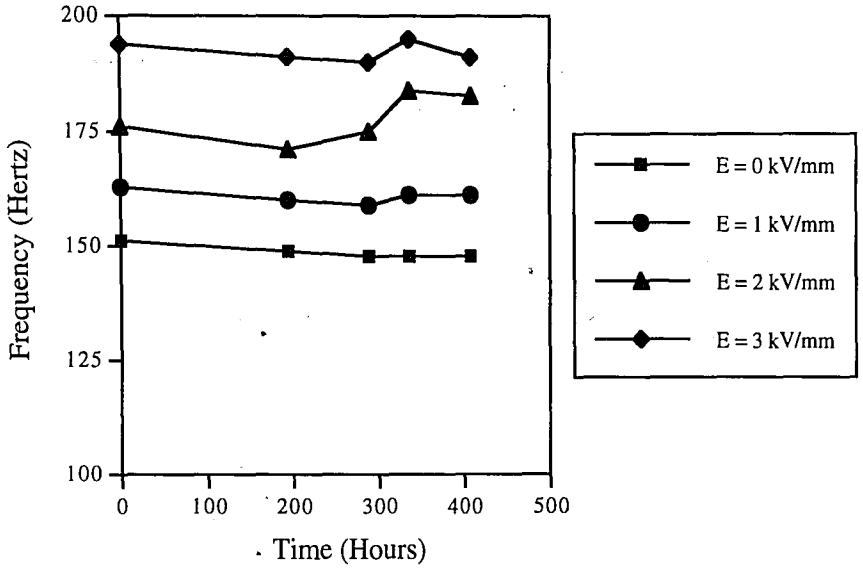

Figure 4.14 Variation of DC beam Mode Three frequency over time.

Table 4.2 Averages and standard deviations of observed natural frequencies for the DC ER material based adaptive structure

	Applied DC Electric Field (kV/mm)			
	0	1.0	2.0	3.0
Mode One				
Mean Frequency (Hz)	13.50	15.5	20.25	25.50
Standard Deviation (Hz)	0.56	1.43	2.24	2.09
Mode Two				
Mean Frequency (Hz)	39.25	43.75	56.75	69.75
Standard Deviation (Hz)	0.69	1.98	3.38	2.24
Mode Three				
Mean Frequency (Hz)	148.50	160.50	177.75	192.25
Standard Deviation (Hz)	1.63	1.12	5.26	2.05

In contrast to the results of AC beams, significant increases in modal frequencies were observed for DC beams at high electric field levels. The largest increase of approximately 89 percent occurred in the case of mode one. Modes two and three also exhibited large increases in modal frequencies as the DC electric field level was increased.

Although the current output limitations of the TREK amplifier prevented the study of AC beams at electric fields of greater that 1500 V(rms)/mm, the results of Figures 4.12-4.14 clearly showed the difference between AC and DC beams. Namely, the distinct upward shift of frequency/time curves as the electric field was increased.

The loss factors of the DC beam under varying electric fields over time were obtained in the same manner as described previously for the AC beams. Loss factor variations over time for modes one through three of the DC beam are presented in Figures 4.15-4.17, respectively. The DC material based beam also exhibited large deviations in the loss factor due to reasons previously discussed: Changes in ER material properties over time, and perhaps variations in boundary conditions. Similarly, increases in the damping effect were generally observed at higher electric fields.

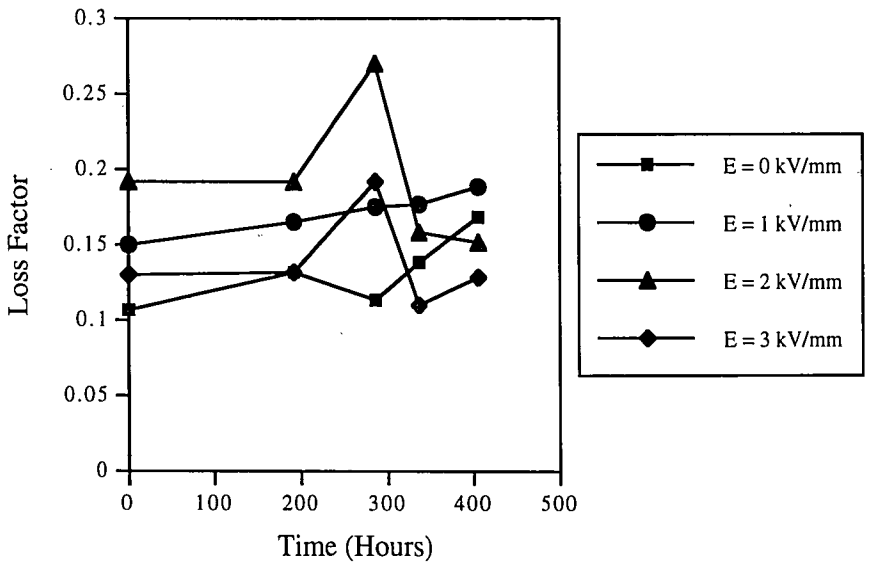

Figure 4.15 Variation of DC beam Mode One loss factor over time.

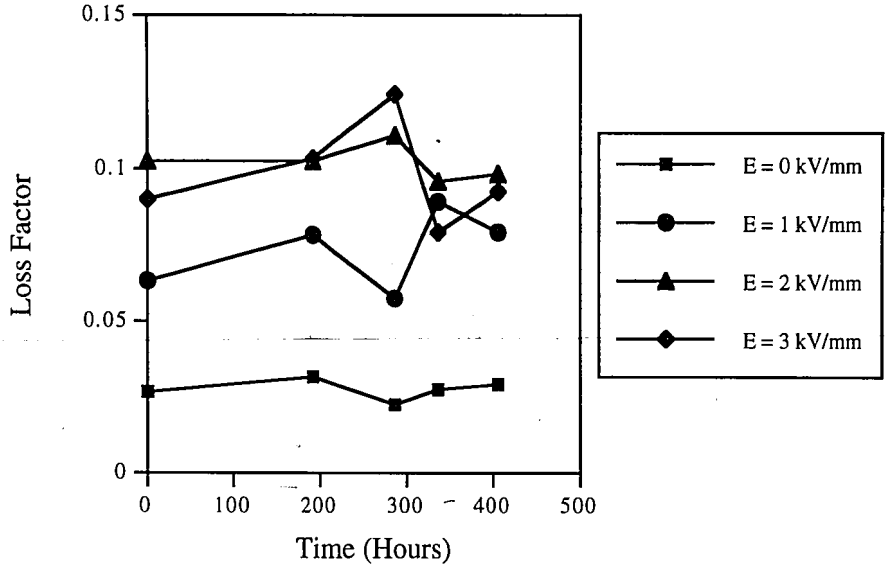

Figure 4.16 Variation of DC beam Mode Two loss factor over time.

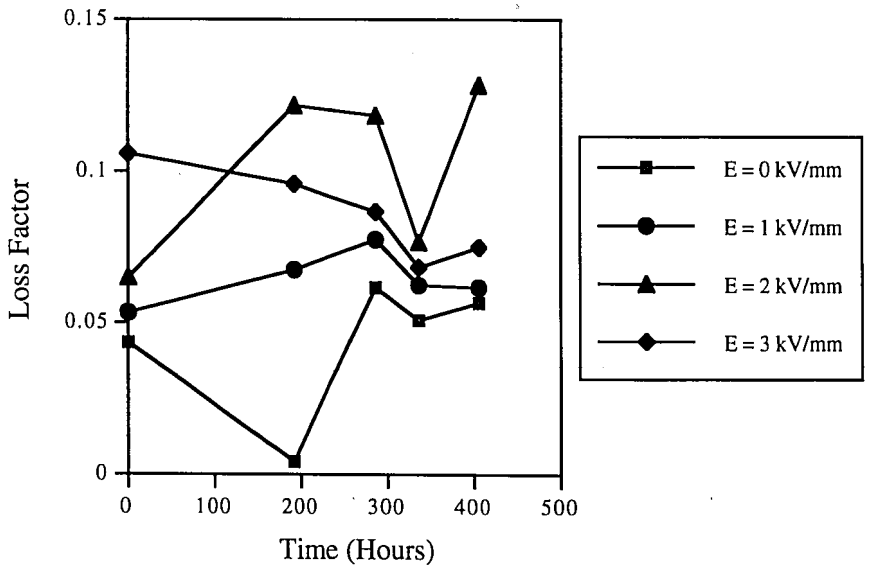

Figure 4.17 Variation of DC beam Mode Three loss factor over time.

4.5.2 ER adaptive beam structural frequency response

Since the properties of the ER material layer directly affect structural vibration response, an alternative approach to present the behavior of these structures under varying electric field intensity is to use frequency response curves. Changes in the properties of the ER material layer directly affect the frequency response curves. Whereas Figures 4.6-4.8 and Figures 4.12-4.14 show increases in natural frequencies of the ER beam in terms of upward shift of the frequency/time curves, the frequency response curves show the characteristics of the beams throughout the frequency range of interest.

The frequency response of the AC material based beam is shown in Figure 4.18. As the electric field is increased, the damping effect of the ER material is noticed in the form of decreased vibration amplitude and a slight shift of the curve towards higher frequency. In viscoelastic terms, modal frequency increases and damping of this class of beams are due to storage modulus (G') and loss modulus (G") changes. It is expected that an ER material with a high G' value will contribute to increasing modal frequencies; less energy is lost to viscous dissipation. For an ER material with a high G" value, damping takes place in terms of viscous dissipation; less is contributed to increasing the overall stiffness. The behavior of the AC ER material beam shown in Figure 4.18 seemed to suggest large changes in loss modulus with changes in electric field and relatively small changes in storage modulus—since significant modal damping increases but only slight natural frequency increases were observed when the electric field strength was increased.

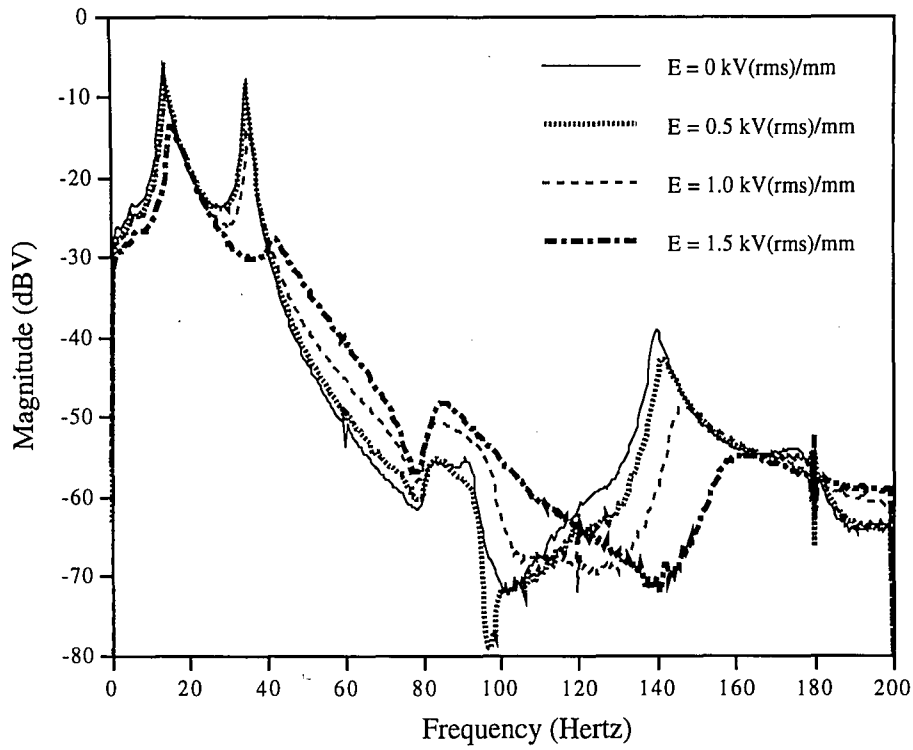

Figure 4.18 Frequency response of the AC adaptive beam under varying electric field strength.

The typical frequency response of a DC ER material based adaptive beam is shown in Figure 4.19. At higher electric field levels, the DC material based beam exhibited a decrease in amplitude, like that of the AC beam previously discussed. However, the single most important feature that differentiates AC and DC beams is the distinct shift towards higher frequencies, i.e. significant increase in modal frequencies as electric field is increased. As previously mentioned, the increases in modal frequencies of the DC beam may be attributed to fundamental differences in rheological properties. Again, an ER material with high storage-modulus changes with electric field application will increase significantly in stiffness, thereby increasing the natural frequencies of the entire structure.

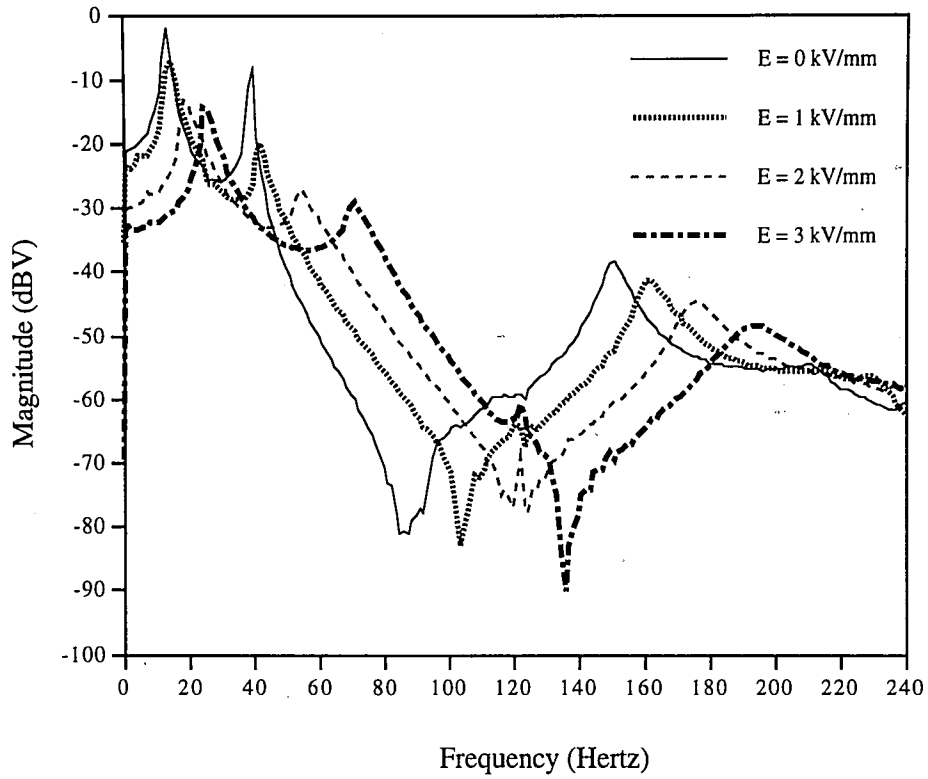

Figure 4.19 Frequency response of the DC adaptive beam under varying electric field strength.

The amount of viscous dissipation and energy stored is only qualitatively represented by frequency response curves: Figures 4.18 and 4.19. But in order to further understand the causes for such differences in frequency response, it is imperative for the experimenter to know the quantitative rheological properties and behavior of the ER materials under small, dynamic strains.

4.5.3 Effect of ER rheology on structural response

The interpretation of structural vibration response of AC and DC ER beams requires the results of Chapter 3 of this thesis. Specifically, the results of Sections 3.4.3 and 3.4.4. In these sections, the rheological behavior of both AC and DC ER materials was analyzed at small strains.

Since it was already proven from Sections 3.4.3 and 3.4.4 that both ER materials behaved non-linearly at frequency ranges from 1 to 16 Hertz, only the results at 10 Hertz will be shown. Also, since the main interest is to determine the effect of rheology on beam response, frequency and electric field data from Sections 3.4.3 and 3.4.4 were chosen to match those of actual beam conditions. For both ER materials, data from an excitation frequency of 10 Hertz was chosen. For the AC material, data at an electric field of 2 kV(rms)/mm was superimposed over DC material data at an electric field of 3 kV/mm. It is expected that a superposition of $G_n^{'}$ and $G_n^{''}$, as well as ϕ and τ values will reveal the ratios of rheological properties to each other. Of particular interest is the proportions of $G_n^{'}$ and $G_n^{''}$ to each other at small strains. As previously discussed (Section 4.5.2), the relative proportions of $G_n^{'}$ and $G_n^{''}$ directly affect the frequency response of the ER adaptive structures due to damping. A valid point may be raised as whether or not to plot $\tan \delta$ (Equation 2.19) as a function of strain, since $\tan \delta$—as discussed in Section 2.2—is a direct measurement of damping capacity. But upon closer examination, one realizes that Equation 2.19 is a ratio of linear-viscoelastic G" divided by linear-viscoelastic G'. Since it was already proven that both AC and DC ER materials examined are nonlinear viscoelastic, $\tan \delta$ relationship may not be used. Instead, interpretation of ER rheology influence on beam response requires the knowledge of fundamental viscoelastic properties, i.e. nonlinear storage and loss moduli, and phase angle. Selected results from Sections 3.4.3 and 3.4.4 are re-plotted and presented in Figures 4.20 and 4.21.

In Figure 4.20, the viscoelastic properties of the two ER materials and PDMS are shown. As it was shown in Section 3.4.2 and again in Figure 4.20, PDMS is a linear viscoelastic material. To find the G' and G" dependence on frequency, a frequency sweep may be performed—provided that the applied strain is below the yield strain. For both ER materials however, it is shown in Figure 4.20 and as it has already been established in Sections 3.4.3 and 3.4.4 that both ER materials exhibit nonlinear behavior. Adopting the

conventions of Sections 3.4.3 and 3.4.4, the nonlinear viscoelastic storage and loss moduli are referenced as G_n' and G_n'', respectively.

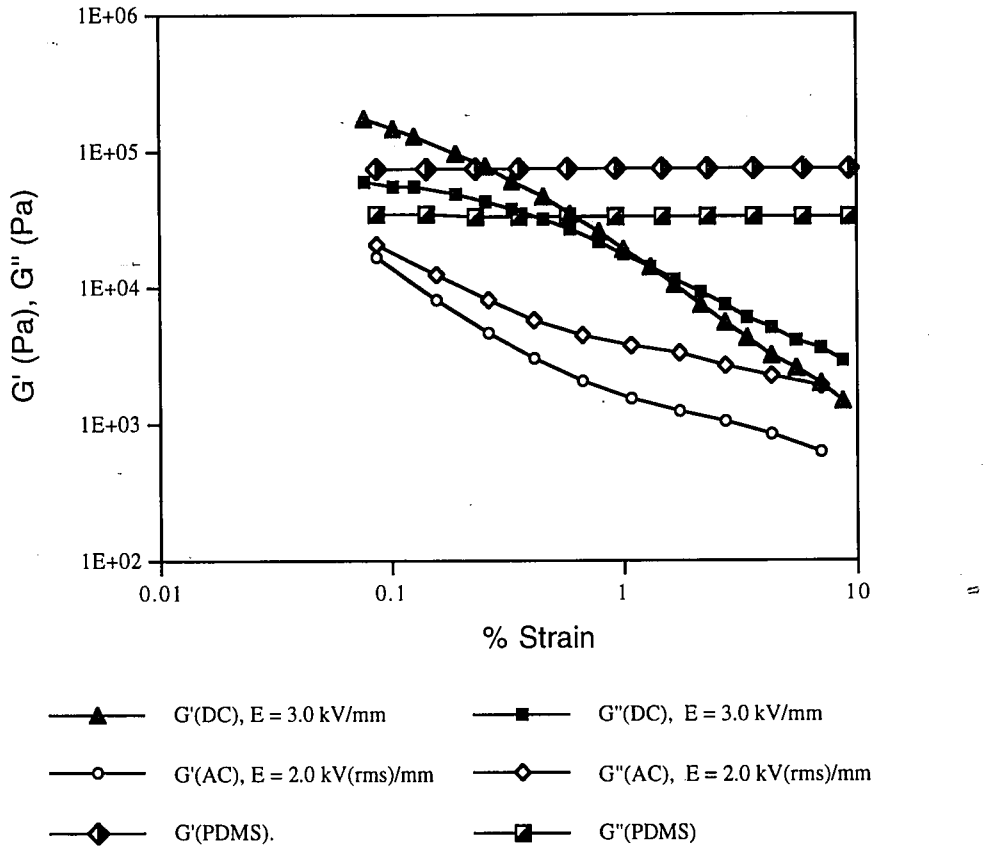

Figure 4.20 Effect of strain on the complex shear moduli of LORD ER materials and PDMS at a strain frequency of 10 Hertz.

An explanation for the higher increase in natural frequencies for the DC ER material based beam could be made from Figure 4.20. The nonlinear storage modulus (G_n') is greater than the nonlinear loss modulus (G_n'') for up to approximately one percent strain. A high G_n' value consequently means that overall, the ER beam is stiffer at high electric fields and will correspondingly have higher natural frequencies. The characteristics of AC material behavior is different from the DC material. While nonlinear behavior is also

observed at small strains, G_n'' is greater than G_n' within the entire strain range investigated. A high value of G_n'' is associated with large quantities of energy lost to viscous dissipation. Vibration damping of the ER beam is achieved in this case, but the penalty on the tunable nature of the system is apparent in relatively lower increases in natural frequencies (Section 4.5.2).

The phase angle ϕ as a function of strain is shown in Figure 4.21(a). By analyzing the phase angle behavior, the properties of the viscoelastic material in question may be compared to that of the elastic and viscous materials. While a polymer like PDMS has constant ϕ values as strain increased, both ER materials became more viscous in behavior as strain was increased. Clearly, the ER-200 is more viscous in behavior than the ER-III for the strain range tested. It should be emphasized that no abrupt transitions in phase angle from low values (<45 degrees) to high values of near 90 degrees exist in Figure 4.21(a). Such transitions, if they were to occur, would represent a transition between pre-yield and post-yield behavior. The lack of such transitions support the conclusion of nonlinear behavior of Figure 4.20. The shear stresses of the ER materials in Figure 4.21(b) do not show yielding, further supporting this finding.

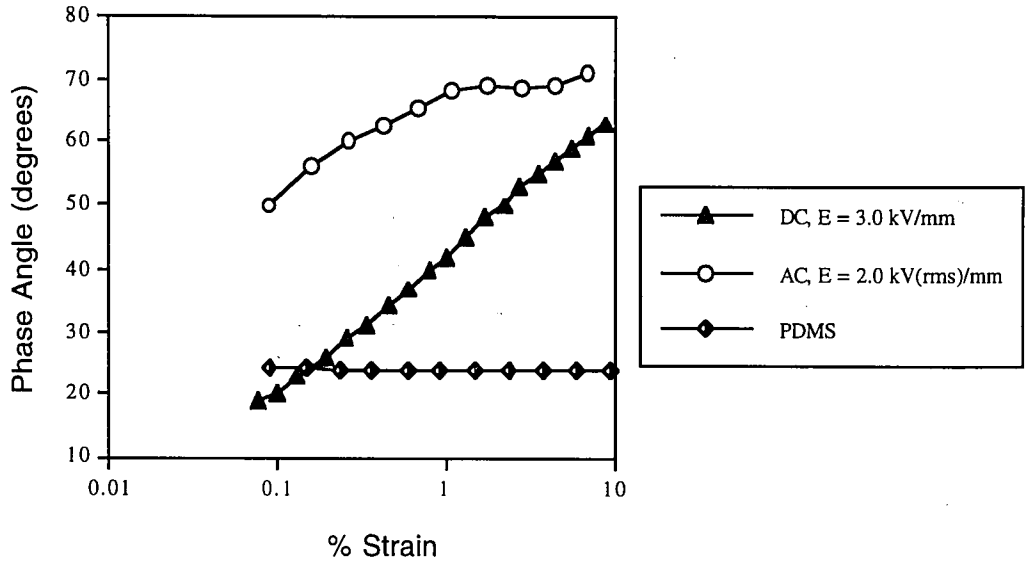

(a)

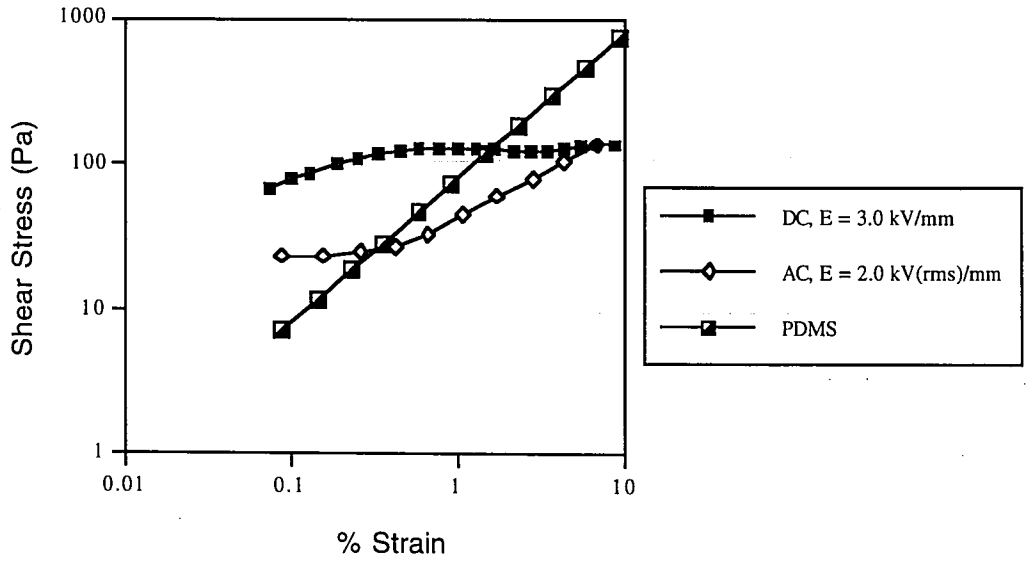

(b)

Figure 4.21 Viscoelastic properties of LORD ER materials and PDMS at a strain frequency of 10 Hertz. (a) Effect of strain on the phase angle, and (b) effect of strain on the shear stress.

Evidences in greater detail are presented in Figures 4.22 and 4.23 in order to support the observed differences in the frequency response curves of AC and DC ER adaptive beams (Figures 4.18 and 4.19). In these Figures, the nonlinear storage and loss moduli are plotted as functions of strain and electric field. It can be observed that both G_n' and G_n'' are strongly influenced by the electric field strength. As field strength increased, the moduli shifted upward readily. As previously discussed, for increases in natural frequencies of ER adaptive structures, elastic behavior, or high G_n' is desired. Though the current output limitations of the TREK prevented the study of the AC beam behavior at above 1.5 kV(rms)/mm, rheological experiments on the Rheometrics RDA II—with smaller electrode surface area—were successfully conducted for up to 3.0 kV(rms)/mm . From Figure 4.22(a), interpolation of experimental data at a strain of 0.1% for electric field strength of 1.5 kV(rms)/mm yielded a G_n' value of approximately 4,500 Pa. But for the ER-III at 0.1% strain and 3.0 kV/mm, G_n' was measured to be 180,000 Pa. This large G_n' difference of the two ER materials was the cause for the comparably larger increases in natural frequencies of the DC adaptive beam. Also from Figure 4.22(a), another problem with the AC ER material is apparent: the current density for the AC ER material is higher than suitable for adaptive structures application. If it had been possible to maintain an AC electric field of 3.0 kV(rms)/mm, greater G_n' values could have been obtained. Consequently the structural-stiffness controllability of the AC adaptive beam would be notably improved.

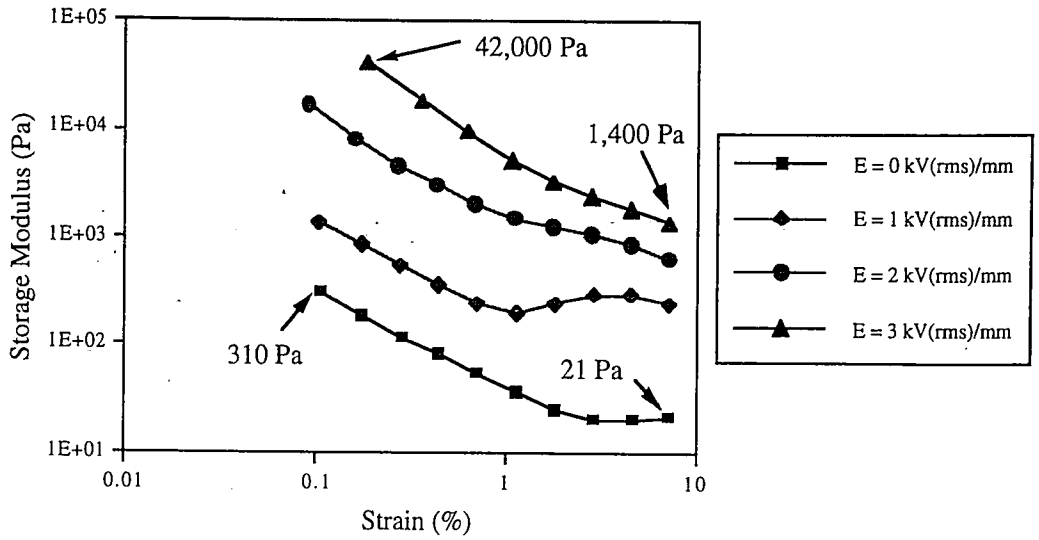

(a)

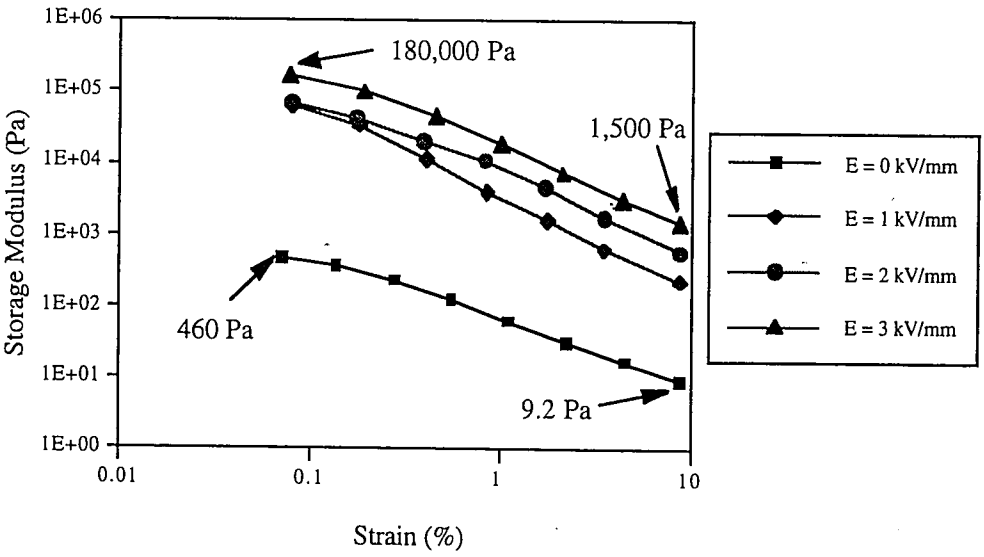

(b)

Figure 4.22 Influence of electric field strength on the nonlinear storage moduli of LORD ER materials at a strain frequency of 10 Hertz. (a) VersaFlo ER-200 and (b) VersaFlo ER-III.

From Figure 4.23(a)-(b), the nonlinear loss modulus can also be seen to be strongly affected by external field strength. For both ER materials, G_n'' increased significantly with increases in field strength. The damping of the AC beam—as shown in terms of decreasing amplitude in Figure 4.18—was easily obtained by electric field strength increases. Even though it has been shown that the stiffness controllability of the ER-III is better than that of the ER-200, it may be observed from Figure 4.23(b) that at small strains, significant damping may also be obtained for this material at high electric field levels. Furthermore, it can be observed from Figure 4.23 that at higher electric fields, the damping (i.e. energy absorption) capability of the DC ER material is comparable to that of the AC ER material. From these quantitative results, the causes of the differences in frequency response between the AC and DC ER material based adaptive beams were found. Both ER materials at small strain levels and high electric field strengths were shown to have damping characteristics comparable to polymeric materials. However, the stiffness control of the DC ER material was superior to that of the AC material due primarily to lower electrical power requirements.

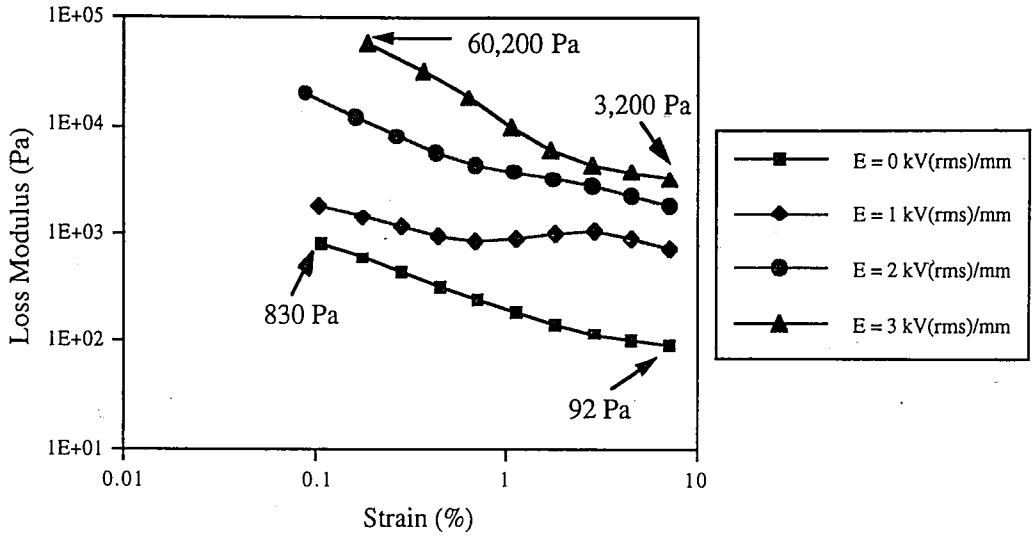

(a)

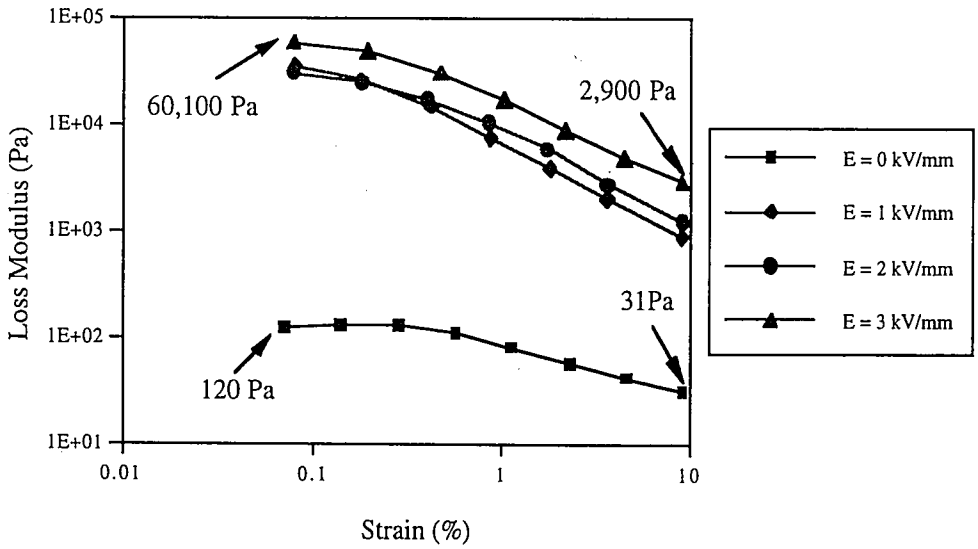

(b)

Figure 4.23 Influence of electric field strength on the nonlinear loss moduli of LORD ER materials at a strain frequency of 10 Hertz. (a) VersaFlo ER-200 and (b) VersaFlo ER-III.

4.5.4 Response of ER structures to the application of electric field

The ideal time response of ER material based structures to on-off states in electric fields as well as changing field strengths is instantaneous, as depicted by Figure 4.5. However, the actual responses obtained are far from ideal, as shown by Figure 4.24, which is the time response of the DC beam at 14 Hertz with a 3000 V/mm electric field applied for a time of 5 seconds.

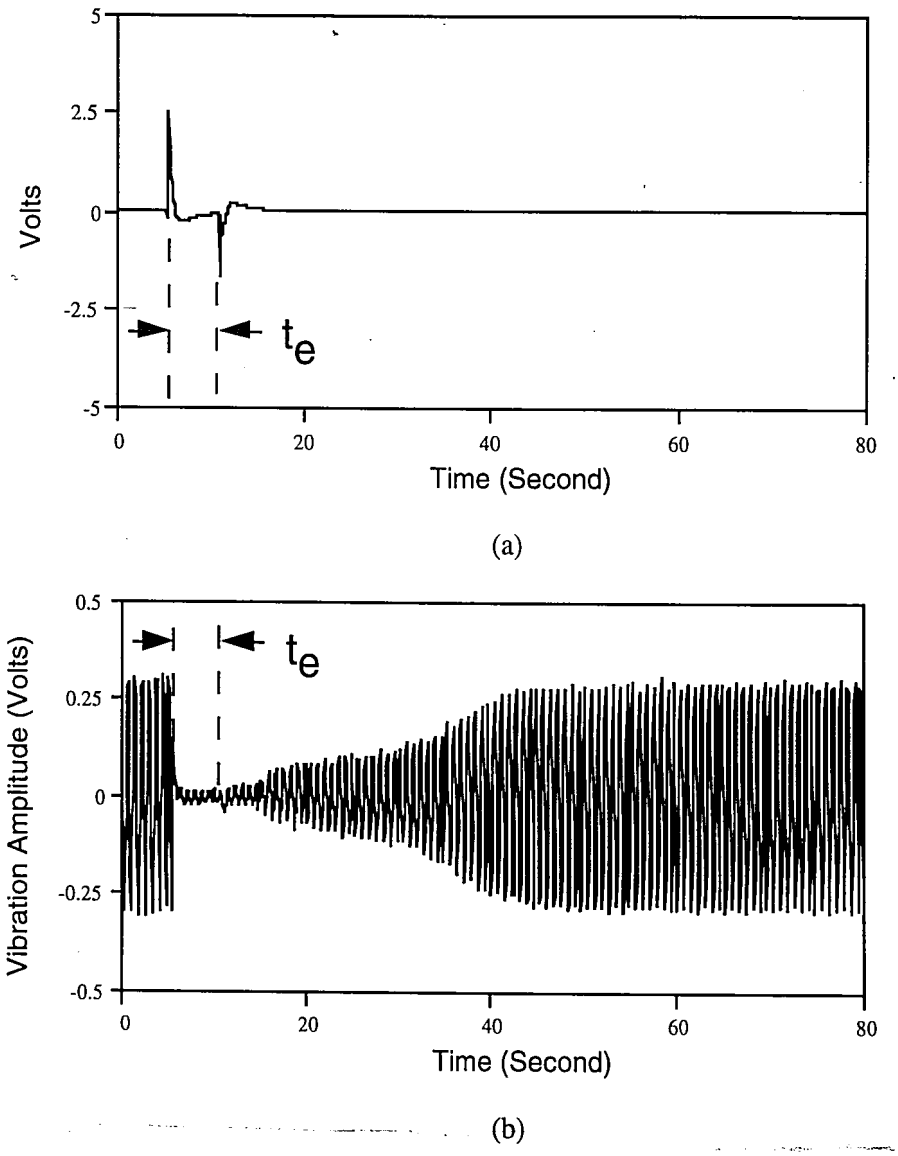

Figure 4.24 Actual response. (a) Output of TREK high voltage amplifier, and (b) DC beam vibration amplitude history at 14 Hertz with ΔE of 3000 V/mm and 5 second application time.

It is expected that the response time of ER adaptive structures to the sudden application of electric field is fast, since available literature indicates a fast response time for ER materials. The results of present experiments for DC and AC ER adaptive structures are presented in Figure 4.25. The results indicate that the response time of these structures to the application of an electric field is indeed fast. In general, the beams reached steady state oscillation within five seconds of the application of the electric field. Also, the higher the ΔE, the faster the beam responded. Again, the current output limitations of the TREK prevented the study of the AC beam at greater than 1500 V(rms)/mm, but there is no question in the trend of response time as ΔE is increased. It can be observed that for both AC and DC beams, mode two response times were shorter than those for mode one. This is simply due to the larger vibration amplitude at mode one. Therefore, more damping energy and time is needed for the beam to establish dynamic, electric-field-on equilibrium.

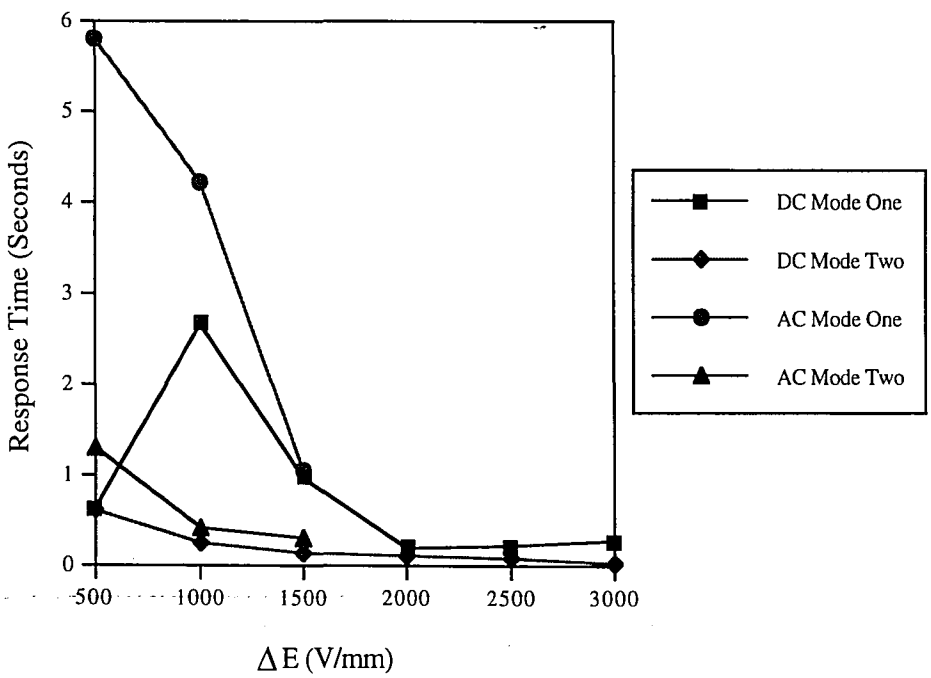

Figure 4.25 ER adaptive beam Switch-On Time.

4.5.5 Response of ER structures to the removal of electric field

The Switch-Off Time for the AC beam is presented in Tables 4.3 and 4.4 for excitation frequencies of 15 and 34 Hertz, respectively. From these Tables, the effect of ΔE and electric field duration time (t_e) on the response time could not be clearly established since holding one variable constant, e.g. t_e, the trend of the other variable i.e. ΔE did not show a consistent pattern of increase or decrease. In all cases however, the beam responded to switch off of AC electric fields in less than three seconds, which is advantageous from a controls perspective. This is true for vibration frequencies of 15 and 34 Hertz, ΔE of up to 1500-0 V(rms)/mm, and for t_e values of up to 120 seconds. By knowing the time delay (three seconds) of AC structures, control schemes could be designed to function in applications where vibration suppression is desired over a wide range of frequencies. The response time to on and off states of electric fields for the AC beam is short, i.e. from a controls perspective, vibration suppression of the AC beam poses no time-response based problem in the lower frequency range. A problem does exist with ER adaptive structures based on this particular AC ER material. As stated previously, the behavior of AC adaptive beams containing this material is inadequate due to high current requirements which in turn lead to a lack of overall structural-stiffness control.

Table 4.3 Response time (in seconds) of the AC ER material based beam at 15 Hertz

	Response Time (sec)		
	ΔE (V(rms)/mm)		
t_e (Seconds)	500-0	1000-0	1500-0
5	2.20	2.35	2.14
30	1.93	2.48	2.42
60	1.86	2.41	1.95
120	1.72	1.73	1.39

Table 4.4 Response time (in seconds) of the AC ER material based beam at 34 Hertz

	Response Time (sec)		
	ΔE (V(rms)/mm)		
t_e (Seconds)	500-0	1000-0	1500-0
5	1.15	1.64	1.93
30	1.41	1.78	1.55
60	1.38	1.90	1.84
120	1.46	2.10	1.93

Unexpected experimental difficulties were encountered in obtaining the Switch-Off Time of the DC beam. Namely, for electromagnetic actuator input voltages similar to those applied to the AC beam (2 V_{rms}), the DC beam response time was observed to be long (>5 minutes), especially at high ΔE and t_e values. The mechanisms causing the formation of fibrils in the DC ER material do not vanish readily upon the removal of electric field. This, in effect, means that a "memory" is developed in the DC ER material where particles in fibrils in the "on" state do not return to random distribution after the removal of the electric field.

It was noticed in the switch-off experiments that when the DC beam did not return to zero-field amplitude, slight increases in electromagnet input voltage (or vibration actuation force) brought on the zero-field behavior immediately. Since both DC and AC materials were found to be nonlinear viscoelastic, i.e. the complex shear moduli were functions of strain, it is conceivable that the time responses were related to strain amplitude by means of energy dissipation; though it is unclear why the phenomena was not observed in the AC material.

The results of Switch-Off Time as a function of t_e and ΔE are shown in Figures 4.26-4.28 for three discrete values of input actuation voltage: 6, 8, and 10 V(rms). All tests performed were at the first fundamental mode of the beam, i.e. 14 Hertz. Essentially, these Figures show the effect of t_e, ΔE, and actuation voltage on response time. ΔE had the greatest influence on response time at values greater than 1000 V/mm. Figures 4.27

and 4.28 also show that—in general—the greater the t_e, the longer the beam took to return to zero-field behavior. But at ΔE of 3000 V/mm and t_e equal to 60 seconds, the response time reached a maximum value and then showed a decreasing trend. As the vibration actuation voltage (i.e. disturbance force) was increased, the response time was reduced significantly as shown.

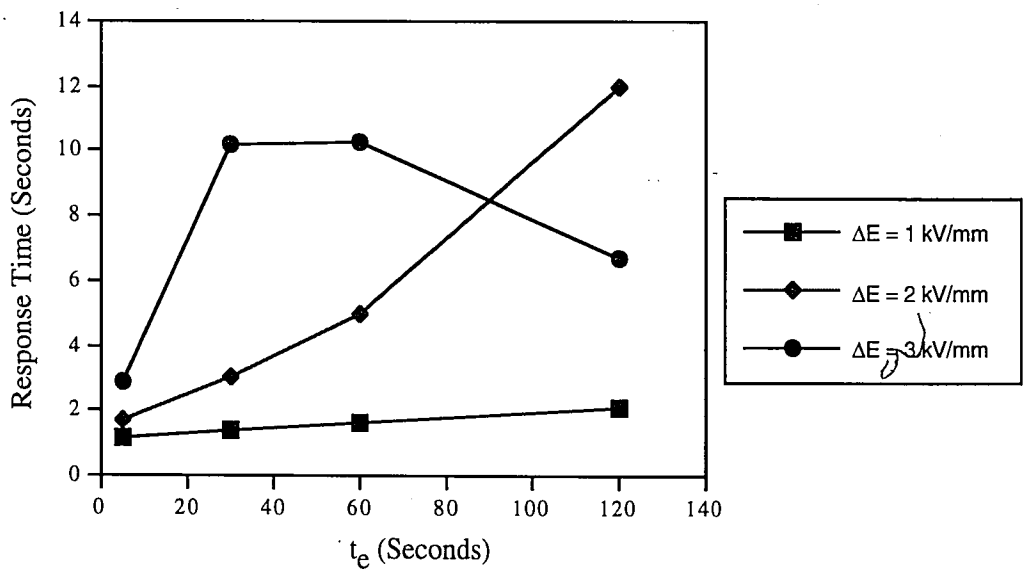

Figure 4.26 DC beam Switch-Off Time at 14 Hertz subjected to electromagnet input voltage of 6 V_{rms}.

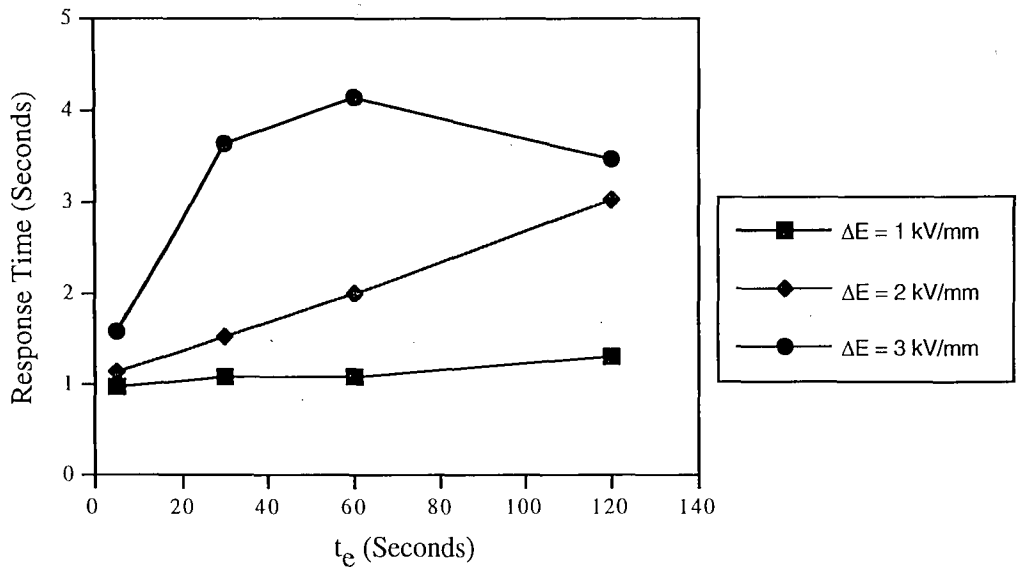

Figure 4.27 DC beam Switch-Off Time at 14 Hertz subjected to electromagnet input voltage of 8 V_{rms}.

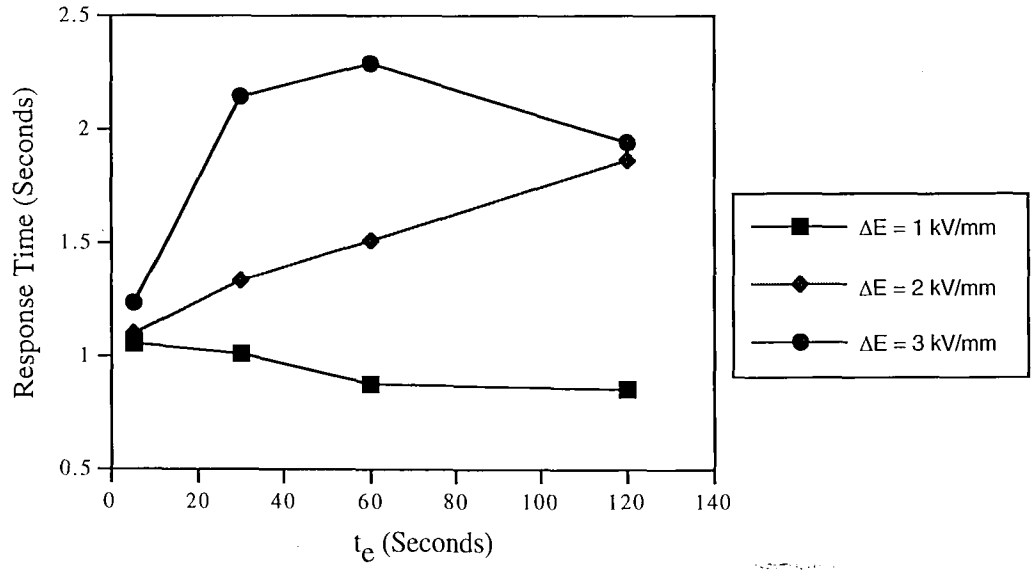

Figure 4.28 DC beam Switch-Off Time at 14 Hertz subjected to electromagnet input voltage of 10 V_{rms}.

The results of the switch off time analysis discussed above showed that the utilization of DC ER materials in structural vibration is frequency range sensitive. Since more energy and motion is needed to disperse the fibrils upon the removal of the electric field, the rapid control of structural vibration may therefore be limited—with this material—to a low frequency range. While the DC ER material could still be used for a high frequency range, the response time at the high range is expected to be long.

4.6 Chapter Summary

A question that arises is: can AC ER materials be utilized for structural damping since AC beams switch on and off relatively fast? There is certainly an advantage from the controls perspective. But observations from Figure 4.18 yield slight increases in natural frequencies due to electric field increases; whereas Figure 4.19 for the DC ER material beam shows large increases in natural frequencies as the DC electric field is increased. Given the behavior observed in Figure 4.18, the optimum electric field for AC beam vibration amplitude minimization is always the highest electric field value. For adaptive structures based on the DC ER material, however, Figure 4.19 supports the notion that the optimum electric field level changes with vibration frequency (Yalcintas et al., 1993). In order to successfully design and implement a truly tunable structure, DC behavior is more desirable, i.e. specific electric fields may be applied at discrete vibration frequencies throughout the frequency range to obtain minimum amplitude; nevertheless, the time response characteristic of the AC ER material is needed.

Indeed, the problems encountered in using ER materials as the damping layer in adaptive structures are not fully solved. One such problem is that for materials such as LORD Corporation ER-III, the particle chains do not disperse immediately upon removal of an electric field. Better ER materials having the mechanical properties of ER-III, the time response of ER-200, and low electrical current requirement are needed for structural damping. ER materials do have potential for such applications, provided that superior fluids

are developed. The rheology of ER materials, specifically, the nonlinear viscoelastic behavior over the frequency range of interest must be further studied and modeled. The understanding of the fundamental rheology of these behaviorally complex materials is essential for further understanding the reliability and controllability of ER material based structures.

CHAPTER 5: CONCLUSIONS AND FUTURE WORK

5.1 Conclusions

Electrorheological (ER) materials are preferred for use in the damping of structures due to their fast, controllable rheological properties. Since understanding fundamental ER rheology was necessary for the design and modeling of ER material based adaptive structures, rheological experiments were performed on two types of commercial ER materials. Both AC and DC materials were found to be viscoelastic. However, linear viscoelastic theory could not be used to describe material properties under varying electric field strengths and strain frequencies. This was due to the observed nonlinear behavior (strain dependence) of both materials even at small strains. Both strain frequency and electric field intensity affected the nonlinear storage and loss moduli. Increases in electric field strength significantly increased the nonlinear complex shear moduli, while the effect of frequency on the shear moduli remained unclear and required further investigation.

The reliability and controllability issues of AC and DC ER material based structures were addressed. Both types of structures exhibited stable modal frequencies over time. Another indication of reliability—modal loss factor—displayed large variations over time, but showed no trend. The cause of which is thought to include factors such as variations in boundary conditions, and most importantly, changing ER material properties over time. Though not consistently observed, structural damping generally increased with increasing electric field strength. Inconsistent increases in modal frequencies in response to electric fields were observed between AC and DC structures. Evidence from rheological experiments proved that this was due to the differences—between AC and DC materials—in the contribution of nonlinear storage and loss moduli to the overall nonlinear complex modulus. The higher value of nonlinear storage modulus of the DC material at small strains was found to have caused consistent increase of natural frequencies of the adaptive beam.

For the AC material, the dominance of nonlinear loss modulus at small strains contributed significantly to structural damping, and less towards overall stiffness.

In terms of controllability, both AC and DC beams responded rapidly to application of electric field. In most cases, vibration amplitude was minimized within five seconds. Response time decreased as electric field strength increased. Upon removal of the electric field, the AC structure returned to zero-field behavior within three seconds; application time and field strength had no significant influence on response time . Time response of the DC structure to the switch off of the electric field was also studied. Factors which influenced the beam's return to zero-field behavior included electric field strength, application time, and external excitation amplitude. Results indicated that although DC ER materials are preferred for adaptive-structures application, extraordinarily long response time may be expected for high vibration frequencies.

From the results of rheological experiments, it is concluded that a nonlinear-viscoelastic phenomenon is encountered when an ER adaptive structure is under small amplitude vibration. The modeling of ER adaptive structures is complicated by the observed strain dependence, since strain amplitude varies according to mode shapes and location along the structure. Although ER materials offer controllable rheological properties, the utilization of ER materials as the damping layer in adaptive structures requires reconsideration due to this non-linearity. The full implementation of an ER material based adaptive structure with sensing and controls capabilities may not be realized with the present ER materials. The advancement of these dynamically tunable structures requires superior ER materials with balanced viscoelastic properties as well as instantaneous dispersion of ER particulate matter upon electric field removal.

5.2 Future Work

The utilization of ER materials as the damping layer in adaptive structures requires reconsideration due to the nonlinear effects. Present methods and models assuming a damping layer with uniform properties may be insufficient for accurate prediction of ER adaptive structural responses.

Pertinent to the understanding of these structures is the knowledge of nonlinear-viscoelastic behavior and properties of the ER materials. While the field of nonlinear viscoelasticity is not new, considerable effort is required in the initiation of research in this area. Methods which could be used include Fourier Transform—primarily a method for the quantification of ER materials' energy dissipation and energy storage capabilities throughout a frequency spectrum. Essentially, this method takes the Fourier Transform of the stress response of the viscoelastic material under induced strain; examination of the stress response in the frequency spectrum provides information on linearity and dynamic moduli. More fundamental methods utilize linear viscoelastic equations, but add in nonlinear terms as appropriate for describing the observed nonlinear phenomenon. Still other methods evaluate the stress response of a nonlinear-viscoelastic material by the use of constitutive relations. Many of these methods have been widely used in the field of polymer science and polymer rheology.

Potential problem areas of utilizing commercial rheometers for yielding (static or dynamic) investigations do exist, especially for testing high viscosity viscoelastic materials. Problems such as wall slip, insufficient strain resolution, undefined deformation, and transducer drift of the strain measuring system could lead to unreliable results. Very slow, steady shearing, or creep analysis of the ER materials should be examined, since in these constant-stress tests the above mentioned problems could be avoided or minimized. Investigation of ER materials under creep conditions could be beneficial in distinguishing the linear/nonlinear behavior and properties. Consequently, further understanding of the characteristics of these complex materials may be obtained.

REFERENCES

Block, H., J. P. Kelly, A. Qin, and T. Watson. (1990). "Materials and Mechanisms in Electrorheology," *Transactions of the American Chemical Society* , 6(1):6-14.

Boyle, F.P. (1992). "Performance Characterization of ER Fluids: Durability," *Proceedings of the International Conference on Electrorheological Fluids*, R. Tao (Ed.), World Scientific Publishing Co., New Jersey, pp. 236-245.

Brooks, D. (1993). "Applicability of Simplified Expressions for Design with Electro-Rheological Fluids," *Journal of Intelligent Material Systems and Structures*, 4:409-414.

Brooks, D., J. Goodwin, C. Hjelm, L. Marshall, and C. Zukoski. (1986). "Visco-Elastic Studies on an Electro-Rheological Fluid," *Journal of Colloids and Surfaces*, 18(1986):293-312.

Choi, Y., A.F. Sprecher, and H. Conrad. (1992). "Response of Electrorheological Fluid-Filled Laminate Composites to Forced Vibration," *Journal of Intelligent Material Systems and Structures*, 3:17-29.

Conrad, H. and A.F. Sprecher. (1991). "Characteristics and Mechanisms of Electrorheological Fluids," *Journal of Statistical Physics,* 64:1073-1091.

Conrad, H., A.F. Sprecher, Y. Choi, and Y. Chen. (1991). "The temperature dependence of the electrical properties and strength of electrorheological fluids," *Journal of Rheology*, 35(7):1393-1409.

Coughlin, C.S. and R.N. Capps. (1994). "Particle size effects in the electrorheological behavior of silica-poly(dimethylsiloxane) mixtures," *Proceedings of the SPIE, Smart Structures and Intelligent Systems*, N.W. Hagood (Ed.), 2190:19-27.

Coulter, J.P., K.D. Weiss, and J.D. Carlson. (1993a). "Engineering Applications of Electrorheological Materials," *Journal of Intelligent Material Systems and Structures*, 4:248-259.

Coulter, J.P., D.L. Don, M. Yalcintas, and P.J. Biermann. (1993b). "An Experimental Investigation of Electrorheological Material Based Adaptive Plates," submitted for publication.

Coulter, J.P., K.D. Weiss, and J.D. Carlson. (1992). "Electrorheological Materials and Their Usage in Intelligent Material Systems and Structures, Part II: Applications," *Recent Advances in Adaptive and Sensory Materials and Their Applications*, C.A. Rogers, R.C. Rogers (Eds.), Technomic Publishing Co., Inc., Lancaster, Pennsylvania, pp. 507-523.

Don, D.L. (1993). *An Investigation of Electrorheological Material Adaptive Structures*, Masters Thesis, Lehigh University, Bethlehem, Pennsylvania.

Ehrgott, R. and S. Masri. (1992). "Experimental Studies of Electro-Rheological Materials for Application in Adaptive Structures," *Proceedings of the Third International Conference on Adaptive Structures*, B.K. Wada, M. Natori, and E. Breitbach (Eds.), Technomic Publishing Co., Inc., Lancaster, Pennsylvania, pp. 161-175.

Ferry, J.D. (1980). *Viscoelastic Properties of Polymers*, John Wiley and Sons, Inc., N.Y.

Filisko, F.E. and L.H. Radzilowski. (1990). "An intrinsic mechanism for the activity of alumino-silicate based electrorheological materials," *Journal of Rheology*, 34(4):539-552.

Flanders, S.W., L.I. Burke, and M. Yalcintas. (1994). "Alternate Neural Network Architectures for Beam Vibration Minimization," submitted to The Proceedings of the ASME Winter Annual Meeting for publication.

Fox, R.W. and A.T. McDonald. (1985). *Introduction to Fluid Mechanics*, John Wiley & Sons, Inc., NY.

Gamota, D.R., A.S. Wineman, and F.E. Filisko. (1993). "Fourier transform analysis: Nonlinear dynamic response of an electrorheological material," *Journal of Rheology*, 37(5):919-933.

Gamota, D.R. and F.E. Filisko. (1991a). "Linear/Non-Linear Mechanical Properties of Electrorheological Materials," *Proceedings of the International Conference on Electrorheological Fluids*, R. Tao (Ed.), World Scientific Publishing Co., New Jersey, pp. 246-263.

Gamota, D.R. and F.E. Filisko. (1991b). "Dynamic mechanical studies of electrorheological materials: Moderate frequencies," *Journal of Rheology*, 35(3):399-425.

Gamota, D.R. and F.E. Filisko. (1991c). "High frequency dynamic mechanical study of an aluminosilicate electrorheological material," *Journal of Rheology*, 35(7):1411-1425.

Gandhi, M.V. and B.S. Thompson. (1990). "Dynamically-Tunable Smart Structures Featuring Electro-Rheological Fluids," *U.S.-Japan Workshop on Smart/Intelligent Materials and Systems*, I. Ahmad, A. Crowson, C.A. Rogers, and M. Aizawa (Eds.), Technomic Publishing Co., Inc., Lancaster, Pennsylvania, pp. 319-326.

Gandhi, M.V. and B.S. Thompson. (1989). "Dynamically-Tunable Smart Composites Featuring Electro-Rheological Fluids," in *Fiber Optic Smart Structures and Skins II*, E. Udd (Ed.), Boston, MA: SPIE-The International Society for Optical Engineering, 1170:294-304.

Gandhi, M.V. and B.S. Thompson. (1988). "A New Generation of Revolutionary Ultra-Advanced Intelligent Composite Materials Featuring Electro-Rheological Fluids," in *Smart Materials, Structures, and Mathematical Issues*, C.A. Rogers (Ed.), Technomic Publishing Co., Inc., Lancaster, Pennsylvania, pp. 63-68.

Gast, A.P. and C.F. Zukoski. (1989). "Electrorheological Fluids as Colloidal Suspensions," in *Advances in Colloid and Interface Science*, Elsevier Science Publishers B.V., 30(1989):153-202.

Gong, H., L.M. King, and T.B. Cher. (1993). "Influence of a Locally Applied Electro-Rheological Fluid Layer on Vibration of a Simple Cantilever Beam," *Journal of Intelligent Material Systems and Structures*, 4:379-384.

Han, L., A. Voloshin, M. Yalcintas, and J.P. Coulter. (1994). "Electrorheological adaptive structures with embedded sensing and control," *Proceedings of the SPIE, Smart Structures and Intelligent Systems*, N.W. Hagood (Ed.), 2190:2-12.

Hartsock, D.L., R.F. Novak, and G.J. Chaundy. (1991). "ER fluid requirements for automotive devices," *Journal of Rheology*, 35(7):1305-1326.

Hill, J.C., N.A. Vaz, D.J. Klingenberg, and C.F. Zukoski. (1992). "Experimental and Theoretical Response Times of Electrorheological Fluids," *Proceedings of the International Conference on Electrorheological Fluids*, R. Tao (Ed.), World Scientific Publishing Co., New Jersey, pp. 280-288.

Hill, J.C. and T.H. Van Steenkiste. (1991). "Response times of electrorheological fluids," *Journal of Applied Physics*, 70(3):1207-1211.

Hosseini-Sianaki, A., W.A. Bullough, R. Firoozian, J. Makin, R.C. Tozer. (1992). "Experimental Measurements of the Dynamic Torque Response of an Electro-Rheological Fluid in the Shear Mode," *Proceedings of the International Conference on Electrorheological Fluids*, R. Tao (Ed.), World Scientific Publishing Co., New Jersey, pp. 219-235.

Hunter, L.W., F.F. Mark, D.A. Kitchin, M.R. Feinstein, N.A. Blum, B.R. Platte. F.G. Arcella, D.R. Kuespert, and M.D. Donohue. (1993). "Optical Effects of Electro-Rheological Fluids," *Journal of Intelligent Material Systems and Structures*, 4:415-418.

Hunter, R.J. (1989). *Foundations of Colloid Science, Volume II*, Oxford University Press, NY.

Hunter, R.J. (1987). *Foundations of Colloid Science, Volume I*, Oxford University Press, NY.

Johnson, A.R., J. Makin, W.A. Bullough, R. Firoozian, and A. Hosseini-Sianaki. (1993). "Fluid Durability in a High Speed Electro-Rheological Clutch," *Journal of Intelligent Material Systems and Structures*, 4:527-532.

Jordan, T.C., M.T. Shaw, and T.C.B. McLeish. (1992). "Viscoelastic response of electrorheological fluids. II. Field strength and strain dependence," *Journal of Rheology*, 36(3):441-463.

Jordan, T.C. and M.T. Shaw. (1989). "Electrorheology," *IEEE Transactions on Electrical Insulation*, 24(5):849-878.

Klass, D.L. and T.W. Martinek. (1967). "Electroviscous Fluids. I. Rheological Properties," *Journal of Applied Physics*, 38(1):67-74.

Morishita, S. and T. Ura. (1993). "ER Fluid Applications to Vibration Control Devices and an Adaptive Neural-Net Controller," *Journal of Intelligent Material Systems and Structures*, 4:366-372.

Otsubo, Y., M. Sekine, and S. Katayama. (1992). "Electrorheological properties of silica suspensions," *Journal of Rheology*, 36(3):479-496.

Shiang, A.H. and J.P. Coulter. (1994). "Controllability and Reliability Issues Related to Electrorheological Material Adaptive Structures," *Proceedings of the Second International Conference on Intelligent Materials*, C.A. Rogers, G.G. Wallace (Eds.), Technomic Publishing Co., Inc., Lancaster, Pennsylvania, pp. 1117-1130.

Sperling, L.H. (1992). *Introduction to Physical Polymer Science*, John Wiley & Sons, Inc., N.Y.

Tanaka, K., T. Yoshida, and K. Koyama. (1992). "Transient Response of ER Fluids," *Proceedings of the International Conference on Electrorheological Fluids*, R. Tao (Ed.), World Scientific Publishing Co., New Jersey, pp. 289-299.

Thurston, G.B. and E.B. Gaertner. (1991). "Viscoelasticity of electrorheological fluids during oscillatory flow in a rectangular channel," *Journal of Rheology*, 35(7):1327-1343.

Tschoegl, N.W. (1989). *The Phenomenological Theory of Linear Viscoelastic Behavior: An Introduction*, Springer-Verlag, Berlin.

Weiss, K.D., J.D. Carlson, and J.P. Coulter. (1993). "Material Aspects of Electrorheological Systems," *Journal of Intelligent Material Systems and Structures*, 4:13-34.

Weiss, K.D., J.P. Coulter, and J.D. Carlson. (1992). "Electrorheological Materials and Their Usage in Intelligent Material Systems and Structures, Part I: Mechanisms, Formulations and Properties," *Recent Advances in Adaptive and Sensory Materials and Their Applications*, C.A. Rogers, R.C. Rogers (Eds.), Technomic Publishing Co., Inc., Lancaster, Pennsylvania, pp. 605-621.

Wereley, N.M. (1994). "Active damping of flexible rotor blades using ER fluid based actuators," *Proceedings of the SPIE, Smart Structures and Intelligent Systems*, N.W. Hagood (Ed.), 2190:13-18.

Winslow, W.M. (1949). "Induced Fibration of Suspensions," *Journal of Applied Physics*, 20(12):1137-1140.

Yalcintas, M., J.P. Coulter, and D.L. Don. (1993). "Structural Modeling and Optimal Control of Electrorheological Material Based Adaptive Beams," submitted to ASME Journal of Vibration and Acoustics for publication.

Yalcintas, M. and J.P. Coulter. (1993). "Analytical Modeling of Electrorheological Material Based Adaptive Beams," submitted to the Journal of Composite Engineering for publication.

Yen, W.S. and P.J. Achorn. (1991). "A study of the dynamic behavior of an electrorheological fluid," *Journal of Rheology*, 35(7):1375-1384.

VITA

Andy Hsien-Tzu Shiang was born in Taipei, Taiwan, Republic of China on September 12, 1968 to parents of Mr. and Mrs. Cheng-Teh Shiang. He immigrated to the United States with his family in November of 1980. After finishing elementary and secondary schooling in Albany, New York, he entered Rensselaer Polytechnic Institute of Troy, New York. The author became a naturalized citizen of the United States in February of 1990. Upon graduation from Rensselaer in May of 1991 with a Bachelor of Science in Mechanical Engineering, he started professional employment as a mechanical engineer in the Nuclear Services Division of Gilbert/Commonwealth Inc. of Reading, Pennsylvania. In fall of 1992, he entered Lehigh University for part-time studies towards a Master of Science. After resigning from Gilbert/Commonwealth in November of 1992, he entered Lehigh University in January of 1993 as a full-time graduate research assistant under the direction of Dr. John P. Coulter. In December of 1994, the author received his Master of Science degree in Mechanical Engineering. The author's post-masters plans are to continue his studies towards a doctorate in mechanical engineering and ultimately teach at the university level.

END OF TITLE